AFRRI REPORTS

(2)

July • August • September 1988

Defense Nuclear Agency
Armed Forces Radiobiology Research Institute
Bethesda, Maryland 20814-5415

UNCLASSIFIED

SECURITY CLASSIFICATION OF THIS PAGE

REPORT DOCUMENTATION PAGE

1a. REPORT SECURITY CLASSIFICATION UNCLASSIFIED	1b. RESTRICTIVE MARKINGS
2a. SECURITY CLASSIFICATION AUTHORITY	3. DISTRIBUTION/AVAILABILITY OF REPORT Approved for public release; distribution unlimited.
2b. DECLASSIFICATION/DOWNGRADING SCHEDULE	
4. PERFORMING ORGANIZATION REPORT NUMBER(S) SR88-20 - SR88-29	5. MONITORING ORGANIZATION REPORT NUMBER(S)
6a. NAME OF PERFORMING ORGANIZATION Armed Forces Radiobiology Research Institute 6b. OFFICE SYMBOL (If applicable) AFRRI	7a. NAME OF MONITORING ORGANIZATION
6c. ADDRESS (City, State and ZIP Code) Defense Nuclear Agency Bethesda, Maryland 20814-5145	7b. ADDRESS (City, State and ZIP Code)
8a. NAME OF FUNDING/SPONSORING ORGANIZATION Defense Nuclear Agency 8b. OFFICE SYMBOL (If applicable) DNA	9. PROCUREMENT INSTRUMENT IDENTIFICATION NUMBER
8c. ADDRESS (City, State and ZIP Code) Washington, DC 20305	10. SOURCE OF FUNDING NOS. PROGRAM ELEMENT NO.: NWED PROJECT NO.: TASK NO.: WORK UNIT NO.: QAXM
11. TITLE (Include Security Classification) AFRRI Reports, Jul-Sep 1988	
12. PERSONAL AUTHOR(S)	
13a. TYPE OF REPORT Reprints/Technical 13b. TIME COVERED FROM _____ TO _____	14. DATE OF REPORT (Yr., Mo., Day) 1988 November 15. PAGE COUNT 85
16. SUPPLEMENTARY NOTATION	

17. COSATI CODES			18. SUBJECT TERMS (Continue on reverse if necessary and identify by block number)
FIELD	GROUP	SUB. GR	

19. ABSTRACT (Continue on reverse if necessary and identify by block number)

This volume contains AFRRI Scientific Reports SR88-20 through SR88-29 for Jul-Sep 1988.

20. DISTRIBUTION/AVAILABILITY OF ABSTRACT UNCLASSIFIED/UNLIMITED ☐ SAME AS RPT. ☒ DTIC USERS ☐	21. ABSTRACT SECURITY CLASSIFICATION UNCLASSIFIED
22a. NAME OF RESPONSIBLE INDIVIDUAL M. E. Greenville	22b. TELEPHONE NUMBER (Include Area Code) (202)295-3536 22c. OFFICE SYMBOL ISDP

DD FORM 1473, 83 APR EDITION OF 1 JAN 73 IS OBSOLETE.

UNCLASSIFIED

SECURITY CLASSIFICATION OF THIS PAGE

CONTENTS:

Scientific Reports

RADIATION RESEARCH 115, 595–604 (1988)

Prevention and Treatment of the Gastric Symptoms of Radiation Sickness

ANDRE DUBOIS AND NANCY FIALA

Laboratory of Gastrointestinal and Liver Studies, Digestive Diseases Division, Department of Medicine, Uniformed Services University of the Health Sciences, and Department of Physiology, Armed Forces Radiobiology Research Institute, Bethesda, Maryland 20814

AND

CHESTER A. BOWARD AND VICTOR BOGO

Department of Behavioral Sciences, Armed Forces Radiobiology Research Institute, Bethesda, Maryland 20814

DUBOIS, A., FIALA, N., BOWARD, C. A., AND BOGO, V. Prevention and Treatment of the Gastric Symptoms of Radiation Sickness. *Radiat. Res.* **115**, 595–604 (1988).

Currently available treatments for radiation-induced nausea and vomiting either are ineffective or reduce performance. The new antiemetic and gastrokinetic agent zacopride was tested in rhesus monkeys to assess its behavioral toxicity and its ability to inhibit radiation-induced emesis. Zacopride (intragastric, 0.3 mg/kg) or a placebo was given blindly and randomly in the basal state and 15 min before a whole-body 800 cGy ^{60}Co γ-radiation dose (except for the legs which were partially protected to permit survival of some bone marrow). We determined (1) gastric emptying rates; (2) the presence and frequency of retching and vomiting; and (3) the effect of zacopride on the performance of a visual discrimination task in nonirradiated subjects. No vomiting, retching, or decreased performance was observed after either placebo or zacopride in the control state. Following irradiation plus placebo, 70 emeses were observed in 5 of 6 monkeys, and 353 retches were observed in all 6 monkeys. In contrast, only 1 emesis was observed in 1 of 6 monkeys and 173 retches were seen in 4 of 6 monkeys after irradiation plus zacopride ($P < 0.01$). Zacopride also significantly inhibited radiation-induced suppression of gastric emptying. When given after the first vomiting episode in a separate group of irradiated monkeys, zacopride completely prevented any subsequent vomiting. The present results demonstrate that intragastric administration of zacopride significantly inhibited radiation-induced retching, vomiting, and suppression of gastric emptying in rhesus monkeys and did not cause detectable behavioral side effects when given to nonradiated monkeys. This observation has important implications in the treatment of radiation sickness.

INTRODUCTION

Therapeutic and accidental exposure to doses of radiation greater than 150 cGy causes nausea, vomiting, and suppression of gastric emptying in man, monkeys, and dogs (*1–4*). In addition, the normally low doses of radiation that may be encountered in space could play a role in the man–space program, because some of the symptoms observed in space sickness and radiation sickness are similar (*5*). Medications cur-

0033-7587/88 $3.00

rently available to treat radiation- and space-induced nausea and vomiting either are ineffective or reduce performance ability. For example, we previously reported (*4, 6*) that metoclopramide, but not domperidone, effectively prevents radiation-induced vomiting in rhesus monkeys. However, metoclopramide is known to cause involuntary movements in treated patients (*7*).

Recently, several benzamide derivatives of the metoclopramide class have been introduced for the treatment of emesis and/or gastroparesis, and these derivatives may not have behavioral side effects. Therefore, we evaluated the action of one of these agents, zacopride, on radiation-induced vomiting and gastric suppression in rhesus monkeys. Specifically, we studied the possibility of preventing and treating radiation-induced vomiting and suppression of gastric emptying using zacopride. We also determined the possible side effects of this therapeutic agent on gross behavior and on performance of a visual discrimination task.

MATERIAL AND METHODS

Twenty-four male domestic rhesus monkeys, *Macaca mulatta*, mean weight 3.1 ± 0.2 kg, were used in these experiments. Monkeys were quarantined on arrival and screened for evidence of disease before being released from quarantine. They were maintained in an AALAC accredited facility and were held in individual stainless steel cages in conventional holding rooms maintained at 21 ± 1°C with 50 ± 10% relative humidity. Animals were on a 12-h light/dark full-spectrum lighting scale with no twilight and were provided with tap water *ad libitum*, commercial primate chow, and fruits.

After adaptation to a primate-restraining chair, six monkeys were trained to discriminate between a circle and a square (correct) randomly presented every 10 s on backlit press-plates, mounted on an eye-level response panel (*8*). An incorrect response or failure to respond within 0.8 s resulted in a 3-mA shock. Incoming efficiency on the visual discrimination task was 97 ± 2% in the six monkeys. Percentage correct choice was assessed during 18 min (100 trials) before, and for 180 min (1000 trials) after, oral administration of a placebo or zacopride (AHR 11190B, A. H. Robins Co, Richmond, VA). A repeated measure design was used as follows: (a) baseline control without oral administration of fluid; and (b) blind administration of either 0.3 mg/kg zacopride in 5% glucose solution or 0.2 ml/kg of 5% glucose solution.

Twelve other chair-adapted monkeys were studied on 3 separate days after an overnight fast as follows: (1) and (2) on two control days after random and blind intragastric administration of either placebo (0.2 ml/kg) or zacopride (0.3 mg/kg), and (3) on irradiation day after intragastric administration of either placebo or zacopride given blindly and in random order 15 min before exposure. These doses of zacopride were selected based on previous monkey experiments (unpublished observations) demonstrating that these doses did not produce noticeable side effects. Studies were performed in the morning and started 30 min after drug administration and 15 min after either sham-radiation (on control days) or radiation exposure.

On control days, the animals were brought to the exposure room and the doors were closed for 3 min, but no radiation was delivered. On irradiation day, monkeys were placed between two large, 10^5-Ci ^{60}Co irradiators, and the animals received nonuniform radiation exposure through positioning of lead wall shields in front of and behind their legs (*9*). Phantom studies demonstrated that a 1-min exposure resulted in midtissue doses of 800 cGy for torso and abdomen, 896 cGy for head, 584 cGy for femurs, and 425 cGy for tibiae (*9*).

The six remaining monkeys were studied once in the basal state without treatment and again after irradiation as described above but without drug administration prior to exposure. After one episode of vomiting had occurred, 0.3 mg/kg zacopride was given intragastrically, and the study was performed as described above. If vomiting recurred again within 3 min of zacopride administration, a second dose of medication was administered.

Each monkey was monitored for 3 h on control days and 6 h on irradiation days using a videocamera and a video cassette recorder. The videotapes were blindly evaluated at a later time for vomiting, retching, and any other side effect. During this evaluation, vomiting was defined as a succession of strong and brief contractions of thoracic and abdominal muscles leading to the expulsion of gastric contents through the mouth; retching was defined as nonproductive vomiting (*4*).

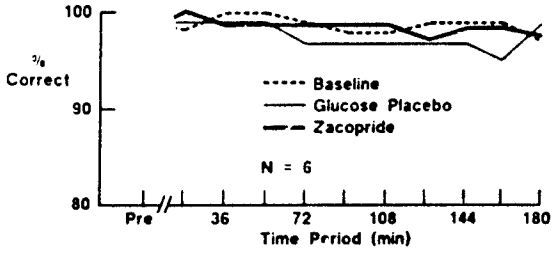

FIG. 1. Effect of zacopride on visual discrimination performance. Six monkeys were tested repeatedly at 2-week intervals without treatment (baseline), after oral placebo, and after oral zacopride administration (0.3 mg/kg).

A previously described and validated marker dilution technique (*10*) was used to determine concurrently gastric secretion and gastric emptying during a 40-min fasting period and for 60 min after the injection of an 80-ml water meal (postmeal period). In the present studies, as previously reported (*4*), this technique was slightly modified in that [^{99m}Tc]DTPA (diethylenetriamine pentacetic acid) was used as the marker instead of phenol red. This intubation method requires only the sequential sampling of the gastric contents, and it permits the concurrent measurement of intragastric volume, gastric emptying, and gastric secretion. A 12-French double lumen nasogastric tube was placed in the stomach and its position was verified by the water recovery test (*11*). Starting 45 min later, samples of the mixed gastric contents were aspirated just before and immediately after intragastric administration of 5 to 20 ml of a [^{99m}Tc]DTPA test solution (30 μCi/100 ml H_2O; pH 7.4; 37°C). After centrifugation of the samples, the clear supernatants were assayed for ^{99m}Tc concentrations using an autogamma counter (1282 Compugamma LKB Instruments, Inc., Gaithersburg, MD). These determinations were repeated every 10 min during the basal period and after intragastric instillation of an 80-ml water meal containing [^{99m}Tc]DTPA (3 μCi/100 ml; pH 7.4; 37°C).

Intragastric volumes of fluid (V_1, V_2, ...) and amounts of ^{99m}Tc (Tc_1, Tc_2, ...) were determined at the time of each sampling using the marker dilution principle (*4, 10, 12, 13*). Fractional emptying rate (g) was then determined for each 10-min interval (t) between two dilutions, assuming that emptying was a first-order process (exponential) during a given 10-min interval. However, since g was allowed to vary from interval to interval, no general assumption was required regarding emptying over the total duration of the experiment. We used the following equation:

$$g = -[\log_e(Tc_2/Tc_1)]/t.$$

Net fluid output (R_v) in milliliters per minute was then determined for the corresponding interval, assuming that R_v remained constant over the given interval and using the equation:

$$R_v = [V_2 - V_1 \cdot \exp^{-gt}] \cdot g/[1 - \exp^{-gt}].$$

Intragastric volumes of fluid and masses of ^{99m}Tc were then recalculated, taking into account these first estimates of fractional emptying and fluid output, which were in turn recalculated. This iterative process was repeated until the improvement of the solution was less than 1% per iteration.

These calculations were performed using a locally developed program and a PDP-10 computer (Division of Computer Research and Technology, National Institutes of Health, Bethesda, MD). The assumptions involved have been described and discussed elsewhere (*10*) and are based on original contributions by Hildes and Dunlop (*12*) and George (*13*). However, in contrast to their method, the present technique allows correction for emptying and secretion that occur during the 1-min marker dilution interval, and this technique can be applied during fasting. On irradiation day, intervals with occurrence of vomiting were not taken into account for calculation of g and R_v.

Statistical evaluation of visual-discrimination performance data was assessed using a two-way analysis of variance. The statistical significance of differences observed for fractional emptying rate and fluid output was evaluated using a three-factor (treatment, time, and monkey) analysis of variance with repeated mea-

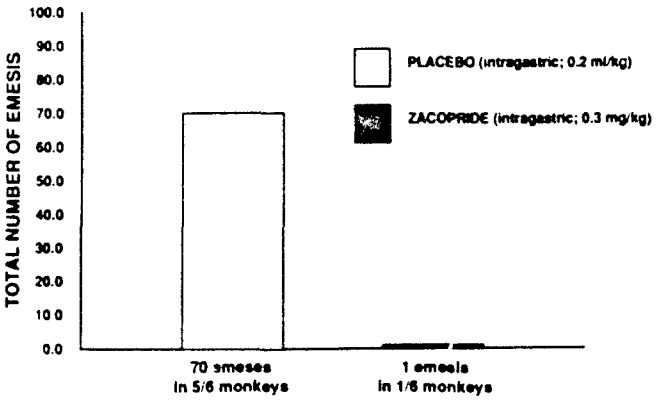

FIG. 2. Effect of zacopride on the total number of radiation-induced emeses. Placebo or zacopride was given intragastrically 30 min before irradiation, and the number of emeses was determined using a videotape. Emesis was defined as a succession of strong and brief contractions of thoracic and abdominal muscles leading to expulsion of gastric contents through the mouth.

sures on the last two factors (*10*). This was done using the program LDU-040 (K. L. Dorn) and an IBM 370 computer (Division of Computer Research and Technology, National Institutes of Health, Bethesda, MD). For vomiting and retching data, statistical analysis was performed using the Behrens–Fisher test (*14*).

RESULTS

No vomiting, retching, or other side effects were observed after placebo alone or zacopride alone. Similarly, zacopride did not significantly modify performance as assessed with a visual discrimination task in nonirradiated animals (Fig. 1).

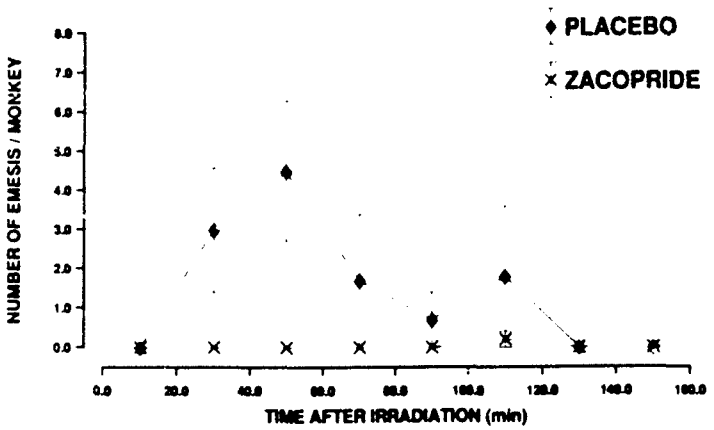

FIG. 3. Effect of zacopride on time course of radiation-induced emesis. Placebo or zacopride was given intragastrically 30 min before irradiation. The number of emeses as determined using a videotape was averaged for each 20-min period. Emesis was defined as a succession of strong and brief contractions of thoracic and abdominal muscles leading to the expulsion of gastric contents through the mouth. Values are means ± SE.

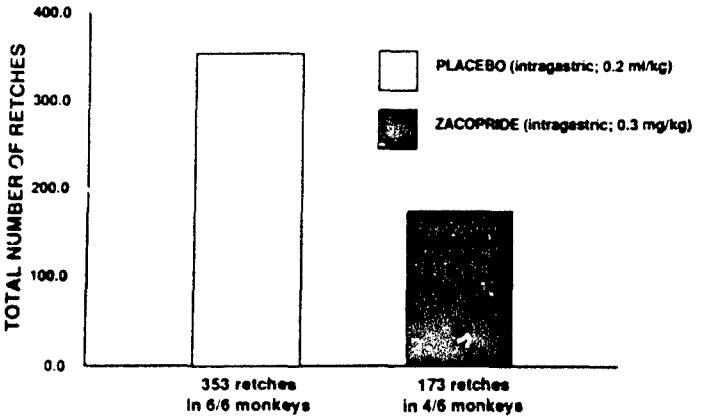

FIG. 4. Effect of zacopride on the number of radiation-induced retches. Placebo or zacopride was given intragastrically 30 min before irradiation, and the number of retches was determined using a videotape. Retching was defined as a nonproductive vomiting.

Following irradiation, 70 emeses were observed in 5 of 6 monkeys after placebo (the 6th monkey experiencing only retching, as described below), compared to only 1 emesis in 1 of 6 monkeys after zacopride (Fig. 2; $P < 0.01$). As illustrated by the time course of emesis following irradiation (Fig. 3), most vomiting occurred during the first hour after placebo, whereas the only vomiting after zacopride was seen at about 2 h. Similarly, 353 retches were observed in 6 of 6 monkeys after placebo compared to 173 retches in 4 of 6 monkeys after zacopride (Fig. 4; $P < 0.01$). In addition,

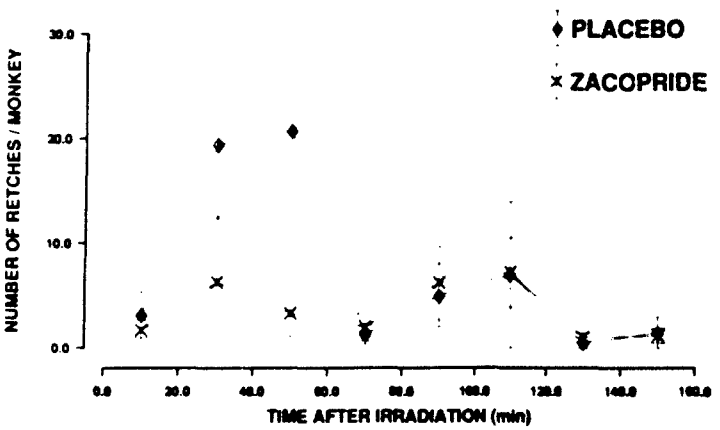

FIG. 5. Effect of zacopride on the time course of radiation-induced retching. Placebo or zacopride was given intragastrically 30 min before irradiation, and the number of retches determined using a videotape was averaged for each 20-min period. Retching was defined as nonproductive vomiting. Values are means + SE.

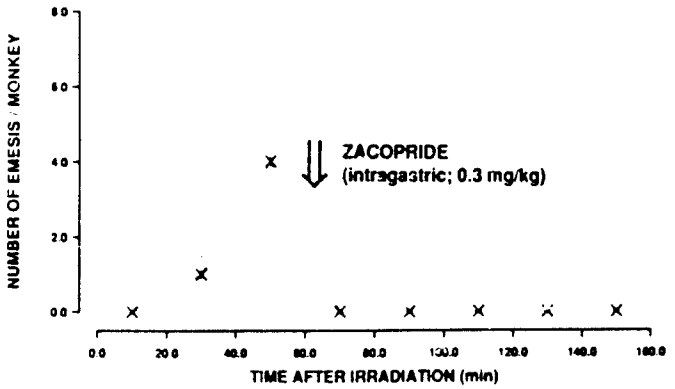

FIG. 6. Effect of zacopride administered after the first emesis on the time course of radiation-induced vomiting. Zacopride was given intragastrically after the first emesis had occurred (i.e., between 50 and 60 min after irradiation) and the number of emeses determined using a videotape was averaged for each 20-min period. Values are means ± SE.

most retching occurred during the first hour after placebo, and zacopride significantly reduced the number of retches during that period, but not during the second hour (Fig. 5). When compared to placebo given before irradiation, administration of zacopride to another group of irradiated monkeys after vomiting had started (i.e., about 30 min after irradiation) significantly inhibited the occurrence of retching and vomiting during the subsequent 100 min of observation (retches: 2 vs 84; emeses: 0 vs 25; $P < 0.05$). The time course of this effect is depicted graphically in Figs. 6 and 7.

Zacopride did not significantly modify fractional gastric emptying (FER) in the control state during fasting or after a water meal (Table 1). After irradiation plus

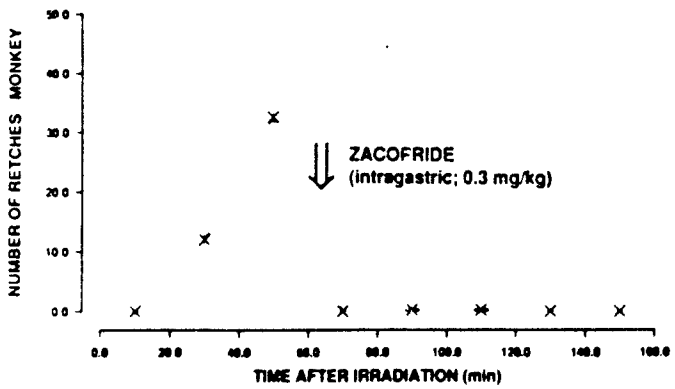

FIG. 7. Effect of zacopride administered after the first emesis on the time course of radiation-induced retching. Zacopride was given intragastrically after the first emesis had occurred (50–60 min after irradiation), and the number of retches determined using a videotape was averaged for each 20-min period. Values are means ± SE.

TABLE I

Effect of Zacopride, Radiation, and a Water Meal on Fractional Emptying Rate (in %/min)

	Control		*Postirradiation*	
	Fasting	*Postmeal*	*Fasting*	*Postmeal*
Placebo	3.42 ± 0.92	4.21 ± 0.64	1.15 ± 0.20*	0.36 ± 0.12*
Zacopride	4.86 ± 0.49	4.37 ± 0.69	2.72 ± 0.84*†	0.66 ± 0.20*†

Note. Values are ±SE.

* $P < 0.05$ compared to control.

† $P < 0.05$ compared to placebo using ANOVA with repeated measures.

placebo, gastric emptying was significantly slowed during fasting and after a meal (Table I; $P < 0.05$), effects which were significantly inhibited by zacopride ($P < 0.05$). However, irradiation still produced significant suppression of both fasting and postmeal FER even after zacopride ($P < 0.05$).

DISCUSSION

In the present studies, we determined the emetic and gastroplegic effects of nonuniform γ irradiation, studied the efficacy of zacopride in the prevention and treatment of radiation-induced vomiting and gastric suppression, and evaluated the potential side effects of this medication in the rhesus monkey.

In the basal nonirradiated state, intragastric administration of zacopride did not induce vomiting, retching, or abnormal behavior. In addition, zacopride did not impair performance on a visual discrimination task, demonstrating that it was not behaviorally toxic for this task. This finding was recently confirmed using a murine motor performance task ((*15*) and unpublished observations). Determining if a new drug has behavioral toxicity is important because this side effect may be as limiting as the adverse effect (emesis) the drug is designed to treat, e.g., in an emergency radiation situation (*16*).

Following irradiation, we determined the precise time course of vomiting and retching as well as the alterations of gastric emptying. Retching and vomiting started about 30 min after irradiation, decreased markedly after 70 min, and disappeared after 120 min. The present 30-min delay differs markedly from previous observations of a delay of almost 1 h after irradiation with doses of 400–550 cGy (*2*) and of a delay of less than 5 min following a dose of 1200 cGy (*17*). Thus, the interval between irradiation and vomiting appears to be inversely proportional to the dose received. In contrast, both the emetic response and the gastric suppression were similar to those observed after total-body irradiation in the same animal model with midtissue doses to the torso and abdomen identical to those used in the present experiments (800 cGy) (*4*). This dose of 800 cGy was selected because it was twice the ED_{50} for vomiting as previously determined by others for monkeys (*2*, *17*). However, due to the exposure system chosen for the present experiments, the head midtissue doses were 30% higher than in our previous studies (*4*), and the tibia and femur midtissue doses

were, respectively, 47% and 27% lower. Taken together, these data suggest that the abdomen and torso are the most important targets for the initiation of the prodromal syndrome.

In the monkey exposed to 800 cGy ^{60}Co, intragastric administration of zacopride 15 min before irradiation prevented radiation-induced vomiting. In addition, zacopride significantly inhibited retching, although the time course of retching appears to have been only minimally altered by zacopride (Fig. 5). Due to the small number of subjects, the difference did not reach a level of statistical significance, but it is probable that the effect shown on Fig. 5 was real. In addition, intragastric administration of zacopride after the first episode completely suppressed retching and vomiting for the subsequent 100 min. Since zacopride did not significantly modify radiation-induced retching and vomiting from 60 to 120 min after exposure, the duration of the antiemetic effect of zacopride in the present model appears to be about 1 h. Similarly, zacopride inhibited the suppression of gastric emptying induced by irradiation during fasting and after the water meal. Thus, after irradiation plus zacopride, gastric emptying was decreased by only 40% during fasting and by 85% after the meal. Since the meal was given about 1 h after zacopride, it appears that the duration of the gastrokinetic effect of the drug, like that of its antiemetic effect, was approximately 1 h. Taken together, these observations suggest that the current formulation of zacopride should be administered twice: once before irradiation and once after exposure. Although the improvement of gastric emptying induced by zacopride using the present frequency and dose of administration is not complete, it markedly improves the possibility of oral rehydration after exposure to radiation. It is most remarkable that zacopride has an antiemetic effect even when given intragastrically after irradiation and that it can actually interrupt radiation-induced vomiting and retching.

The mechanism by which radiation causes emesis and gastric inhibition, as well as the mechanism by which zacopride prevents these effects, remains hypothetical. The central nervous system appears to play a pivotal role in radiation-induced prodromal symptoms, as suggested by the observed rise of plasma β-endorphin following irradiation (*4*). This rise is similar to the one observed after exposure to stress (*18, 19*), which is known to inhibit gastric function (*20*). Thus the rise of plasma β-endorphin may be responsible in part for radiation-induced vomiting and gastric inhibition, since this type of effect has been observed after exogenous administration of opioids (*21*). Irradiation could cause the release of β-endorphin or of another humoral mediator by initially activating the peripheral end of afferent nerves. A direct effect of irradiation on the brain appears unlikely for at least three reasons. First, shielding of the area postrema (chemoreceptor trigger zone) does not prevent radiation-induced vomiting (*22*). Second, increasing the dose delivered to the head by 50% in the present study does not modify significantly the symptoms (*4*). Third, ablation of the area postrema in cats does not prevent radiation-induced vomiting (*23*). Zacopride is a benzamide derivative with gastrokinetic properties which does not protect against emesis caused by apomorphine-induced activation of the dopamine receptors of the area postrema (*24*). However, intravenous (iv) or intracerebroventricular zacopride prevents emesis induced by either iv chemotherapy agent (*25*). Since zacopride is not a dopamine antagonist, it is not neuroleptic and does not cause extrapyramidal, cardiovascular, or autonomic nervous system side effects. Given these facts, it is probable that zacopride

prevents radiation-induced vomiting and retching by acting at a site different than the area postrema, either centrally or at the periphery, but the exact mechanism of action remains to be defined.

In conclusion, we observed that radiation-induced emesis was accompanied by suppression of gastric emptying in monkeys. In addition, intragastric administration of zacopride significantly inhibited radiation-induced retching, vomiting, and suppression of gastric emptying. Although zacopride does not appear to cause detectable adverse behavioral side effects, further studies are needed to confirm this perception. The present observations have important implications in the treatment of radiation sickness and it will be important to determine if they can be confirmed in clinical studies.

ACKNOWLEDGMENTS

We thank Drs. R. S. Alphin and W. Smith, A. H. Robins Co., Richmond, Virginia, for generously supplying the zacopride and placebo. We also thank N. Fleming, M. Flynn, J. Stewart, and J. Warrenfeltz for their valuable support in animal handling and radiopharmaceutical preparation and administration. This research was supported by the Armed Forces Radiobiology Research Institute, Defense Nuclear Agency, under work unit 00059. The opinions and assertions contained herein are those of the authors and should not be construed as official or reflecting the views of the Department of Defense or the Uniformed Services University of Health Sciences or the Defense Nuclear Agency. The experiments reported herein were conducted according to the principles set forth in the *Guide for the Care and Use of Laboratory Animals*, Institute of Animal Resources, National Research Council, DHEW Publ. No. (NIH) 78-23.

RECEIVED: February 8, 1988; REVISED: April 12, 1988

REFERENCES

1. R. A. CONARD. Some effects of ionizing radiation on the physiology of the gastrointestinal tract: A Review. *Radiat. Res.* **5**, 167–188 (1956).
2. G. R. MIDDLETON and R. W. YOUNG. Emesis in monkeys following exposure to ionizing radiation. *Aviat. Space Environ. Med.* **46**, 170–172 (1975).
3. A. DUBOIS, J. P. JACOBUS, M. P. GRISSOM, R. ENG, and J. J. CONKLIN. Altered gastric emptying and prevention of radiation induced vomiting in dogs. *Gastroenterology* **86**, 444–448 (1984).
4. E. D DORVAL, G. P. MUELLER, R. R. ENG, A. DURAKOVIC, J. J. CONKLIN, and A. DUBOIS. Effect of ionizing radiation on gastric secretion and gastric motility in monkeys. *Gastroenterology* **89**, 374–380 (1985).
5. J. R. LACKNER and A. GRAYBIEL. Etiological factors in space motion sickness. *Aviat. Space Environ. Med.* **54**, 675–681 (1983).
6. A. DUBOIS. Aspects of radiation-induced gastrointestinal injury and radioprotection. *Pharmacol. Ther.* **39**, 67–72 (1988).
7. K. SCHUETZE-DEERIEU. Metoclopramide. *Gastroenterology* **77**, 768–779 (1979).
8. J. W. THORPE and R. W. YOUNG. Monkey performance after partial body irradiation. *Aerosp. Med.* **42**, 503–507 (1971).
9. R. I. MONROY, R. R. SKELLY, P. TAYLOR, A. DUBOIS, R. A. DONAHUE, and T. J. MACVITTIE. Recovery from severe hematopoietic suppression using recombinant human granulocyte-macrophage colony stimulating factor. *Exp. Hematol.* **16**, 344–348 (1988).
10. A. DUBOIS, G. H. NATHESON, P. VAN EERDEWEGH, and J. D. GARDNER. Gastric emptying and secretion in the rhesus monkey. *Am. J. Physiol.* **232**, 186–192 (1977).
11. J. M. FINDAY, R. J. PRESCOTT, and W. SIRCUS. Comparative evaluation of water recovery test and fluoroscopic screening in positioning a nasogastric tube during gastric secretory studies. *Br. Med. J.* **4**, 458–461 (1972).

12. J. A. HEDDLE and D. L. DUNLOP, A Method for estimating the rates of gastric secretion and emptying. *Can. J. Med. Sci.* **29**, 83–89 (1951).
13. J. D. GEORGE, New clinical method for measuring the rate of gastric emptying: The double sampling test meal. *Gut* **9**, 237–242 (1968).
14. G. W. SNEDECOR and W. G. COCHRAN, *Statistical Methods*, 5th ed., pp. 87–98. Iowa State Univ. Press, Ames, Iowa, 1980.
15. V. BOGO, T. A. HILL, and R. W. YOUNG, Comparison of accelerod and rotarod sensitivity in detecting ethanol- and acrylamide-induced performance decrement in rats: Review of experimental considerations of rotating rod systems. *Neurotoxicology* **2**, 765–787 (1981).
16. V. BOGO, N. J. JACOBS, and J. F. WEISS, Behavioral toxicity and efficacy of WR2721 as a radioprotectant. *Radiat. Res.* **104**, 182–190 (1985).
17. J. E. MATTSON and M. G. YOCHMOWITZ, Radiation-induced emesis in monkeys. *Radiat. Res.* **82**, 191–199 (1980).
18. R. GUILLEMIN, T. VARGO, J. ROSSIER, S. MINICK, N. LING, C. RIVIER, W. VALE, and F. BLOOM, β-endorphin and adrenocorticotropin are secreted concomitantly by the pituitary gland. *Science* **197**, 1367–1369 (1977).
19. J. ROSSIER, F. FRENCH, C. RIVIER, N. LING, R. GUILLEMIN, and F. BLOOM, Foot-shock induced stress increases β-endorphin in rat blood but not brain. *Nature* **270**, 618–620 (1977).
20. A. DUBOIS and B. H. NATTESON, Habituation of gastric function suppression in monkeys after repeated free-operant avoidance sessions. *Physiol. Psychol.* **6**, 524–528 (1978).
21. P. T. SHEA-DONOHUE, N. ADAMS, J. ARNOLD, and A. DUBOIS, Effects of met-enkephalin and naloxone on gastric emptying and secretion in rhesus monkeys. *Am. J. Physiol.* **245**, G196–G200 (1983).
22. H. I. CHINN and S. C. WANG, Locus of emetic action following irradiation. *Proc. Soc. Exp. Biol. Med.* **85**, 472–477 (1954).
23. H. L. BORISON, L. E. MCCARTHY, E. B. DOUPE, J. JOHNSON, and R. BORISON, Acute radiation-induced vomiting in area postrema-ablated cats. *Radiat. Res.* **109**, 430–439 (1987).
24. R. S. ALPHIN, W. L. SMITH, C. B. JACKSON, D. A. DROPPLEMAN, and L. F. SANCILIO, Zacopride (CERR-11190B), a unique and potent gastrointestinal, prokinetic and antiemetic agent in laboratory animals. *Dig. Dis. Sci.* **33**(10), 482S (1988) [Abstract].
25. W. L. SMITH, L. M. CALLAHAM, and R. S. ALPHIN, The emetic activity of centrally administered cisplatin and its antagonism by zacopride. *J. Pharm. Pharmacol.* **40**, 142–143 (1988).

GASTROENTEROLOGY 1988;95:500–7

Prospects for Management of Gastrointestinal Injury Associated With the Acute Radiation Syndrome

ANDRE DUBOIS and RICHARD I. WALKER
Digestive Diseases Division, Department of Medicine, Uniformed Services University of the Health Sciences and Armed Forces Radiobiology Research Institute, Bethesda, Maryland

The effect of total-body ionizing radiation on the digestive tract is dose-dependent and time-dependent. At low doses (1.5 Gy), one observes only a short prodromal syndrome consisting of nausea, vomiting, and gastric suppression. At doses >6 Gy, the prodromal syndrome is more marked, and it is followed after a 2–5-day remission period by a subacute syndrome, characterized by diarrhea and hematochezia. This gastrointestinal syndrome is superimposed onto a radiation-induced bone marrow suppression. The combination of intestinal and hemopoietic syndromes results in dehydration, anemia, and infection, leading eventually to irreversible shock and death. The treatment of prodromal symptoms is based on the administration of antiemetics and gastrokinetics, although an effective treatment devoid of side effects is not yet available for human therapy. The treatment of the gastrointestinal subacute syndrome remains difficult and unsuccessful after exposure to total body doses >8–10 Gy. Supportive therapy to prevent infection and dehydration may be effective if restoration or repopulation of the intestinal and bone marrow stem cells does occur. In addition, bone marrow transplantation may improve the prospect of treating the hemopoietic syndrome, although the experience gained in Chernobyl suggests that this treatment is difficult to apply in the case of nuclear accidents. Administration of radioprotectants before irradiation decreases damage to healthy cells, while not protecting cancerous tissues. In the future, stimulation of gastrointestinal and hemopoietic progenitor cells may be possible using cell growth regulators, but much remains to be done to improve the treatment of radiation damage to the gastrointestinal tract.

During the past 30 yr, much has been learned about the physiologic mechanisms causing radiation injury, and the recent events in Chernobyl have heightened the general awareness to nuclear hazards. The medical experience in Russia should alert physicians that high-dose total-body radiation injury can occur and we must be prepared to treat such injuries.

The first comprehensive description of the acute radiation syndrome in humans was provided by Hempelmann and colleagues (1) based on the experience they acquired while treating 10 patients involved in two radiation accidents at Los Alamos National Laboratory on August 21, 1945, and on May 21, 1946. These cases pointed out the complexity of the pathophysiology of radiation injury.

In his classic 1956 paper, Quastler (2) hypothesized that total-body irradiation arrests the production of new epithelial cells from the crypts of Lieberkuhn. The diminished replacement of epithelial cells combined with normal sloughing of differentiated cells leads to the depletion of mature intestinal surface epithelial cells. This loss of epithelial cells causes a breakdown of the barrier between the intestinal luminal contents and permits entry of toxic substances into the systemic circulation, which can be lethal. In addition, as discussed by Moore (3), changes of the metabolic balance observed after total-body irradiation may bear similarities with those seen after surgical injury. In both situations, there is an increase in the extracellular component at the expense of intracellular metabolism, increased urinary nitrogen excretion, loss of nitrogen and potassium, and a tendency to retain sodium.

In 1965, Bond and his colleagues (4) reviewed the accumulated human and animal experience; they postulated a disturbance of cellular kinetics in multiple-organ systems that manifested itself in distinct components: the hemopoietic syndrome, the gastro-

0016-5085/88/$3.50

intestinal syndrome, and the cardiovascular or central nervous system syndrome. They also recognized that the acute radiation syndrome is characterized by an acute phase, also called prodromal syndrome, and a subacute phase, also called bone marrow and gastrointestinal syndromes. These two phases of radiation sickness are separated by an apparent remission during which the patient may be completely symptom-free.

Although we recognize that bone marrow depression with its hematologic and immunologic sequelae is of extreme importance and represents a medical problem frequently encountered in irradiated persons, we have elected to review specifically the less commonly considered gastrointestinal component of the acute radiation syndrome. The large amount of information on the pathophysiology of radiation-induced gut dysfunction is summarized along with its implications for current and future therapeutic intervention. The long-term effects of radiation (such as enteropathy, fibrosis, and carcinogenesis) will not be considered here, and the reader is referred to the reviews by Morgenstern et al. (5) and Fry (6).

It must be remembered that the degree of gastrointestinal injury following irradiation will depend upon a variety of conditions. For example, many of the side effects described in this review are not observed after exposure to similar doses during local irradiation or in preparation for bone marrow transplantation. It is not known whether this is entirely due to the low dose rate, to the fractionated irradiation, or to concurrent treatment with antibiotics or bone marrow infusion. Furthermore, neutron radiation is much more destructive to intestinal crypt cells than are similar quantities of γ-photons. Once injury to the gastrointestinal tract has reached sufficient levels to produce symptoms associated with the acute radiation syndrome, mechanisms of organ failure and interventions would be expected to be the same regardless of the circumstances of their origin. Therefore, this review reports primarily data obtained from experiences with photons delivered promptly, as may occur in an accident. However, these findings should be pertinent to any situation in which the total dose received and the dose rate are above a given threshold.

Pathophysiology of Gastrointestinal Injury

Acute Radiation Sickness or Prodromal Syndrome

Immediately after total body irradiation with doses >1.5 Gy, vomiting is frequently observed in all the mammals that can vomit, i.e., cats, dogs, monkeys, and humans, but not in those that cannot, such as rats and mice (7). The median effective dose for vomiting is ~2 Gy for total body exposure to γ-rays; it is believed to be ~2 Gy for neutron irradiation also, although some differences may exist in animals (8). In humans, radiation-induced vomiting is preceded and accompanied by nausea and anorexia (1,4); in animals, hypersalivation, chewing, and yawning are observed, and these symptoms may be considered to be the physiologic equivalents of nausea (9). In addition, gastric emptying, gastric motility, and gastric secretion are temporarily suppressed (10,11). For doses >9 Gy, diarrhea is often observed, and the prognosis is particularly poor if diarrhea is explosive and bloody. These symptoms may be explained by the gross alterations of the myoelectric activity of the small intestine that were observed in dogs exposed to 9.4-Gy abdominal γ-radiation; an initial increase of intestinal motility immediately after exposure was followed by decreased motility 1–4 days later (12).

These symptoms are potentially important from a diagnostic standpoint because they can be used within 1 or 2 h of exposure to qualitatively estimate the dose of radiation received. Similar symptoms are observed after local irradiation, although to a lesser extent. In the case of local irradiation, the threshold for vomiting and diarrhea is lowest for the abdomen, the irradiation of which causes nausea and vomiting after doses greater than about 1.5 Gy (8).

The mediators involved in these early effects of radiation are unknown. Direct or indirect radiation effects on the central nervous system probably play a pivotal role, although areas of the brain that are involved remain ill defined, as is the nature of the neurotransmitters mediating these effects (13). The vomiting center and the vagal nuclei are thought to be necessary, but the precise role of the area postrema is still controversial (14–16). The stimulation of the central nervous centers could result from the radiation-induced release of free radicals, or from other substances such as the endotoxins produced by intestinal microorganisms that have been shown to enter the bloodstream of animals (17) and humans (18) after irradiation. Alternatively, the peripheral afferent nerves could be directly stimulated by these endogenous substances. Whatever initiates the general response of the body, a release of various circulating chemicals (i.e., β-endorphin, histamine, prostaglandins, endotoxins) has been observed after total-body irradiation, but their role in producing the early effects of radiation remains to be defined. β-Endorphin could play a role because endogenous and exogenous opiates are known to cause vomiting (19), to slow gastric emptying, and to suppress gastric acid output (20). The role of histamine in the pathogenesis of the symptoms of the prodromal

syndrome remains unclear and probably involves histamine H_1-receptors; histamine H_2-receptor agonists do not cause vomiting and they stimulate gastric secretion and gastric emptying (21), whereas the opposite is observed after total-body irradiation (11). In contrast, prostaglandins could be candidates as mediators of the observed symptoms because (a) they are released after irradiation (22,23) and (b) their effects are similar to those occurring after total-body irradiation (24,25). Finally, the fact that combined vagotomy and high spinal cord section prevents radiation-induced vomiting (16) suggests that an afferent or efferent nervous mechanism, or both, is involved, although the neurotransmitter mediating this effect has not yet been defined (26). In general, there are no morphologic changes of gastrointestinal smooth muscles or intestinal mucosa during the prodromal syndrome (12), although some alterations of parietal cell ultrastructure have been described (11).

Subacute Gastrointestinal Syndrome

Radiation-induced vomiting usually ceases within 24 h of total-body irradiation, and gastric function is normal 2 days after 8-Gy γ-exposure (11). Patients and animals then experience a relatively symptom-free period that may last 2–7 days, depending on the dose received. If this dose is >5 Gy, a second phase of radiation sickness appears within 1 wk of irradiation. One observes stomatitis, abdominal bloating, gastrointestinal ileus, diarrhea, and guaiac-positive or bloody stools (4) as well as sepsis, dehydration, and shock. This syndrome is characterized by electrolyte imbalance (27,28) and, as shown by metabolic balance studies (3), bears similarities with the situation observed during the postoperative period and after surgical injury.

The cause of these symptoms is complex, and their pathogenesis is still not completely understood. After doses of radiation >2 Gy, the turnover of intestinal cells is decreased, leading to atrophy of the villi (4). In addition, radiation produces alterations of transport in the rabbit ileum as evaluated in vitro with Ussing chambers. Short circuit current, transepithelial potential, and resistance were all increased dose-dependently 1–4 days after total-body exposure to 7.5–12-Gy γ-radiation (29). These changes are similar to those observed after administration of bacterial toxins or secretagogues, and they may be responsible for decreased intestinal absorption of electrolytes, fluids, and nutrients in vivo (30,31).

An intestinal injury with immunologic and physiologic consequences is increased permeability of the epithelial barrier. This concept is consistent with findings of Fine and coworkers (32–34), who detected bacterial endotoxin of intestinal origin in the plasma of animals after a variety of severe trauma episodes. Endotoxin-containing particles in the intestine may penetrate the epithelial barrier via the intercellular route. The incidence of disrupted intercellular tight junctions followed a biphasic pattern similar to that seen for the detection of endotoxin in mouse livers after irradiation (35). This increase in intestinal permeability after irradiation could be due to the action of humoral mediators on this organ. A variety of vasoactive substances have been shown to increase intestinal permeability to endotoxin (36). For example, severe disruption of the tight junction complex was seen in rabbits infused with histamine but not in those animals given saline (37).

Although not always associated directly with mortality, endotoxin may have profound effects on radiation victims. For example, endotoxins may contribute to immunosuppression in the host, but they can also produce subsequent beneficial effects in compromised subjects (38), such as stimulation of bone marrow repair after irradiation (39). Sublethal endotoxemia may be beneficial in other types of trauma as well. For example, Spillert et al. (40) reported that endotoxin decreased burn severity when given to mice immediately after thermal injury. On the other hand, endotoxins released shortly after irradiation of animals (17) or humans (18) may also contribute to early performance decrements associated with radiation.

Endogenous enteric bacteria appear not to play a major role in pure intestinal radiation death described after doses >12 Gy as there was no sepsis or endotoxemia at the time of death in rats with acute intestinal injury (41). Furthermore, preirradiation contamination of the gastrointestinal tract with *Pseudomonas aeruginosa* did not modify survival time of animals dying from pure intestinal syndrome within 3–4 days of irradiation (42). In contrast, postirradiation infection from endogenous enteric bacteria was an important factor after exposure to the lower doses of radiation that cause later death by a combination of intestinal and hemopoietic injuries (42).

Intestinal microorganisms are a major source of infection in irradiated individuals. Changes in the numbers of facultatively anaerobic bacteria, which could become opportunistic pathogens after irradiation, have been monitored in experimental animals (35). Ilea were removed from rats at intervals after sublethal (5 Gy) or lethal (10 Gy) cobalt 60 irradiation and cultured quantitatively for microorganisms. The facultative flora were significantly reduced in numbers 24 h after sublethal irradiation but reached preirradiation levels 7–11 days later. Lethal (10 Gy)

radiation also caused a reduction in numbers of facultative flora at 24 h after irradiation but, in contrast to sublethally irradiated rats, facultative populations began to increase by 7 days postirradiation and were increased several times above normal levels by day 11. This period of excessive colonization of the ileum by facultatively anaerobic flora coincided with the beginning of the time that deaths occurred in rats. Disturbed intestinal microecology has also been seen in other animal models of irradiation injury and has been associated with sepsis and death (35). Changes in the intestinal flora, coupled with impairment of the normal barrier function of the gastrointestinal tract, allow the bowel to serve as a reservoir for pathogens that can enter the portal and systemic circulations and fuel the ongoing septic process. This process may become rapidly overwhelming in a subject further compromised by marrow failure and profound immunosuppression.

In addition, loss of colonization resistance is associated with shifts in microbial populations in compromised individuals. Van der Waaij (43) has shown that opportunistic pathogens in the digestive tract are the major source of infection in animals with decreased defensive capacity. Colonization-resistant anaerobic flora contribute to the control of these facultatively anaerobic pathogens, but when colonization resistance is lost, the opportunistic flora are able to multiply excessively on mucosal surfaces. This event is associated with invasion of normally sterile tissues by endogenous flora. Selective decontamination of the digestive tract with antibiotics that eliminate pathogens but do not disturb anaerobic flora (which maintain colonization resistance) has successfully been used to prevent infection in patients with burns (44) or granulocytopenia (45).

There is a relationship between numbers of intestinal microorganisms and their translocation to mesenteric lymph nodes (46). Increased numbers of bacteria in the lumen of irradiated subjects could cause opportunistic infections through this process. Recent data may help identify the route by which translocation occurs, suggesting that M cells overlying lymphoid follicles of the gastrointestinal tract are part of a major antigen-sampling system (47). Some bacteria can attach to and be transported through these cells, where they should be processed by macrophages and lymphocytes as an initial step in the mucosal immune response. If the normal function of this system is impaired by radiation or other trauma, an easy route of ingress to the body would be provided.

Many organisms colonizing the intestine, including those conferring colonization resistance, are localized in the mucous barrier, a major structure ~450 μm thick overlying the epithelium (48). Any alteration of normal intestinal barrier function could enhance the likelihood of systemic infection as well as permit intestinal contents to damage the epithelial lining. Irradiation may cause a reduction of mucus secretion either through a decrease in the number of goblet cells in the mucosa or through lymphocyte (T cell) loss from radiation exposure (49). Bile secretion could also affect mucus integrity (50). Although the mechanism is unknown, it was recently shown that the continuity of the mucous blanket can be degraded after irradiation (51). Although other physiologic and immunologic changes are probably also involved in influencing postirradiation microbiologic events in the intestine, destruction of the mucous barrier could alter colonization resistance and permit pathogen access to the epithelium.

Alterations of Intestinal Blood Flow and Microcirculation

The role of alterations of intestinal blood flow in the pathophysiology of the acute, subacute, and chronic radiation syndromes remains unclear. Measurements of total small intestinal blood flow in rats exposed to 5-Gy total-body γ-radiation failed to demonstrate consistent changes. In contrast, intestinal blood flow decreased during the first 2 h after exposure to 10 Gy but increased significantly by 4–6 h postirradiation (52–54). In rats exposed to whole-body γ-radiation of either 9 or 10 Gy, Suskevic and Uklonskaya (55) observed marked fluctuations in blood flow in the first hours after irradiation. An initial decrease was followed by a pronounced increase at 6 h postirradiation and then by a sharp decrease from the second to the third day.

Extended observations of postirradiation blood flow to the small intestine showed a continued decrease at 6 and 12 mo after abdominal x-irradiation, with a fractionated (1.91 Gy/day) exposure of 28.71 Gy. However, both the jejunum and ileum showed a blood flow at control level when exposed to only a single dose of 5.74 Gy x-radiation (56). In contrast, blood flow to the large intestine was increased through the 6 mo of postirradiation observation, but began a decline to below control levels by 12 mo postirradiation.

Thus, variations exist according to the species, organs, source of radiation, method of exposure (fractionated or single), technique of blood flow measurement, and time of measurement after irradiation. The response appears to be triphasic after exposure to doses >6 Gy: an initial decrease in blood flow is followed in a few hours by an increase that lasts a few days and, in turn, gives way to a long-lasting decrease in total blood flow.

The microcirculation of the intestine also appears

to be altered after irradiation. Seventy-two hours after exposure to 15-Gy mixed neutron-γ-radiation, the villous capillary network of the dog small intestine appeared histologically intact and continuous, despite mucosal cell destruction, but the intestinal capillary blood flow per gram of mucosa was increased at that time (57). Occlusive endothelial changes were found in the submucosal arterioles of rats 4 days after exposure to 14.6-Gy x-radiation (58). Similarly, clinical evidence of microvascular changes in humans with radiation bowel disease has been furnished by Carr et al. (59). These studies also indicated that alterations were observed in the mucosal vasculature in patients 1–28 mo after radiotherapy. In addition, Suskevic and Uklonskaya (55) observed that permeability increased fourfold in rats 3 days after exposure to whole-body γ-radiation of 9–10 Gy.

In cats exposed to doses of up to 15 Gy, the microvasculature of the intestine was found to be normal 4 days to 4 mo postirradiation (60). However, after exposure to 15–30 Gy, decreased vascularity was observed in all layers of the bowel, including variations in luminal width and obstruction of vessels, which occurred more frequently at the higher doses (60). These vascular changes may be responsible for a decreased capillary filtration coefficient, which has been observed after irradiation. In addition, later experiments provided evidence of ultrastructural changes that correlated with these changes in capillary filtration coefficient, suggesting that the early decrease in this coefficient seen in the groups exposed to 20 and 25 Gy may result from pericapillary fibrosis.

Prospects for Management

Prodromal Syndrome

The prevention and treatment of radiation-induced vomiting can be achieved with neuroleptics (chlorpromazine, promethazine) or even general anesthesia (61). However, this type of approach is not desirable because of the side effects of these medications, which further depress gastric emptying and appetite and may increase the risk of pulmonary infection.

A more promising approach has been the use of antidopaminergic agents. The oldest dopamine antagonist is metoclopramide which, in addition to its antiemetic properties, has a potent gastrokinetic effect and prevents radiation-induced vomiting and gastroplegia in monkeys (62). This gastrokinetic action appears to be independent of its antidopaminergic properties and may be related to a metoclopramide-induced release of acetylcholine and other neuropeptides within the myenteric plexus (63). However, therapeutic doses of metoclopramide do not seem to be effective in humans if given after vomiting has started (64). In addition, this medication may cause extrapyramidal side effects, because it crosses the blood-brain barrier and inhibits striatal dopamine receptors (65). In contrast, the peripheral dopamine antagonist domperidone does not cause central side effects because it inhibits only the dopamine receptors located outside the blood-brain barrier (66) and it prevents radiation-induced vomiting in the dog (10). However, domperidone does not appear to be effective against either radiation-induced gastroplegia or radiation-induced vomiting in the monkey (10,11). In contrast, clinical trials seem to indicate that domperidone may be effective in humans (67), although double-blind placebo-controlled studies will be necessary to confirm this finding.

A number of newer antiemetic and gastrokinetic agents are currently being tested in both animals and patients. Recently, one of these medications (Zacopride, A. H. Robins Co., Richmond, Va.) was found to be effective in the prevention and treatment of the prodromal syndrome (vomiting, retching, and gastric emptying suppression) in monkeys while not causing undesirable side effects (68).

Subacute Radiation Syndrome

The treatment of the subacute gastrointestinal syndrome is based on supportive therapy to prevent infection and dehydration, although ultimate survival depends on bone marrow and intestinal stem cell restoration or repopulation. This therapy includes plasma volume expansion, platelets, and antibiotics, which enhance survival after intestinal injury caused by radiation. With these therapeutic measures, survival may be possible up to 15 Gy, but total-body irradiation above 20 Gy is not manageable. Finally, the prognosis becomes much more serious if irradiation injury is combined with thermal or mechanical injury, as may occur in an accident such as the Chernobyl disaster.

Current research is attempting to prevent the damage to the intestine by using a variety of radioprotectants. These compounds appear to reduce initial damage to stem cells in the crypts and thereby decrease the effect of a given dose of radiation. Under experimental conditions a dose reduction factor can then be calculated to quantitatively evaluate the efficacy of radioprotectants. For example, the thiol derivative group (ethiofos or WR-2721) improves survival of the stem cells of the intestinal crypts in addition to those of the bone marrow and has a dose reduction factor of 1.25–1.60 (31,69). Furthermore, ethiofos enemas in rats demonstrated a

dose reduction factor of 1.8 compared with controls (70). As the compound was not absorbed into the circulation, it appears that ethiofos can exert its radioprotective action by a direct, nonsystemic effect on gastrointestinal mucosa. Recent evidence has also been presented suggesting that the use of prostaglandins alone and especially in combination with WR-2721 could prevent damage to the epithelial cells of intestinal villi, being therefore truly radioprotective and cytoprotective (69).

Stem cell survival in the intestine is a probable event, even if radioprotectants are not used. For this reason, the induction or administration of cell growth regulators after radiation offers future possibilities for enhancement of intestinal recovery. This approach is already being applied to the stem cell compartment of the bone marrow of irradiated subjects (71).

Other methods to promote intestinal recovery may be closer at hand. Postirradiation enteropathy is exacerbated by bile and pancreatic proteases (72,73). Effects of these substances may be enhanced when the mucous barrier is lost after injury (51,74). These problems can be alleviated and cellular recovery enhanced in experimental animals fed elemental diets containing amino acids before irradiation (74–76). Finally, therapeutic effectiveness of elemental diets has also been shown in patients undergoing radiation therapy (77), and numerous other compounds such as micronutrients (e.g., selenium, vitamins A and E) are also currently under study as potential radioprotectants.

Summary

Three types of injury occur in the gastrointestinal tract after radiation. Emesis and gastric suppression are caused by mechanisms still unknown, and have effects that complicate radiotherapy and the treatment of people receiving exposures in accident or weapon detonation scenarios. Sufficient damage to the epithelial barrier and the intestinal microcirculation impairs gastrointestinal function, which can have lethal consequences. The mucosal immune system and the ecology of the colonization resistant flora are also disrupted after radiation exposure. Thus, mortality and morbidity are increased by infectious complications, as well as physiologic failure.

Progress is being made to control the physiologic and immunologic consequences of radiation injury to the gastrointestinal tract. New-generation antiemetics may soon control some debilitating effects of radiation. Furthermore, supportive therapy with fluids and platelets, as well as controlled diets, can now minimize some radiation injury. Radioprotectants, possibly in combination with growth factors that enhance stem cell recovery, may soon be available to prevent or to rapidly repair gastrointestinal damage. Selective decontamination with poorly absorbed antibiotics can now offset some consequences of immune suppression in the intestine and future studies may reveal means to nonspecifically enhance mucosal immunity as systemic immunity can now be stimulated.

References

1. Hempelmann LH, Lisco H, Hoffman JG. The acute radiation syndrome: a study of nine cases and a review of the problem. Ann Intern Med 1952;36:279–510.
2. Quastler H. The nature of intestinal radiation death. Radiat Res 1956;4:303–20.
3. Moore FD. Metabolic care of the surgical patient. Philadelphia: WB Saunders, 1959:921–4.
4. Bond VP, Fliedner TM, Archambeau JO. Mammalian radiation lethality: a disturbance in cellular kinetics. New York: Academic, 1965.
5. Morgenstern L, Thompson R, Friedman NB. The modern enigma of radiation enteropathy: sequelae and solutions. Am J Surg 1977;134:166–72.
6. Fry RJM. Experimental radiation carcinogenesis: What have we learned? Radiat Res 1981;87:224–39.
7. Conard RA. Effect of x-irradiation on intestinal motility in the rat. Am J Physiol 1951;165:375–85.
8. Young RW. Mechanisms and treatment of radiation-induced nausea and vomiting. In: Davis CJ, Lake-Bakaar GV, Grahame-Smith DG, eds. Nausea and vomiting: mechanisms and treatment. Berlin: Springer-Verlag, 1986:94–109.
9. Dubois A, Mueller G, O'Connell L, Durakovic A. Abnormal gastric emptying and prevention of radiation-induced vomiting in primates (abstr). Gastroenterology 1985;88:1370.
10. Dubois A, Jacobus JP, Grissom MP, Eng RR, Conklin JJ. Altered gastric emptying and prevention of radiation-induced vomiting in dogs. Gastroenterology 1984;86:444–8.
11. Dorval ED, Mueller GP, Eng RR, Durakovic A, Conklin JJ, Dubois A. Effect of ionizing radiation on gastric secretion and gastric motility in monkeys. Gastroenterology 1985;89:374–80.
12. Summers RW, Flatt AJ, Prihoda M, Mitros FA. Small intestinal motility in dogs after irradiation injury. Dig Dis Sci 1987;32:1402–10.
13. Borison HL, Borison R, McCarthy LE. Role of the area postrema in vomiting and related functions. Fed Proc 1984; 43:2955–8.
14. Chinn HI, Wang SC. Locus of emetic action following irradiation. Proc Soc Exp Biol Med 1954;85:472–4.
15. Brizzee KR, Neal LM, Williams PM. The chemoreceptor trigger zone for emesis in the monkey. Am J Physiol 1955; 180:659–62.
16. Borison HL. Site of emetic action of x-radiation in the cat. J Comp Neurol 1957;107:439–53.
17. Walker RI, Ledney GD, Galley CB. Aseptic endotoxemia in radiation injury and graft-vs-host disease. Radiat Res 1975; 62:242–9.
18. Maxwell A, Gaffin SL, Wells MT. Radiotherapy, endotoxemia and nausea. Lancet 1986;i:1148–9.
19. Lefebvre RA, Willems JL, Bogaert MG. Gastric relaxation and vomiting by apomorphine, morphine and fentanyl in the conscious dog. Eur J Pharmacol 1981;69:139–45.
20. Shea-Donohue PT, Adams N, Arnold J, Dubois A. Effects of

Met-enkephalin and naloxone on gastric emptying and secretion in rhesus monkeys. Am J Physiol 1983;245:G196–200.
21. Dubois A, Nompleggi D, Myers L, Castell DO. Histamine H_2 receptor stimulation increases gastric emptying (abstr). Gastroenterology 1978;74:1028.
22. Steel LK, Rafferty MA, Wolfe WW, et al. Urinary excretion of cyclic nucleotides, creatinine prostaglandin E_2 and thromboxane B_2 from mice exposed to whole-body irradiation from an enhanced neutron field. Int J Radiat Biol 1986;50:695–715.
23. Dubois A, Dorval ED, Steel L, Fiala N, Conklin JJ. Effect of ionizing radiation on prostaglandins and gastric secretion in rhesus monkeys. Radiat Res 1987;110:289–93.
24. Nompleggi D, Myers L, Castell DO, Dubois A. Effect of a prostaglandin E_2 analog on gastric emptying and secretion in rhesus monkeys. J Pharmacol Exp Ther 1980;212:491–5.
25. Shea-Donohue PT, Myers L, Castell DO, Dubois A. Effect of prostacyclin on gastric emptying and secretion in rhesus monkeys. Gastroenterology 1980;78:1476–9.
26. Carpenter DO, Briggs DB, Knox AP, Strominger NL. Radiation-induced emesis in the dog: effects of lesions and drugs. Radiat Res 1986;108:307–16.
27. Caster WO, Armstrong WD. Electrolyte metabolism after total body x-irradiation. Radiat Res 1956;5:189–204.
28. Gits J, Gerber GB. Electrolyte loss, the main cause of death from the gastrointestinal syndrome? Radiat Res 1973;55:18–28.
29. Gunter-Smith PJ. Gamma radiation affects active electrolyte transport by rabbit ileum: basal Na and Cl transport. Am J Physiol 1986;250:G540–5.
30. Lushbaugh CC, Sutton J, Richmond CR. The question of electrolyte loss in the intestinal death syndrome of radiation damage. Radiat Res 1960;13:814–24.
31. Herrera J, Gage T, Mohaupt T, Vigneulle R, Dubois A. Effects of radiation on intestinal absorption in dogs: protection by WR-2721 (abstr). Gastroenterology 1987;92:1434.
32. Cuevas P, Ishiyama M, Koizumi S, Woodruff P, Kaufman A, Fine J. Role of endotoxemia of intestinal origin in early death from large burns. Surg Gynecol Obstet 1974;138:725–30.
33. Ravin HA, Fine J. Biological implications of intestinal endotoxins. Fed Proc 1962;21:65A.
34. Woodruff PWH, O'Carroll DE, Koizumi S, Fine J. Role of the intestinal flora in major trauma. J Infect Dis 1973;128:290–4.
35. Walker RI, Porvaznik M. Association of bacteria and endotoxin with post trauma events. In: Ninneman J, ed. Immunologic consequences of thermal and traumatic injury. Baltimore: University Park Press, 1983:1–15.
36. Cuevas P, Fine J. Production of fatal endotoxic shock by vasoactive substances. Gastroenterology 1973;64:285–91.
37. Porvaznik M, Baker W, Walker RI. Disruption of the goblet cell intercellular junction following histamine infusion of the rabbit ileum. Experientia 1983;39:514–8.
38. Walker RI. Potential uses of endotoxin in compromised subjects. In: Nowotny A, ed. Beneficial effects of endotoxin. New York: Plenum, 1983:197–212.
39. MacVittie TJ, Walker RI. Endotoxin-induced alterations in canine granulopoiesis: colony-stimulating factor, colony-forming cells in culture, and growth of cells in diffusion chambers. Exp Hematol 1978;6:613–8.
40. Spillert CR, Ghuman SS, McGovern PJ Jr, Lazaro EJ. Effects of endotoxin in murine burns. Adv Shock Res 1981;5:163–6.
41. Geraci JP, Jackson KL, Mariano MS. The intestinal radiation syndrome: sepsis and endotoxin. Radiat Res 1985;101:442–50.
42. Geraci JP, Jackson KL, Mariano MS. Effects of pseudomonas contamination or antibiotic decontamination of the intestine on acute radiation lethality. Radiat Res 1985;104:395–405.
43. Van der Waaij D. The colonization resistance of the digestive tract in experimental animals and its consequences for infection prevention, acquisition of new bacteria and the prevention and spread of bacteria between cage mates. In: van der Waaij D, Verhoef J, eds. New criteria for antimicrobial therapy: maintenance of digestive tract colonization resistance. Amsterdam: Excerpta Medica 1979:43–53.
44. Van Saene HKF, Klasen JJ, Sauer EW. Selective decontamination in burn patients: effects on wound healing. Preliminary results. In: van der Waaij D, Verhoef J, eds. New criteria for antimicrobial therapy: maintenance of digestive tract colonization resistance. Amsterdam: Excerpta Medica 1979:216–22.
45. Mulder NH, Nieweg HO, Sleijfer DT, et al. Infection prevention in granulocytopenic patients by selective decontamination of the digestive tract. In: van der Waaij D, Verhoef J, eds. New criteria for antimicrobial therapy: maintenance of digestive tract colonization resistance. Amsterdam: Excerpta Medica 1979:113–6.
46. Steffen EK, Berg RD. Relationship between cecal population levels of indigenous bacteria and translocation to the mesenteric lymph nodes. Infect Immun 1983;39:1252–9.
47. Sneller MC, Strober W. M cells and host defense. J Infect Dis 1986;154:737–41.
48. Rozee KR, Cooper D, Lam K, Costerton JW. Microbial flora of the mouse ileum mucous layer and epithelial surface. Appl Environ Microbiol 1982;43:1451–63.
49. Lake AM, Bloch KJ, Neutra MR, Walker WA. Intestinal goblet cell mucus release. II. In vivo stimulation by antigen in the immunized rat. J Immunol 1979;122:834–7.
50. Sullivan MF, Hulse EV, Mole RH. The mucus-depleting action of bile in the small intestine of the irradiated rat. Br J Exp Pathol 1965;46:25–44.
51. Walker RI, Brook I, Costerton JW, MacVittie T, Myhal ML. Possible association of mucous blanket integrity with postirradiation colonization resistance. Radiat Res 1985;104:346–57.
52. Delgado G, Butterfield AB, Dritschilo A, et al. Measure of blood flow by the multiple radioactive microsphere technique in radiated gastrointestinal tissue. Am J Clin Oncol 1983;6:463–7.
53. Janossy G. Intestinal blood flow in gastrointestinal irradiation syndrome in the rat. Acta Med Acad Sci Hung 1969;26:13–21.
54. Janossy G. Cardiac output and its distribution in the terminal stage of the gastrointestinal irradiation syndrome ("radiation shock"). Acta Med Acad Sci Hung 1969;26:23–9.
55. Suskevic LN, Uklonskaya LI. Changes in certain functional properties of the vessels of the intestines in whole body gamma irradiation at superlethal doses. Radiobiologiya 1975;15:771–5.
56. Volenec K, Vodicka I, Chmelar V, Brich P, Vavrova E. Changes in regional blood flow at late intervals after single and fractionated x-ray irradiation in rats. Sb Ved Pr Lek Fak Univ Karlovy 1979;22:459–69.
57. Kabal J, Baum SJ, Wyant DE. Canine intestinal vasoactivity during the development of the gastrointestinal radiation syndrome. Radiat Res 1972;50:528–38.
58. Eddy HA, Casarett GW. Intestinal vascular changes in the acute radiation intestinal syndrome. In: Sullivan MF, ed. Gastrointestinal radiation injury. New York: Excerpta Medica 1968:385–95.
59. Carr ND, Pullen BR, Hasleton PS, Scofield PF. Microvascular studies in human radiation bowel disease. Gut 1984;25:448–54.
60. Eriksson B. Microangiographic pattern in the small intestine of the cat after irradiation. Scand J Gastroenterol 1982;17:887–95.
61. Cordts RE. Animal-model studies of radiation-induced

emesis and its control. Technical Report SAM-TR-86-26. San Antonio, Tex.: U.S. Air Force School of Aerospace Medicine, 1982.
62. Dubois A, Danquechin Dorval E, O'Connell L, Durakovic A, Conklin JJ. Treatment of vomiting and of gastric emptying suppression in primates after gamma irradiation. J Nucl Med 1984;25:96A.
63. Crosswell AR, Buyniski JP. Metoclopramide mechanism of action studies in the chemically or field stimulated guinea-pig ileum. Fed Proc 1984;43:3867A.
64. Sokol GH, Greenberg HM, McCarthy S, Sledjeski L, Lyman G. Radiation induced nausea: the comparative efficacy of oral metoclopramide versus prochlorperazine and placebo. A double blind randomized study (abstr). Proc Am Soc Clin Oncol Annu Meet 1986;5:970.
65. Schulze-Delrieu K. Metoclopramide. Gastroenterology 1979; 77:768–79.
66. Laduron PM, Leysen JE. Domperidone, a specific in vitro dopamine antagonist, devoid of in vivo central dopaminergic activity. Biochem Pharmacol 1979;28:2161–5.
67. Bernier J, Huys J. Domperidone in the symptomatic treatment of radiotherapy-induced nausea and vomiting. Postgrad Med J 1979;55(Suppl 1):50–4.
68. Dubois A, Fiala N, Bogo V. Prevention and treatment of the gastric symptoms of radiation sickness. Radiat Res (in press).
69. Hanson WR. Radiation protection of murine intestine by WR-2721, 16-16 dimethyl prostaglandin E_2 and the combination of both agents. Radiat Res 1987;111:361–73.
70. France HG Jr, Jirtle RL, Mansbach CM II. Intracolonic WR 2721 protection of the rat colon from acute radiation injury. Gastroenterology 1986;91:644–50.
71. Monroy RL, Skelly RR, Davis TT, et al. Enhanced hematopoietic recovery after bone marrow transplantation in a monkey model using recombinant human granulocyte-macrophage colony stimulating factor (GM-CSF). Fed Proc 1987;46:1365.
72. Geraci JP, Dunston SG, Jackson KL, Mariano MS, Holeski C, Eaton DL. A reexamination of the role of bile in radiation induced intestinal death in rats. Radiat Res 1987;109:47–57.
73. Morgenstern L, Hiatt N. Injurious effect of pancreatic secretions on postradiation enteropathy. Gastroenterology 1967; 53:923–9.
74. Langlois P, Williams HB, Gurd FN. Effect of an elemental diet on mortality rates and gastrointestinal lesions in experimental burns. J Trauma 1972;12:771–6.
75. Hugon JS, Bounous G. Elemental diet in the management of the intestinal lesions produced by radiation in the mouse. Can J Surg 1972;15:18–26.
76. Mohiuddin M, Kramer S. Therapeutic effect of an elemental diet on proline absorption across the irradiated rat small intestine. Radiat Res 1978;75:660–3.
77. Bounous G. The use of elemental diets during cancer therapy. Anticancer Res 1983;3:299–304.

Received November 12, 1987. Accepted March 7, 1988.

Address requests for reprints to: Andre Dubois, M.D., Ph.D., Department of Medicine, Room A3075, Uniformed Services University of the Health Sciences, Bethesda, Maryland 20814.

The opinions and assertions contained herein are the private ones of the authors and are not to be construed as official policy or as reflecting the views of the Department of Defense.

INT. J. RADIAT. BIOL., 1988, VOL. 54, NO. 4, 545 562

Alterations in phosphate metabolism during cellular recovery of radiation damage in yeast

PATRICIA K. HOLAHAN, STEVEN A. KNIZNER, CAROLINE M. GABRIEL and CHARLES E. SWENBERG†

Radiation Biochemistry Department,
Armed Forces Radiobiology Research Institute,
Bethesda, Maryland 20814-5145, U.S.A.

Received 14 August 1987; revision received 13 April 1988; accepted 14 April 1988.

We have examined alterations in phosphate pools during cellular recovery from radiation damage in intact, wild-type diploid yeast cells using ^{31}P nuclear magnetic resonance (NMR) spectroscopy. Concurrent cell survival analysis was determined following exposure to ^{60}Co γ-radiation. Cells held in citrate-buffered saline (CBS) showed increased survival with increasing time after irradiation (liquid holding recovery, LHR) with no further recovery beyond 48 h. Addition of 100 mmol dm^{-3} glucose to the recovery medium resulted in greater recovery. In the presence of 5 mmol dm^{-3} 2-deoxyglucose (2-DG), LHR was completely inhibited. NMR analyses were done on cells perfused in agarose threads and maintained under conditions similar to those in the survival studies. ATP was observable by NMR only when glucose was present in the recovery medium. In control cells, ATP concentrations increased and plateaued with increasing recovery time. With increasing radiation dose the increase in ATP was of lesser magnitude, and after 2000 Gy no increase was observed. These observations suggest that either the production of ATP in irradiated cells is suppressed or there is enhanced ATP utilization for repair of radiation damage. In CBS with 100 mmol dm^{-3} glucose, a dose-dependent decrease in polyphosphate (polyP) was detectable with no concurrent increase in inorganic phosphate (P_i). In the absence of an external energy source, such as glucose, there was a slight increase in P_i. This suggests that polyP may be used as an alternative energy supply. When 2-DG was present in the recovery medium, polyP decreased, but there was a simultaneous increase in P_i with increasing radiation dose and recovery time. This suggests that the polyP are hydrolyzed as a source of phosphates for repair of radiation damage.

1. Introduction

Phosphorus (^{31}P) nuclear magnetic resonance (NMR) spectroscopy is currently being used to monitor cellular metabolism and energetics both *in vitro* and *in vivo* (Navon *et al.* 1977, Jacobsen and Cohen 1981, Nicolay *et al.* 1983). *In vitro* NMR spectra can be generated from perchloric acid (PCA) extracts obtained from cells (Navon *et al.* 1977). However, this technique involves total disruption of the cells and therefore does not allow dynamic studies of cell metabolism. In addition, PCA extracts permit the observation of only acid-soluble metabolites. *In vivo* NMR spectroscopy can be used to observe major mobile (unbound) metabolites in cells or tissues. Large macromolecules or highly immobilized (bound) molecules will not

† Reprint requests and correspondence should be addressed to: C. E. Swenberg, Department of Radiation Sciences, AFRRI, Building 42, NMCNCR, Bethesda, MD 20814-5145, U.S.A.

generate an observable NMR resonance. Because NMR spectroscopy has an inherent lack of sensitivity it requires the use of a large number of cells for obtaining spectra with a good signal-to-noise ratio. Cells are densely packed, which results in a nonphysiological state and eventual cell death due to the accumulation of toxic metabolites. A technique that overcomes these difficulties and allows large numbers of cells to be maintained in a viable physiological state has been described by Foxall and Cohen (1983). In this method, cells are embedded in an agarose matrix and can be perfused with media or buffers containing nutrients. Diffusion of metabolites through the agarose reaches a very rapid equilibrium (Foxall *et al.* 1984). In this study we have utilized this technique to monitor phosphate metabolism during liquid holding recovery following ionizing irradiation under a variety of conditions for wild-type diploid yeast.

Diploid yeast (*Saccharomyces cerevisiae*) exhibits well-documented recovery from potentially lethal damage (liquid holding or dark recovery) (Patrick *et al.* 1964). In yeast this recovery has been attributed to the repair of double-strand breaks under nongrowth conditions (Frankenberg-Schwager *et al.* 1980). Since it is known that energy is required for recovery from radiation damage (Jain *et al.* 1977) in addition to cell growth and maintenance (Jain *et al.* 1982), this investigation was undertaken to determine if changes in ^{31}P NMR spectra would correlate with cell sensitivity to radiation killing. Repair requires the synthesis of fragments of nucleic acids, production of repair enzymes, and energy, usually in the form of ATP. Polyphosphates, found in yeast, are polymers of orthophosphate (inorganic phosphate) linked with high-energy phosphoanhydride bonds (Yoshida 1955). The chain length of these polyphosphates can vary from several to several hundred phosphate residues (Harold 1966). These polyphosphates can be separated into four fractions: PP_1, PP_2, PP_3, and PP_4 (Harold 1966, Kulaev 1979). PP_3 and PP_4 are the most highly polymerized (mean chain length of 55 and 260 phosphate residues, respectively) and appear to be located near the cell plasma membrane. Due to their length and association with the plasma membrane, these phosphates are probably not detected by NMR spectroscopy. Fractions PP_1 and PP_2 are much less polymerized, having chain lengths of 2–40 orthophosphate residues, and are located throughout the cell, in the cytoplasm, nucleus and vacuoles (Kulaev 1979). The physiological role of polyphosphates is not known, but it has been proposed that they may serve (a) as a store of phosphate bond energy, (b) as a phosphate reserve, and or (c) as direct phosphorylating agents in metabolic pathways (Mudd *et al.* 1958, Nicolay *et al.* 1983, Wood 1966). ^{32}P investigations (see Kulaev 1979) have shown that fraction PP_2 accumulates during nucleic acid biosynthesis whereas fraction PP_1 is used for the biosynthesis of nucleic acids and nucleotide triphosphates. Hence, we have measured the variations in phosphate pools during liquid holding following γ-irradiation in wild-type yeast using NMR spectroscopy. Changes in the cellular metabolism of phosphates were correlated with cellular recovery determined by cell survival experiments.

2. Materials and methods

2.1. *Cell culture and survival assay*

Wild-type diploid yeast cells (obtained from Yeast Genetic Stock Center, Berkeley, CA; *Saccharomyces cerevisiae*, strain X2180XS288C) were cultured in YEPD medium (1 per cent yeast extract, 2 per cent peptone and 2 per cent dextrose; Gibco Laboratories, Inc., Madison, WI). Long-term cultures were maintained at

4 C on agar (2 per cent) plates. For dark recovery experiments, cells were grown to plateau phase in liquid YEPD broth at 30 C for 24–48 h before experiments. Cells for survival analysis were diluted in phosphate-buffered saline (PBS), and irradiated at a cell density of 1×10^6 cells ml. Prior to irradiation, cells were sonicated for 3 s to ensure a single cell suspension. Cell survival was determined by diluting the cell suspension and plating on nutrient YEPD agar. Cells were held on ice to ensure no repair of radiation damage before plating. Agar plates were then incubated at 30 C for 3–4 days to allow colony formation.

Delayed plating experiments were conducted by holding the cells (10^6 cells ml) in PBS in the dark at 20 C for the indicated times before plating on nutrient agar. As before, the cells were incubated at 30 C to allow colony formation after plating. In some experiments, citrate-buffered saline (CBS) was substituted for PBS during the irradiation and recovery periods.

2.2. *Radiation and or chemical treatment*

Bilateral irradiations were performed using a ^{60}Co γ-irradiator (dose rate approximately 52 Gy min). Cells were irradiated at 4 C in a continuously shaken ice-water bath.

For experiments involving chemical treatments the chemicals were present during irradiation and the recovery period. 2-Deoxy-D-glucose was obtained from Sigma Chemical Co. (St Louis, MO). Solutions were prepared in PBS and filtered through a sterile 0·2 μm Nalgene filter on the day of the experiment. Cells were resuspended in PBS containing the chemicals immediately prior to irradiation.

2.3. *Preparation of cells for NMR experiments*

Assignment of resonances in the NMR spectrum was accomplished by use of PCA extracts of cells. Resonances were assigned by comparing chemical shifts to literature values (Salhany *et al.* 1975, Navon *et al.* 1979) by (1) performing pH titrations and observing changes in chemical shifts, (2) adding certain enzymes (e.g. glucose-6-phosphatase) and noting resulting alterations in the spectrum, and (3) 'spiking' the extract by addition of known phosphorylated compounds and noting spectral changes. When obtaining PCA extracts, cells were irradiated at a cell density of 5×10^6 cells ml and then pelleted, washed, and resuspended in 0·9 per cent NaCl. Phosphates were extracted with cold 6 per cent (w v) perchloric acid, then freeze-thawed three times in a dry ice ethanol slurry. The extract was centrifuged and the supernatant, containing acid-soluble phosphates, was neutralized to pH 7·0 by addition of 2 mol dm^{-3} K_2CO_3. Precipitated $KClO_4$ was removed by centrifugation and subsequent filtration of the extract with a 0·2 μm filter. D_2O was added (10 per cent by volume) to the sample solution.

In vivo dark recovery experiments were conducted using 3×10^9 viable cells. The cells were centrifuged and resuspended in a mixture of 0·2 ml 0·9 per cent NaCl and 1·4 ml low-gelling-temperature (lgt) agarose (FMC Corp, Rockland, ME) to a final concentration of 0·9 per cent lgt agarose. The agarose cell mixture was then extruded, under mild pressure, through narrow (0·5 mm i.d.) Teflon tubing in an ice bath into a 12-mm screw-cap NMR tube (Wilmad, Buena, NJ). Cell loss during extrusion was < 10 per cent. The 'spaghetti-like' agarose threads settled at the bottom of the tube in such a way that all cells were within the radiofrequency transmitter receiver region of the NMR probe. A hollow Kel-F insert was situated in the NMR tube, allowing the continuous perfusion of the cells

during irradiation and acquisition of spectra. Control spectra were acquired before irradiation of cells in the perfusion apparatus.

2.4. *NMR spectroscopy*

^{31}P NMR spectra were acquired at 80·98 MHz with a sweep width of ± 2500 Hz using a Nicolet NT-200 wide-bore NMR with a Nicolet 12-mm tunable probe. When deuterium was not present (for *in vivo* preparations), the shimming of field homogeneity was achieved by optimizing the water free induction decay signal through the ^{1}H decoupler channel. For spectra obtained on PCA extracts, a one-pulse sequence consisting of a 70° pulse (20 μs), repeated every 2·2 s, was signal-averaged for 1000 to 5000 acquisitions. Spectra of perfused cells were also generated using a one-pulse sequence, with a 70° pulse and 200-ms delay, and signal-averaged for 1476 acquisitions. Total acquisition time was 15 min per spectrum, and four spectra were added so that the final spectra represent the average concentrations over a 1 h time interval. Resonance areas were obtained by computer integration using standard Nicolet software and are accurate to ± 10 per cent.

3. Results

When diploid yeast cells were held in phosphate-buffered saline (PBS) following irradiation, there was increased survival with increasing time (figure 1A). This phenomenon has been described as liquid holding or dark recovery and is evidenced by an increased shoulder, D_q (Hall 1987), of the survival curve (table 1). No further recovery was observed beyond 48 h of liquid holding time. Cells held in citrate-buffered saline (CBS) exhibited similar recovery as for cells held in PBS (data not

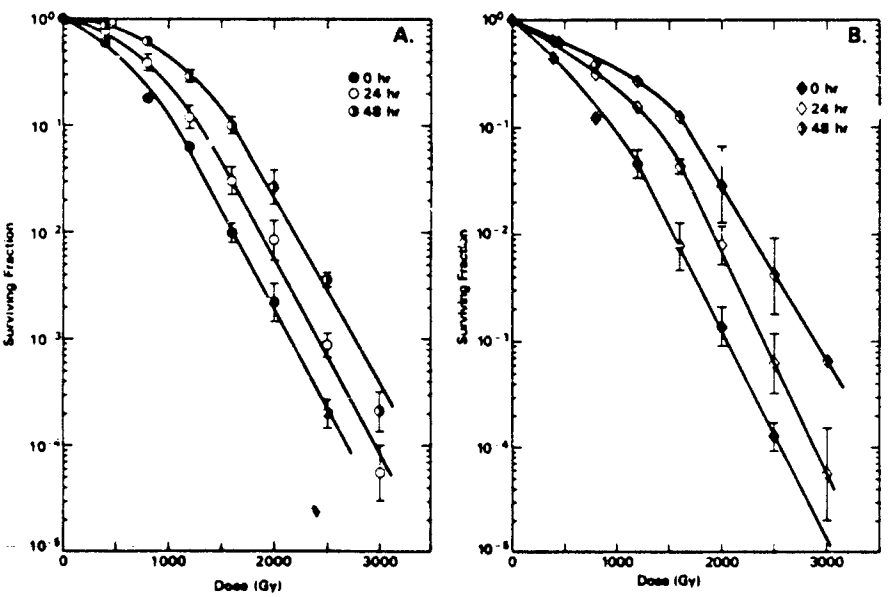

Figure 1. Delayed plating (liquid holding recovery) for wild-type yeast. Cells were irradiated and incubated for 0 (●, ◆), 24 (○, ◇), or 48 (◗, ◗) h in (A) PBS only or (B) PBS with 100 mol dm^{-3} glucose.

Table 1. Recovery of wild-type yeast cells during liquid holding recovery in PBS with or without glucose or 2-deoxyglucose.

	Time after irradiation (h)									
	0		24				48			
	D_0^a	D_q^a	D_0	D_q	RR_1^b	RR_2^b	D_0	D_q	RR_1	RR_2
PBS	250	525	250	760	1·23	1·12	250	1025	1·57	1·29
PBS + 100 mmol dm^{-3} glucose	225	520	225	850	1·43	1·19	225	1050	1·73	1·41
PBS + 5 mmol dm^{-3} 2-deoxy-D-glucose	260	370	230	250	0·90	0·88	230	250	0·90	0·88

[a] D_0, D_q are in units of Gy.

[b] Recovery ratio, defined as dose for delayed plating divided by dose for immediate plating for isosurvival. RR_1, 10^{-1} isosurvival; RR_2, 10^{-2} isosurvival.

shown). When 100 mol dm^{-3} glucose is present in the recovery medium, the shoulder of the survival curve increases more rapidly with no effect on the slope (figure 1 B). Recovery was expressed as the recovery ratio, defined as the dose of radiation after delayed plating divided by the dose after immediate plating to obtain an isosurvival, e.g. 10^{-1} (table 1). This ratio demonstrates that there is greater recovery when glucose is present in the holding medium.

In figure 2, representative NMR spectra of both *in vivo* and *in vitro* preparations of cells are shown. This figure shows the effects of radiation at 2000 Gy on the *in vivo* cell suspension perfused with CBS in the presence of 100 mmol dm^{-3} glucose, for both immediate and 24-h liquid holding time on the NMR spectra. Only in the presence of glucose are the ATP resonances easily resolvable for *in vivo* preparations (peaks 3, 4, and 8). PCA extracts of unirradiated cells were used for the identification of resonance signals. The changes in NMR observable phosphates in PCA extracts of yeast (acid-soluble phosphates) were determined as a function of dose (figure 3). The data are plotted as a percentage of unirradiated controls; the area under each NMR resonance signal was taken to be proportional to the amount of phosphate present. All observable phosphate metabolite concentrations increased with increasing dose. In particular, the sugar phosphates (SP) increased two-fold after 500–2000 Gy, although at higher doses the increase was not as dramatic. The levels of middle phosphates (MP) of long-chain polyphosphates and the α, β, and γ phosphates of ATP also were increased. Only the β-ATP resonance yielded a true indication of ATP levels, since the α and γ resonances also contained contributions from α and β ADP phosphates, respectively. The γ-ATP resonance (bottom panel) overlaps the resonance from the end phosphates (EP) of long-chain polyphosphates. We tentatively attribute this increase in all phosphates with increasing dose to be the radiation-induced disruption of bound intracellular phosphate molecules, which enables more complete extraction of phosphates by PCA.

In vivo ^{31}P NMR spectra were acquired for cells perfused with oxygenated CBS during liquid holding recovery for 24 h following irradiation. NMR spectra were acquired on cells embedded in agarose threads before irradiation as internal controls. The area under each resonance peak was determined relative to the area

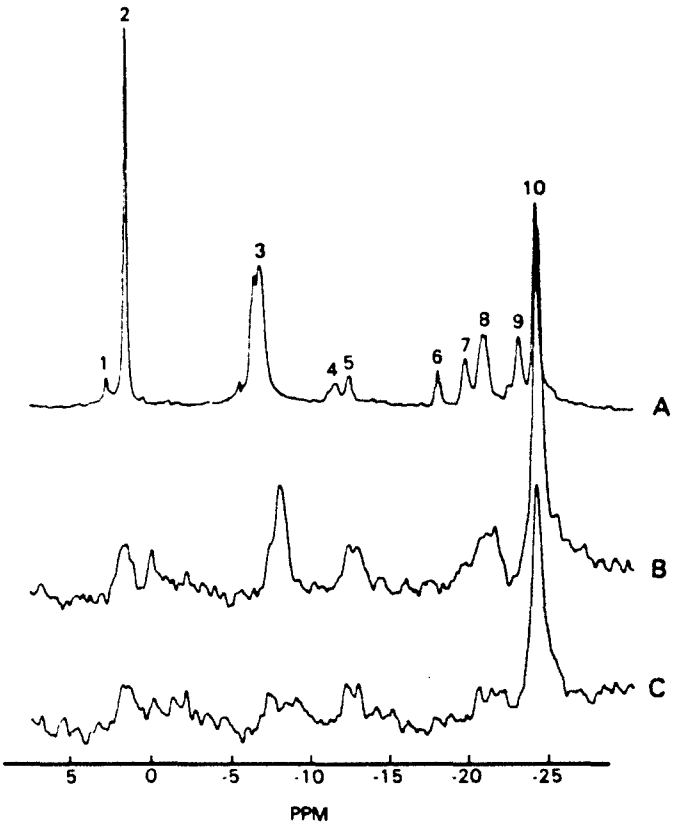

Figure 2. NMR spectra of yeast before and after irradiation. Upper spectrum (A) represents PCA extracts of unirradiated cells used for identification of resonances: (1) sugar phosphates (SP), (2) inorganic phosphate (P_i), (3) end phosphates of polyphosphates and γ-ATP, (4) α-ATP, (5) NAD^+, (6 10) penultimate and middle phosphates of polyphates of polyphosphates. β-ATP also contributes to resonance 8. Remaining spectra are for intact cells in agarose threads. The lower two spectra are from cells that received 2000 Gy and then perfused with PBS containing 100 mmol dm^{-3} glucose for 0 (B) or 24 h (C), during which time dark recovery occurred.

under the initial total spectrum for unirradiated controls. The total NMR observable phosphates (total area of the integrated spectrum) varied during the liquid holding period. Therefore, each integrated area was corrected for the change in total area. These values were then related to the peak area of the preirradiated spectrum. In the presence of PBS there is a large narrow resonance attributable to extracellular P_i. Therefore, in order to observe the NMR resonance associated with intracellular P_i, experiments were conducted with cells perfused with CBS.

For cells irradiated and held in CBS for NMR analysis during liquid holding recovery, the total NMR observable phosphates remained relatively constant (figure 4A). The middle phosphates of long-chain polyphosphates (polyP) remained nearly constant for 24 h in the absence of radiation, with some evidence of periodic variation (figure 4B). There was an initial 20 per cent decrease in in-

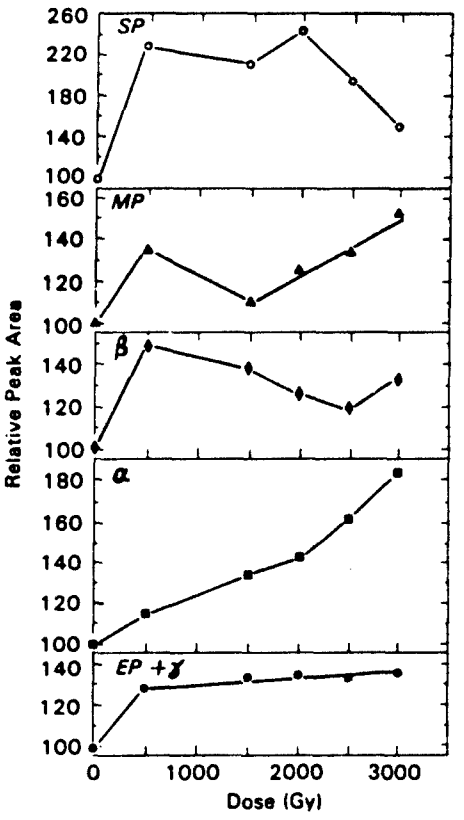

Figure 3. NMR phosphate levels for PCA extracts of yeast as a function of dose. SP, sugar phosphates; MP, middle phosphates of long-chain polyphosphates; β, β-phosphate of ATP; α, α-phosphate of ATP; EP + γ, end phosphates of polyphosphates and γ-phosphate of ATP. See text for details.

organic phosphate, which returned to initial levels 20 h after perfusion was begun (figure 4C). PolyP levels also remained constant following 500 Gy. Following 1000 Gy there was increased utilization of polyP (20 per cent decrease in middle phosphates after 24 h). For both 500 and 1000 Gy, P_i showed an initial decrease and then began to increase 4 h after irradiation. P_i levels were 40 per cent greater than for unirradiated cells at 24 h after irradiation, and appeared to be increasing further.

When 100 mmol dm^{-3} glucose is present in the recovery medium, total phosphate levels increased slightly during the first 16 h for control cells and then returned to baseline levels after 24 h of perfusion (figure 5A). Following 500 Gy, total phosphates increased over the first 6 h after irradiation and then appeared to undergo fluctuations with approximately a 6 h periodicity. At higher radiation doses there is an average continuous decrease (25 per cent over 24 h) with increasing time. However, the periodicity observed for the control and 500 Gy data appears more pronounced. There is a gradual decrease in the middle phosphates of long-chain polyphosphates with increasing time after irradiation (figure 5B), which is more pronounced in the presence of radiation. Control cells showed an initial slight

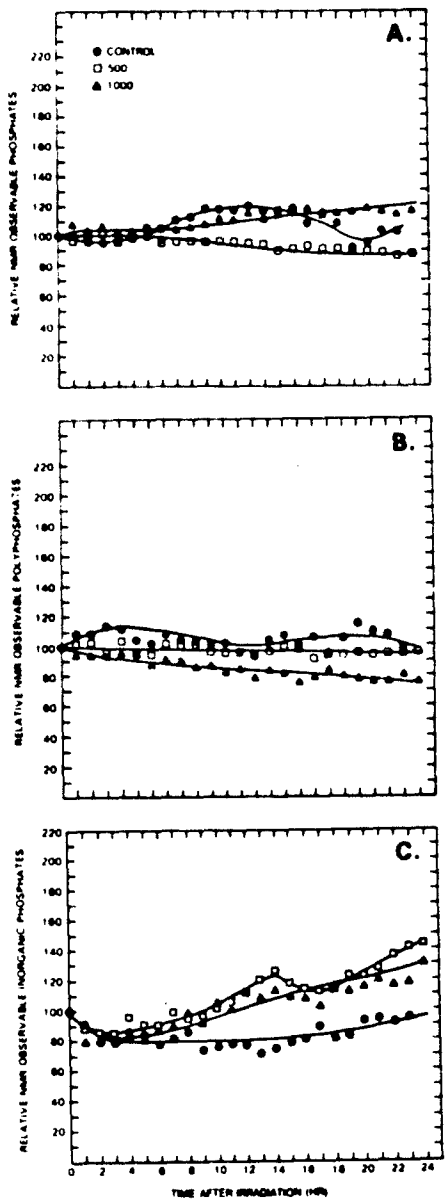

Figure 4. Changes in (A) total NMR observable phosphates, (B) middle phosphates of long-chain polyphosphates (MP), and (C) inorganic phosphate (P_i) during liquid holding recovery of cells perfused with CBS as determined by ^{31}P NMR spectroscopy. Amounts of MP and P_i are corrected for any change in total amount of phosphates. All values are determined relative to preirradiation value. Cells received 0 (●), 500 (□), or 1000 (▲) Gy.

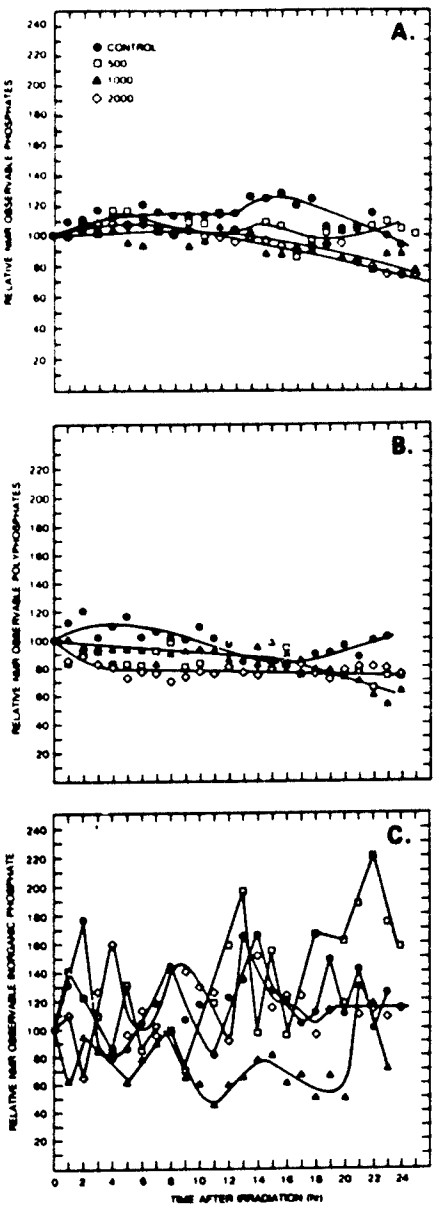

Figure 5. Changes in (A) total NMR observable phosphates, (B) middle phosphates of long-chain polyphosphates (MP), and (C) inorganic phosphate (P_i) during liquid holding recovery of cells perfused with CBS and 100 mmol dm^{-3} glucose as determined by ^{31}P NMR spectroscopy. All values are determined as described in figure 5. Cells received 0 (●), 500 (□), 1000 (▲), or 2000 (◇) Gy.

increase in polyP followed by a gradual decline. However, after 24 h of perfusion, there was no relative change in polyP compared to its initial value. The inorganic phosphate levels showed a very dramatic variation (figure 5C). In the presence of glucose, P_i was present at very low concentrations (< 5 per cent of the total NMR spectra) whereas in the absence of glucose the contribution of P_i to the total spectra was on the order of 25 per cent. There was a periodicity in the amount of P_i with a period of approximately 8 h and this showed a maximum fluctuation of 60 per cent at all doses. This was also observed in the irradiated cells. Due to the small contribution of P_i to the total spectra, the error associated with the determination of its relative area is much larger than with the other resonances. Because of this, we interpreted the data to show that overall there was little change in P_i levels during the recovery period.

In the presence of a glucose analogue, 2-deoxyglucose (2-DG), glycolysis is inhibited. For cells held in recovery medium containing 5 mmol dm^{-3} 2-DG, liquid holding recovery is inhibited (figure 6). There is slightly increased cell killing in the presence of 2-DG, indicating some toxicity. This is also evidenced by the recovery ratio given in table 1. The total NMR observable phosphates decreased for

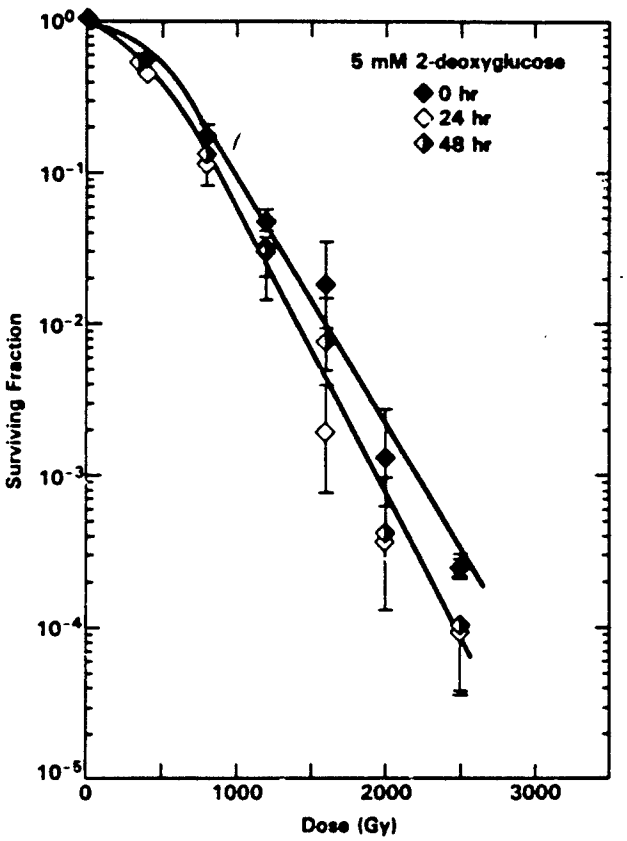

Figure 6. Immediate and delayed plating of wild-type yeast in presence of a glucose analogue, 5 mmol dm^{-3} 2-deoxyglucose (2-DG). Cells were irradiated and held in PBS containing 2-DG for 0 (◆), 24 (◇), and 48 (◑) h.

control cells but increased following 1000 Gy (figure 7A). After 2000 Gy there appear to be fluctuations on the order of 20 per cent with an 8 h periodicity. However, in another control experiment the total phosphates showed an initial increase and then declined. In all experiments with 1000 Gy, total phosphates either remained constant or increased. NMR analysis shows a decrease in the middle phosphates of long-chain polyphosphates (polyP) even in the absence of radiation (figure 7B). This decrease did not correlate with increasing radiation dose. The data shown for 1000 Gy are representative of several experiments, although in some experiments the decrease in polyP was more pronounced. Although in the presence of glucose there was no overall increase in inorganic phosphates (P_i) as a function of time, the presence of 2-deoxyglucose in the recovery medium resulted in a concomitant increase in P_i with decreasing polyP (figure 7C). The most dramatic change in both polyP and P_i was seen following 2000 Gy. Although not shown here, the NMR spectrum displays a very prominent peak associated with 2-deoxyglucose-6-phosphate. It accounts for approximately 25 per cent (determined by ratio of areas) of all observable phosphates by the end of the experiment.

Furthermore, in the presence of glucose it is possible to observe ATP resonances that are beneath the level of detection by NMR in the absence of glucose. The relative amount of ATP was determined from the area of the ^{31}P resonance signal of β-ATP relative to the total amount of NMR observable phosphates (figure 8). There are difficulties in assigning the area under resonance No. 8 (see figure 2) to the ATP content of the cell since PP also contributes to this peak. Judging by PCA extracts β-ATP contributes (to resonance No. 8) approximately 30–35 per cent; however, direct comparison to *in vivo* data is difficult since extractability of ATP and polyphosphates could differ. In our discussion we assume that any variation in resonance No. 8 area is due to changes in ATP. Cells held in CBS containing 100 mmol dm^{-3} glucose with no radiation showed almost a three-fold increase in ATP levels, which plateaued after 8 h of liquid holding. Following irradiation there was less of an increase in ATP levels so that, with 2000 Gy, β-ATP levels remained constant. In cells exposed to 500 Gy there was an initial decrease in the first 4 h followed by an increase, which plateaued after 14 h. With 1000 Gy, ATP levels increased over the first 12 h and then decreased back to preirradiation levels. Cells that received 2000 Gy showed no change in ATP levels during 24 h of liquid holding after an initial decrease in the first 2 h following irradiation.

4. Discussion

The present investigation was undertaken to examine the relationship between high-energy phosphates and the recovery from potentially lethal radiation damage in yeast. Liquid holding recovery in yeast has been shown to be altered by a variety of agents that modify the energy supply, such as 2-deoxyglucose, potassium cyanide, and 2,4-dinitrophenol (Patrick and Haynes 1964, Jain *et al.* 1977). Furthermore, if energy production is inhibited prior to irradiation, there is a reduced capacity for cell survival (Seymour *et al.* 1985). In this study the addition of glucose to the extracellular medium resulted in greater recovery, as demonstrated by a larger recovery ratio (see table 1). In contrast, there was no recovery observed in the presence of 2-deoxyglucose, and there was a reduction of the shoulder of the survival curve (D_q). This decrease in D_q has been attributed to a decrease in the intracellular ATP concentration (Reinhard and Pohlit 1976).

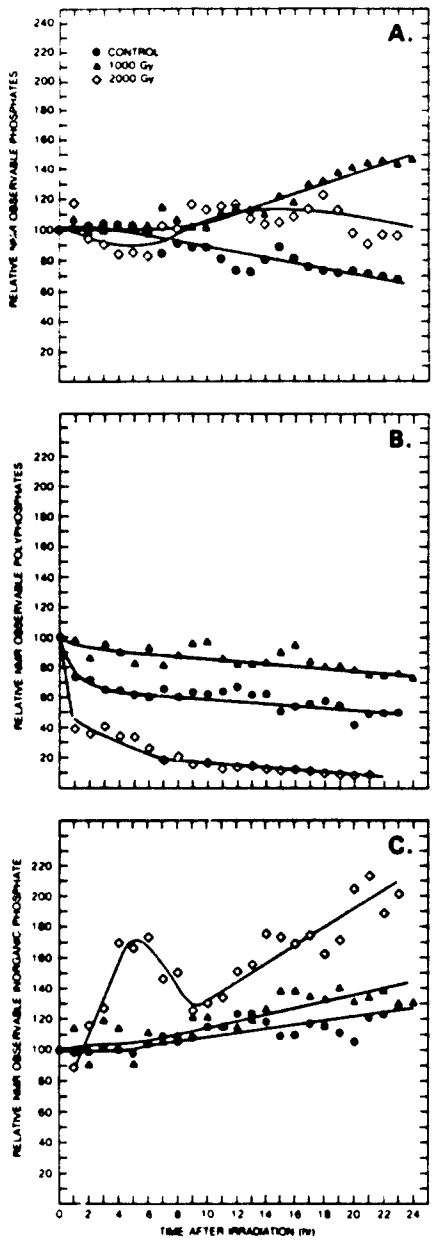

Figure 7. Changes in (A) total NMR observable phosphates, (B) middle phosphates of long-chain polyphosphates (MP), and (C) inorganic phosphate (P_i) during liquid holding recovery of cells perfused with saline and 5 mmol dm^{-3} deoxyglucose as determined by ^{31}P NMR spectroscopy. All values are determined as described in figure 5. Cells received 0 (●), 1000 (▲), or 2000 (◇) Gy.

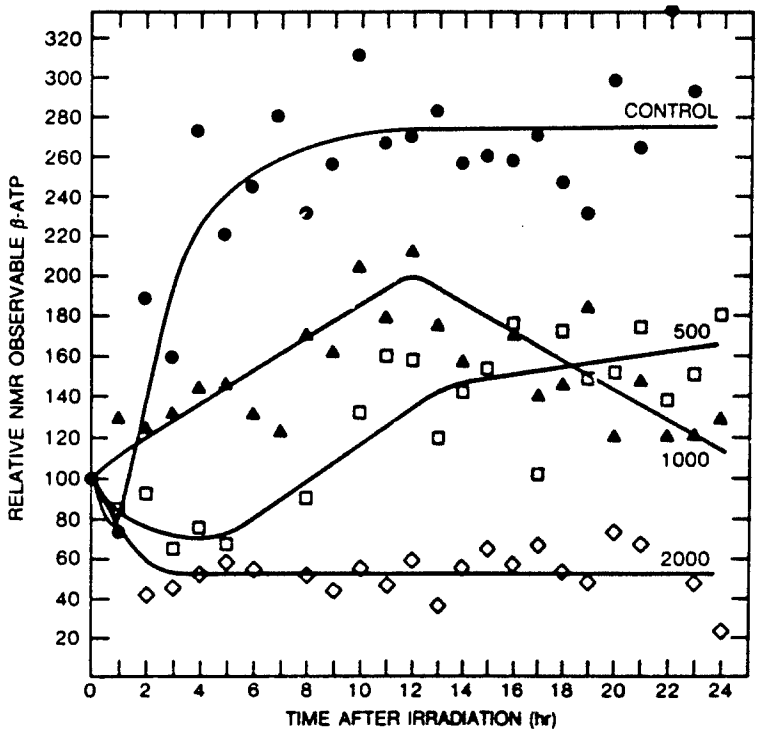

Figure 8. Changes in ATP levels during delayed plating recovery. Amount of ATP was determined from area of the ^{31}P resonance signal of β-ATP relative to total amount of NMR observable phosphates. Cells were irradiated and perfused with CBS containing 100 mmol dm^{-3} glucose. Cells received 0 (●), 500 (□), 1000 (▲), or 2000 (◇) Gy.

For cells perfused with CBS there was both a time- and dose-dependent decrease in polyphosphates. The polyP levels for control cells perfused with CBS displayed a periodicity, with levels increasing to approximately 20 per cent higher than baseline. A possible rationale for this temporal periodicity is that cells could be using the extracellular citrate (after it is transported into the intracellular medium) as a precursor for energy production with the subsequent synthesis of RNA. As has been shown by Kulaev (1979), the PP_2 fraction is synthesized concurrently with nucleic acid biosynthesis. It is hypothesized that these intracellular metabolic cycles have intrinsic cycling times which we tentatively associate with the observed NMR polyP periodicity. For irradiated cells the complex time-dependence of polyP, as measured by NMR spectroscopy, could be interpreted as resulting from interplay between PP_1 and PP_2 contributions to the NMR polyP resonance. As noted above, evidence has been reported suggesting that PP_1 is utilized for the synthesis of nucleic acids and nucleotide triphosphates (Mudd *et al.* 1958, Kulaev 1979). Thus, our irradiated data (at least for doses of 500 and 1000 Gy which showed decreases in polyP with increasing time) suggest that PP_1 is consumed at a greater rate than is the production of PP_2. However, this interpretation assumes that the contribution to the polyP resonance per phosphate is the same for both PP_1 and PP_2 fractions.

When glucose was added to the recovery medium there was again both a time- and dose-dependent decrease in the middle phosphates of the long-chain polyphosphates. The absence of a concurrent increase in P_i suggests the following explanations for this decrease: (a) polyP are being used for the direct phosphorylation of glucose, (b) polyP are being used as a source of phosphates in the repair of DNA damage, or (c) polyP are being used in the synthesis of RNAs which may code for synthesis of repair enzymes. Evidence that the direct phosphorylation of glucose is not the sole explanation comes from our data on phosphate metabolism in the presence of 2-deoxyglucose, a glucose analogue that results in the inhibition of glycolysis. In the NMR analysis of cells irradiated and held in recovery medium containing 2-DG, there was a decrease in the middle phosphates of the long-chain polyphosphates. However, unlike cells that were held in glucose-containing recovery medium, there was a corresponding increase in P_i (figures 5C and 7C). This increase in P_i was also greater than that observed with CBS alone and, in fact, did not show the initial 20 per cent decrease. If polyP were being used solely for glucose phosphorylation, they would be used in the presence of both glucose and 2-deoxyglucose to form glucose-6-phosphate and 2-deoxyglucose-6-phosphate, respectively. In some lower species, polyphosphates can directly phosphorylate glucose with the enzyme polyphosphate glucokinase, but this enzyme has not been identified in yeast (Kulaev 1979). However, it does appear that polyphosphate is used to phosphorylate glucose, although it may be an indirect reaction as chemical energy of polyP bonds do not appear to be directly available to the cells (van Stevenick 1968). PolyP may indirectly phosphorylate ADP or a carrier or enzyme that can mediate the transport of glucose into the cell (van Stevenick 1968). The inorganic phosphate would therefore be expected to show similar changes in both glucose and 2-deoxyglucose, a conclusion not supported by the data reported in figures 5 and 7. Therefore, polyP must be utilized as a phosphate source for more than glucose. Our experimental evidence supporting explanations (b) and (c) as also being viable possibilities is reflected in the changes in P_i. The increase in P_i during recovery in the presence of 2-deoxyglucose suggests that polyP are also being used as a phosphate source for DNA repair and/or RNA synthesis. Polyphosphates decrease during DNA synthesis in the absence of extracellular P_i, suggesting that polyP are being used as a substitute phosphate source (Gillies *et al.* 1981). mRNA synthesis has been shown to increase significantly following irradiation, although there was inhibition of protein synthesis (Skog *et al.* 1985). Therefore, although there may be no increase in total repair enzymes, there are still increased nucleic acid synthesis and repair, which require phosphate. This interaction between polyphosphates and other intracellular macromolecules is illustrated in figure 9. This is a modification of a hypothetical scheme outlined by Kulaev (1979) for high molecular weight polyphosphates in fungi. In this scheme we note the interdependencies exhibited by polyphosphates, nucleotide triphosphates, nucleic acid biosynthesis, and ATP.

The observation that the inhibition of recovery is greater in respiratory-deficient mutants than wild-type yeast (Jain *et al.* 1982) suggests that energy is still supplied by the respiratory pathway. Furthermore, it has been shown that when 2-deoxyglucose is present in the recovery medium, both DNA repair and recovery from potentially lethal radiation damage are reduced (Jain *et al.* 1977, Verma *et al.* 1982). From these investigations the authors concluded that DNA repair depends on ATP. Our data indicated that, in the presence of glucose, ATP concentrations are increased, which is supported by the work of Reinhard and Pohlit (1976). ATP

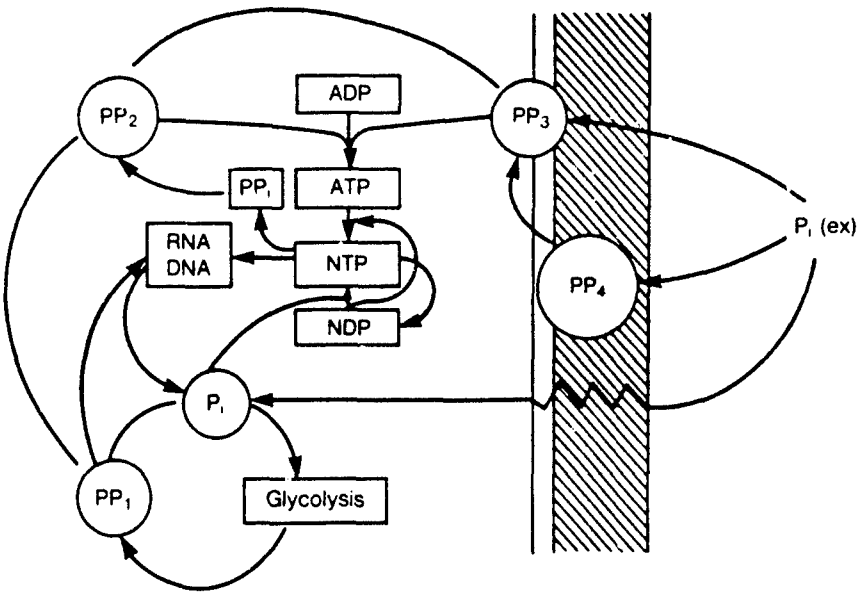

Figure 9. Modification of hypothetical scheme for metabolism of polyphosphates as outlined by Kulaev (1979).

has been shown to be required for the repair of DNA and cellular recovery from radiation damage (Matsudaira *et al.* 1970, Verma *et al.* 1982). In the absence of radiation there is a three-fold increase in ATP during holding time in CBS with glucose. We attribute this increase to the enhanced production of ATP from glycolysis, driven by energy requirements for cell maintenance of protein synthesis and active transport. In addition, even though cells are held in nongrowth medium, there are changes in the number of cells in different phases of the cell cycle. Hence, some of this increase in ATP in the absence of radiation could be attributed to cell cycle variations since it has been shown that ATP doubles through the cell cycle (Skog *et al.* 1982). In the presence of ionizing radiation there is an additional requirement of ATP for cellular repair (Jain *et al.* 1982). The decrease in ATP levels at long holding times for the higher radiation doses suggest that ATP is being used as rapidly as it is produced for the repair of DNA damage. Furthermore, radiation and liquid holding delay cell progression, so that ATP variations through the cell cycle may not be seen. Our results for ATP, reported in figure 8, are similar to data given by Szeinfeld and Blekkenhorst (1987) for transplantable CaNT mouse tumor cells. These authors noted that ATP levels initially increase with time following X-irradiation and then return to control values by 13 h postirradiation. At higher doses, the initial increase in ATP is much less pronounced; this result is consistent with our data, which showed that after 2000 Gy the ATP level actually decreased and then remained constant with increasing holding time. Skog and co-workers (1986) also observed a decrease in ATP following irradiation of Ehrlich ascites tumor cells, but in this case the decrease is related to a lack of substrate for glycolysis rather than increased ATP consumption. Furthermore, these authors showed that a reduction in ATP levels had no effect on radiation-induced changes in cell cycle progression (Skog *et al.* 1983).

In addition, polyP may also be used as an energy source if the ATP concentration is low. Polyphosphate can be used to phosphorylate ADP to form ATP via a reversible reaction catalyzed by polyphosphate kinase (Kulaev 1979). When no glucose was present as an energy source, P_i increased as polyP decreased (figure 4), suggesting that polyphosphates were being used as a supplemental energy source in addition to a source of phosphates. In the presence of an external source of energy (i.e. glucose), the cell was able to synthesize and use ATP; hence polyP was used primarily as a phosphate source. Since ATP was depleted in the presence of 2-deoxyglucose there is a possibility that polyP may be used to provide some energy. However, the cell may not be able to obtain sufficient energy solely from polyphosphate degradation to allow for repair. It appears that yeasts are able to hydrolyze polyP in the presence of 2-deoxyglucose but are unable to utilize either the free phosphates for phosphorylation or the energy release for damage repair.

In conclusion, we note that there are limitations to cellular NMR spectroscopy that should be considered in the discussion of measured phosphate levels. NMR spectroscopy is unable to determine absolute concentrations of a particular phosphate because there could be changes in the balance between immobile and mobile populations of phosphates. If phosphates become bound following radiation, this would also give the appearance of a decrease in phosphate levels. However, because inorganic phosphate increases with the decrease in polyphosphates, it appears that polyP are being hydrolyzed rather than becoming bound. Furthermore, the technique does not distinguish possible differences between irradiated cells committed to full recovery (viable cells) and those destined for reproductive cell death. Thus it remains to be determined if recovery of polyphosphates occurs in viable cells.

Acknowledgements

The authors appreciate the technical assistance of Ms Andrea Lunsford and Ms Colleen Loss in performing the numerous cell survival experiments, and acknowledge the help of Drs Chiwan Chen and Jack Cohen (NIH) for informing and teaching us the technique for viable cell preparation for NMR experiments. We also thank Dr Eric Holwitt for many helpful discussions.

References

Foxall, D. L., and Cohen, J. S., 1983, NMR studies of perfused cells. *Journal of Magnetic Resonance*, **52**, 346–349.

Foxall, D. L., Cohen, J. S., and Mitchell, J. B., 1984, Continuous perfusion of mammalian cells embedded in agarose threads. *Experimental Cell Research*, **154**, 521–529.

Frankenberg-Schwager, M., Frankenberg, D., Blocher, D., and Adamczyk, C., 1980, Repair of DNA double-strand breaks in irradiated yeast cells under nongrowth conditions, *Radiation Research*, **82**, 498–510.

Gillies, R. J., Ugurbil, K., den Hollander, J. A., and Shulman, R. G., 1981, ^{31}P NMR studies of intracellular pH and phosphate metabolism during cell division cycle of *Saccharomyces cerevisiae*. *Proceedings of the National Academy of Sciences, U.S.A.*, **78**, 2125–2129.

Hall, E. J., 1978, *Radiobiology for the Radiologist* (New York: Harper & Row), p. 34.

Harold, F. M., 1966, Inorganic polyphosphates in biology: structure, metabolism, and function. *Bacteriological Reviews*, **30**, 772–794.

Jacobson, L., and Cohen, J. S., 1981, Improved technique for investigation of cell metabolism by ^{31}P NMR spectroscopy. *Bioscience Reports*, **1**, 141–150.

JAIN, V. K., and POHLIT, W., 1973, Influence of energy metabolism on the repair of X-ray damage in living cells. II. Split-dose recovery, liquid-holding reactivation and division delay reversal in stationary populations of yeast. *Biophysik*, **9**, 155–165.

JAIN, V. K., HOLTZ, G. W., POHLIT, W., and POHLIT, S. C., 1977, Inhibition of unscheduled DNA synthesis and repair of potentially lethal X-ray damage by 2-deoxy-D-glucose in yeast. *International Journal of Radiation Biology*, **32**, 175–180.

JAIN, V. K., GUPTA, I., and LATA, K., 1982, Energetics of cellular repair processes in a respiratory-deficient mutation of yeast. *Radiation Research*, **92**, 463–473.

KULAEV, I. S., 1979, *The Biochemistry of Inorganic Polyphosphates* (New York: John Wiley).

MATSUDAIRA, H., FURONO, I., and OTSUKA, H., 1970, Possible requirement of adenosine triphosphate for the rejoining of X-ray-induced breaks in the DNA of Ehrlich ascites-tumour cells. *International Journal of Radiation Biology*, **17**, 339–347.

MUDD, S., YOSHIDA, A., and KOIKE, M., 1958, Polyphosphate as accumulator of phosphorus and energy. *Journal of Bacteriology*, **75**, 224–235.

NAYON, G., OGAWA, S., SHULMAN, R. G., and YAMANE, T., 1977, ^{31}P Nuclear magnetic resonance studies of Ehrlich ascites tumor cells. *Proceedings of the National Academy of Sciences, U.S.A.*, **74**, 87–91.

NAYON, G., SHULMAN, R. G., YAMANE, T., ECCLESHALL, T. R., LAM, K.-B., BARONOFSKY, J. J., and MARMUR, J., 1979, Phosphorus-31 nuclear magnetic resonance studies of wild-type and glycolytic pathway mutants of *Saccharomyces cerevisiae*. *Biochemistry*, **18**, 4487–4499.

NICOLAY, K., SCHEFFERS, W. A., BRUINENBERG, P. M., and KAPTEIN, R., 1983, *In vivo* ^{31}P NMR studies on the role of the vacuole in phosphate metabolism in yeasts. *Archives of Microbiology*, **134**, 270–275.

PATRICK, M. H., and HAYNES, R. H., 1964, Dark recovery phenomena in yeast. II. Conditions that modify the recovery process. *Radiation Research*, **23**, 564–579.

PATRICK, M. H., HAYNES, R. H., and URETZ, R. B., 1964, Dark recovery phenomena in yeast. I. Comparative effects with various inactivating agents. *Radiation Research*, **21**, 144–163.

REINHARD, R. D., and POHLIT, W., 1976, Influence of intracellular adenosine-triphosphate concentration on survival of yeast cells following X-irradiation. *Radiation and Cellular Control Processes*, edited by J. Kiefer. (Berlin: Springer-Verlag), pp. 117–123.

SALHANY, J. M., YAMANE, T., SHULMAN, R. G., and OGAWA, S., 1975, High resolution ^{31}P nuclear magnetic resonance studies of intact yeast cells. *Proceedings of the National Academy of Sciences, U.S.A.*, **72**, 4966–4970.

SEYMOUR, C. B., MOTHERSILL, C., and MORIARTY, M. J., 1985, Glucose analogues alter the response of CHO-K1 cells to gamma irradiation. *Acta Radiologica, Oncology*, **24**, 351–356.

SKOG, S., TRIBUKAIT, B., and SUNDIUS, G., 1982, Energy metabolism and ATP turnover time during the cell cycle of Ehrlich ascites tumour cells. *Experimental Cell Research*, **141**, 23–29.

SKOG, S., TRIBUKAIT, B., and SUNDIUS, G., 1983, Energy metabolism and ATP turnover time during the cell cycle in Roentgen irradiated Ehrlich ascites tumour cells. *Acta Radiologica, Oncology*, **22**, 369–379.

SKOG, S., TRIBUKAIT, B., and NYGAARD, O., 1985, RNA and protein synthesis of irradiated Ehrlich ascites tumour cells. II. Amount of m-RNA and *in vitro* investigations. *Acta Radiologica, Oncology*, **24**, 549–553.

SKOG, S., NORDELL, B., ERICSSON, A., TRIBUKAIT, B., and NISHIDA, T., 1986, Changes in energy metabolism following Roentgen irradiation in *in vivo* growing Ehrlich ascites tumour cells studied by ^{31}P magnetic resonance spectroscopy. *Acta Radiologica, Oncology*, **25**, 63–69.

SZEINFELD, D., and BLEKKENHORST, G., 1987, Effect of X irradiation on adenosine triphosphate and glucose-6-phosphate dehydrogenase in the CaNT mouse tumor. *Radiation Research*, **110**, 305–309.

VAN STEVENINCK, J., 1968, Transport and transport-associated phosphorylation of 2-deoxy-D-glucose in yeast. *Biochimica et Biophysica Acta*, **163**, 386–394.

VERMA, A., SHARMA, R., and JAIN, V. K., 1982, Energetics of DNA repair in UV-irradiated peripheral blood leukocytes from chronic myeloid leukaemia patients. *Photochemistry and Photobiology*, **36**, 627–632.

Wood, H. G., 1966, Inorganic pyrophosphate and polyphosphates as sources of energy. *Current Topics of Cellular Regulation*, **26**, 355–369.

Yoshida, A., 1955, Metaphosphate. II. Heat of hydrolysis of metaphosphate extracted from yeast cells. *Journal of Biochemistry (Tokyo)*, **42**, 163–168.

Circulatory Shock 25:123–130 (1988)

Alterations in Bidirectional Transmembrane Calcium Flux Occur Without Changes in Protein Kinase C Levels in Rat Aorta During Sepsis

R.Z. Litten, J.A. Carcillo, and B.L. Roth

Physiology Department, Armed Forces Radiobiology Research Institute (R.Z.L.), and Surgical Research Division, Naval Medical Research Institute (J.A.C., B.L.R.), Bethesda, Maryland; Department of Anesthesiology, Critical Care Medicine, Child Health and Development, Children's Hospital Medical Center, George Washington University School of Medicine and Health Sciences, Washington, D.C. (J.A.C.)

A depression in aortic contractility has been previously demonstrated in rat intraperitoneal sepsis and during endotoxemia. In this study, we determined whether the mobilization of extracellular calcium (using ^{45}Ca) and the release of intracellular calcium are altered in septic rat aorta when compared to sham-operated controls. The concentration of protein kinase C was also determined by using [^{3}H] phorbol-12,13-dibutyrate (PDBu). We found that calcium influx was unaltered under basal conditions but that the ability of norepinephrine (NE) to augment influx was significantly depressed ($P < .05$; [control vs. septic, 572 ± 54 {SE} vs. 428 ± 30 μmol Ca^{2+}/kg dry wt. aorta]). Calcium influx stimulated by high K^+ was unchanged in aortae between control and septic animals. In the presence of NE, calcium efflux (an indirect measurement of intracellular calcium release) was significantly diminished ($P < .001$) in aortae from septic rats. The concentration of aortic protein kinase C as assessed by PDBu binding sites was unaltered in septic rats when compared with controls. In conclusion, we found that during sepsis alpha$_1$-adrenergic receptor activation of both calcium influx and efflux by NE is decreased; these alterations could be related to the depressed aortic contractility observed in sepsis.

Key words: calcium influx, calcium efflux, norepinephrine

Submitted for publication February 29, 1988.

These findings were presented at the First International Shock Congress, 1987 and published in preliminary form [28].

The opinions and assertions contained herein are the private ones of the authors and should not be construed as reflecting the views of the U.S. Navy, the naval service at large, the Department of Defense, or the Defense Nuclear Agency.

Dr. Roth's present address is Room 5-253, Stanford University Medical Center, Stanford, CA 94304.

Address reprint requests to Dr. R.Z. Litten, Physiology Department, Armed Forces Radiobiology Research Institute, Bethesda, MD 20814-5145.

INTRODUCTION

Human sepsis and septic shock are frequent causes of death in clinical medicine. Septic shock is characterized by peripheral vasodilation with a decreased systemic vascular resistance and hypotension [1–3]. In an attempt to increase the vascular resistance and elevate blood pressure, clinicians usually administer catecholamines and catecholamine derivatives. However, a diminished peripheral vascular responsiveness to catecholamines is commonly observed [4], thus making this approach frequently ineffective.

Alterations in vascular contractility may either involve extrinsic factors (prostaglandins, opioid peptides, etc.) or may be intrinsic to vascular smooth muscle. During endotoxemia and sepsis, previous investigators have demonstrated a diminished ability of NE to induce contraction in rat aorta [see ref. 3 for review]. We previously demonstrated a decrease in the number of aortic alpha$_1$-adrenoceptors and a depressed aortic phosphoinositide (PI) metabolism in this rat model of chronic sepsis [5]. Since we have shown that activation of the alpha$_1$-adrenoceptors with NE results in a stimulation of PI metabolism [6,7], it appears that signal transduction involving alpha$_1$-adrenoceptors is altered in aortae from septic rats.

In this study we determined whether calcium mobilization was altered in aortae from septic rats during the stimulation of alpha$_1$-adrenergic receptors by NE. Calcium influx through calcium channels and calcium efflux, an indication of intracellular calcium release by the sarcoplasmic reticulum [8], were measured in the rat aortae. Both processes in rat aorta are stimulated by the activation of alpha$_1$-adrenoceptors [9]. In addition, we measured the levels of protein kinase C as determined by PDBu binding sites in aortae from septic rats. Activated protein kinase C has been shown to phosphorylate smooth muscle myosin light chain [10,11] as well as alter calcium influx in vascular smooth muscle [12,13] and induce rat aortic contraction [14]. We have also shown that activation of protein kinase C inhibits PI hydrolysis [7], which could explain, in part, the diminished PI turnover observed in the rat aorta during sepsis [5].

MATERIALS AND METHODS

Chronic Rat Sepsis Model

Male Sprague Dawley rats (250–300 g) were obtained from Taconic Farms, Germantown, NY. Control and experimental animals were randomly subjected to sham surgery or cecal ligation with two-hole puncture, respectively, as previously described [15,16]. Twenty-four hours after surgery the surviving animals were killed by decapitation. In our laboratory the model has a 20–30% mortality rate. Surviving animals displayed signs of sepsis originally described by Wichterman et al. [15] including piloerection, a bloody discharge from the nose and mucous membrane, bloody diarrhea, and lethargy.

^{45}Ca Influx

Calcium influx was measured as described by Meisheri and van Breemen [17] with minor modifications [13]. Briefly, 4-mm thoracic aortic rings were incubated at 37°C for 45 min in oxygenated physiological saline (PSS) of the following composition (in mM): NaCl (140), $MgCl_2$ (1), $CaCl_2$ (1.5), KCl (4.6), glucose (10), HEPES buffer (5), pH 7.4 (buffer A). The rings were transferred to PSS (37°C) containing ^{45}Ca (2 μCi/ml) and various experimental protocols as described in figure legends. The rings were then washed in ice-cold PSS for 30 min and placed in a hypotonic 5.0 mM EDTA solution overnight at

room temperature. The aortic rings were removed, dried overnight at 90°C, and weighed. The radioactivity in the hypotonic solution was then detected by liquid scintillation counting.

^{45}Ca Efflux

Calcium efflux was measured in rat aorta by using the procedure of Chiu et al. [9] with minor modifications. Briefly, 4-mm aortic rings were incubated at 37°C for 30 min in oxygenated low-calcium buffer A (0.2 mM instead of 1.5 mM $CaCl_2$). The rings were then loaded with ^{45}Ca for 90 min by using low-calcium buffer A containing 4 μCi/ml of ^{45}Ca. The rings were placed in ice-cold low calcium buffer A for 40 min with a change in solution at 10 min. The rings were then transferred to buffer A (1.5 mM $CaCl_2$) at 37°C for a series of washout procedures wherein the buffer A solutions were changed at 5-, 15-, 20-, and 25-min intervals. A final concentration of 10 μM NE was added to the experimental solution at the start of the 20-min washout period, where an increase in ^{45}Ca release was observed (see Fig. 1). The radioactivity was measured in the washout solution, and the aorta was placed in hypotonic 5.0 mM EDTA solution overnight at room temperature. The aortic rings were removed, dried overnight at 90°C, and weighed. The radioactivity in the hypotonic solution was then counted. The calcium efflux was expressed as cpm ^{45}Ca released into the washout solution per mg dry weight of aorta (see Fig. 1).

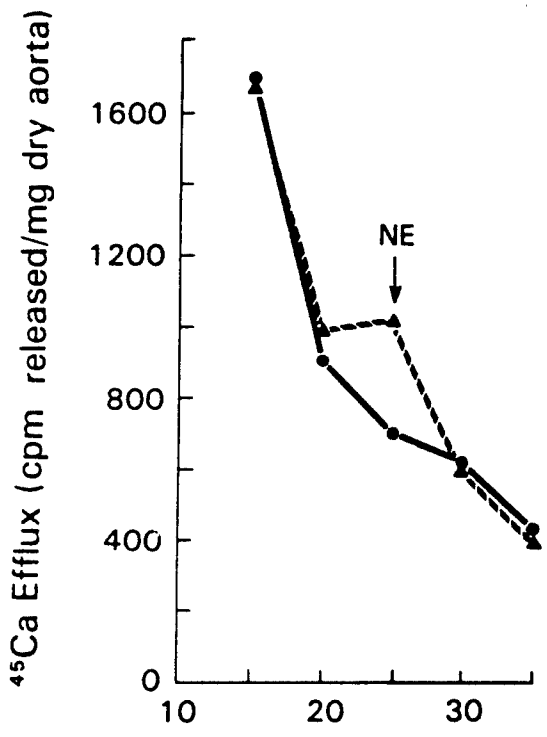

Fig. 1. A typical calcium efflux experiment from rat aortic rings expressed as cpm ^{45}Ca released per mg dry weight of aorta vs. time. At 20 min 10 μM of NE was added to one of the aortic rings (▲), resulting in an increase in calcium release. ● represents calcium efflux without any norepinephrine.

[^{3}H]-Phorbol-12,13-Dibutyrate Binding

PDBu binding was measured as described by Sando and Young [18]. In brief, five aortae were homogenized in 5 ml of homogenization buffer (20 mM Tris-Cl, 0.1 mM phenylmethylsulfonylfluoride, 0.1% beta-mercaptoethanol, 1 mM EGTA, pH 7.40); 100 μl of homogenate was incubated with 0.5 ml of binding buffer (20 mM Tris-Cl, 2 mM $CaCl_2$, 10 mM $MgCl_2$, pH = 6.40, 0.1 mg/ml phosphatidylserine) for 90 min at 22°C. PDBu binding sites were harvested on Whatman GF/B filters with a Brandel Cell Harvester followed by three 5-ml washes with ice-cold 20 mM Tris-Cl (pH 7.40).

Statistical Analysis of the Data

All data reported here represent the mean ± standard error (SEM). The Student's t-test was used for unpaired samples. The Bonferroni inequality was used for simultaneous multiple comparisons [19].

RESULTS

Ca^{2+} Influx

Calcium influx through calcium channels was measured in aortic rings from control and septic rats. We previously showed this to involve a nitrendipine-sensitive process [13]. Under basal conditions there was no difference in calcium influx. The aortic rings were next stimulated by 10 μM NE, a concentration which produced maximal aortic isometric contraction [20] and which in preliminary experiments resulted in maximal influx (not

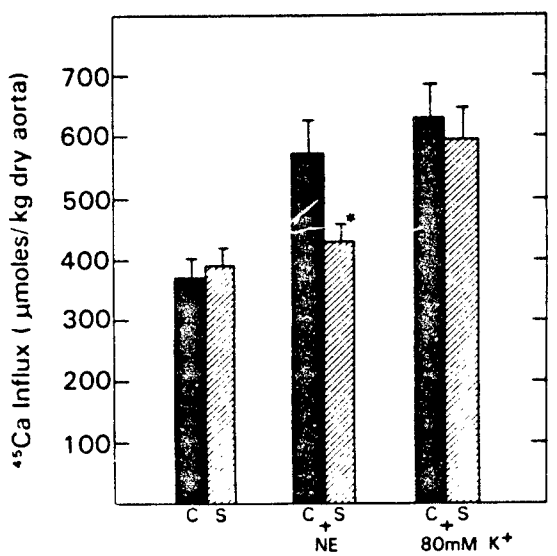

Fig. 2. Calcium influx in control (C) and septic (S) aortic rings. Calcium influx was measured at 5-min incubation time under basal conditions, as well as stimulatory conditions using 10 μM NE and 80 mM K^+. Values are mean ± SEM for 18–34 rings. *$P < .05$ vs. control + NE values. A depression in the NE activation of calcium influx over the basal levels was also observed in aortae from septic rats at incubation times of 10 and 15 min. No difference was observed in the high K^+-stimulated calcium influx between control and septic rats at 10-min incubation time.

shown). We found that the NE-stimulated calcium influx was significantly depressed ($P < .05$) when compared to control values (Fig. 2). Comparison of NE stimulation of calcium influx with the basal levels of calcium influx showed an 88% increase in controls and only a 13% increase in aortae from septic rats. When calcium influx was stimulated by high K^+, there was no significant difference between control and septic animals.

Ca^{2+} Efflux

Calcium efflux was next determined to investigate changes in intracellular calcium release. We found that under basal conditions there was a small but significant ($P < .05$) decrease in calcium efflux in aortic rings from septic animals when compared to controls (Fig. 3). During activation with NE, the calcium efflux was significantly reduced by 33% ($P < .001$ vs. controls) in aortae from septic rats.

Protein Kinase C in Aortae From Septic Rats

As is seen in Table 1, there was no difference in total protein kinase C (as measured by PDBu binding) in aortae from septic and control rats.

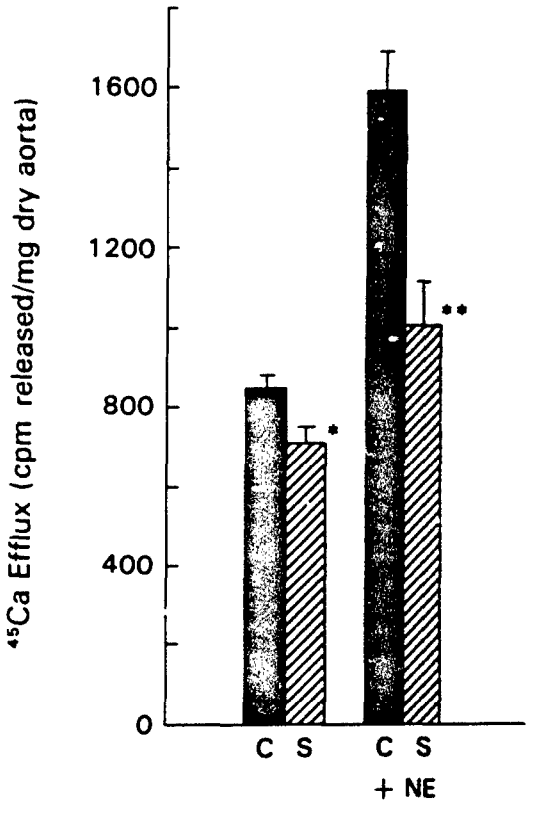

Fig. 3. Calcium efflux in control (C) and septic (S) aortic rings. Calcium efflux was measured in the presence and absence (basal) of 10 μM NE. Values are mean ± SEM for 14–16 rings. *$P < .05$ vs. control values; **$P < .001$ vs. control + NE values.

TABLE I. [^{3}H]phorbol-12,13-Dibutyrate Binding to Aortic Homogenate From Control and Septic Rats[a]

	Total PDBu binding site (dpm/mg)
Control	34,000 ± 3,500
Septic	32,500 ± 4,250

[a]Values are mean ± SEM for three different experiments. Data obtained are described in Materials and Methods. There was no significant difference between control and septic preparations.

DISCUSSION

The findings in this study indicate significant alterations in alpha$_1$-adrenergic receptor-mediated mobilization of extracellular calcium and the release of intracellular calcium in aortae from septic rats. Calcium influx was depressed by 25%, while calcium efflux was reduced by 33% when compared with control values. At the same time, we found that the amount of protein kinase C as assessed by PDBu binding sites was unaltered in aortae from septic rats.

The decrease in calcium mobilization across the calcium channels could be related to the observed depression in aortic contractility during sepsis. This effect could be caused directly by endoxotin or by other circulatory factors such as lymphokines or endothelium-releasing factor(s). We previously showed that the activation of protein kinase C by a phorbol ester increases the calcium influx in rat aorta [13] as well as altering the ability of vasoactive agents to activate PI hydrolysis [21,22]. Since levels of protein kinase C were unchanged it is unlikely that changes in protein kinase C caused the observed change; a more likely explanation is the decrease in receptor levels in rat aorta, as we previously discovered [5]. We also found that PI metabolism was depressed in the rat aorta during sepsis [5], thus creating the possibility of decreased activation of protein kinase C by diacylglycerol (DAG), one of the released products of PI metabolism [23]. Future studies using specific antibodies against protein kinase C could verify this distinction between activation of protein kinase C (i.e., by DAG) and the amount of the enzyme.

The decreased calcium efflux seen in sepsis suggests that intracellular calcium release from the sarcoplasmic reticulum may be depressed in response to NE. This depression could be related to a decrease in inositol-1,4,5-trisphosphate (IP_3), another product of PI metabolism which has been shown to cause calcium release from sarcoplasmic reticulum in vascular smooth muscle [24]. Indeed, recent studies by Chiu et al. [25] in rat aorta as well as our earlier studies [21] indicate a good correlation between PI hydrolysis and intracellular calcium release. Furthermore, we found that levels of phosphatidylinositol-4, 5-biphosphate (PIP_2), the precursor to IP_3, were decreased in aortae from septic rats [5]. Alterations in calcium mobilization from sarcoplasmic reticulum have also been reported in vascular smooth muscle during endotoxic shock. Soulsby et al. [26] showed that the ATP-dependent calcium uptake and calcium-stimulated ATPase activity were depressed by endotoxin in the microsomal-enriched fraction from canine aorta. Since the sarcoplasmic reticulum may be the major system controlling free cytoplasmic calcium in blood vessels [8,27], changes in the release and uptake of calcium from the sarcoplasmic reticulum could be a major factor in explaining the depressed contractility in septic aorta.

Overall, we have demonstrated striking alterations in aortic alpha$_1$-adrenergic receptor-mediated signal transduction during sepsis. We previously showed a decrease in alpha$_1$-

adrenergic receptors and in the alpha$_1$-adrenergic receptor-mediated PI hydrolysis [5]. Furthermore, the decrease in calcium release from sarcoplasmic reticulum, as demonstrated by the decrease in calcium efflux, could be caused by a decrease in PIP_2 hydrolysis. Alpha$_1$-adrenergic receptor stimulation of calcium influx across the calcium channels in the plasmalemma was also depressed in sepsis. In addition, we have also shown an alteration of protein phosphorylation in aortae from septic rats [28] which may reflect changes in the activation, but not the amount, of protein kinase C. Thus these findings suggest that a portion of the diminished responsivity seen in rat aorta during sepsis could be related to perturbations in this receptor-mediated cascade.

Finally, it is important to realize that, similar to these findings in aorta, Spitzer's group found alterations in adrenergic and vasopressin receptor-mediated mobilization of intracellular calcium in hepatocytes [29]. Also, analogous changes in alpha$_1$-adrenergic receptors were also observed in hepatocytes from endotoxemic rats [30] as well as nearly the same alterations in PI metabolism [31].

CONCLUSIONS

During experimental sepsis we found a depressed mobilization of extracellular calcium through calcium channels and depressed calcium efflux, indicating a diminished calcium release from the sarcoplasmic reticulum. The concentration of protein kinase C was not altered. These findings along with our previous results suggest an alteration in aortic alpha$_1$-adrenergic receptor-mediated signal transduction in sepsis.

ACKNOWLEDGMENTS

The authors appreciate the technical assistance of G.T. Gainey and the secretarial assistance of Marianne Owens and Mila M. Ly. This work was supported in part by the Armed Forces Radiobiology Research Institute, Defense Nuclear Agency and Naval Medical Research Institute, Department of Defense, under Work Unit 00169 and Research Task Number MR001.01.1032.

REFERENCES

1. Hess ML, Hastillo A, Greenfield M: Spectrum of cardiovascular functions during gram-negative sepsis. Prog Cardiovasc Dis 23:279–298, 1981.
2. Pomerantz K, Casey L, Fletchen JR, Romwell PW: Vascular reactivity in endotoxin shock: Effect of lidocaine or indomethacin treatment. Adv Shock Res 7:191, 1982.
3. Chernow B, Roth BL: Pharmacologic manipulation of the peripheral vasculature in shock: Clinical and experimental approaches. Circ Shock 18:141–155, 1986.
4. Chernow B, Rainey TG, Lake CR: Endogenous and exogenous catecholamines in critical care medicine. Crit Care Med 10:409–416, 1982.
5. Carcillo JA, Lai J, Venter JC, Roth BL: Molecular properties of altered alpha$_1$-adrenergic receptors in rat intraperitoneal sepsis. Circ Shock 21:302, 1987.
6. Legan E, Chernow B, Parrillo J, Roth BL: Activation of phosphatidylinositol turnover in rat aorta by α_1-adrenergic receptor stimulation. Eur J Pharmacol 110:389–390, 1985.
7. McMillan M, Chernow B, Roth BL: Phorbol esters inhibit alpha$_1$-adrenergic receptor-stimulated phosphoinositide hydrolysis and contraction in rat aorta: Evidence for a link between vascular contraction and phosphoinositide turnover. Biochem Biophys Res Commun 134:970–974, 1986.
8. Johns A, Leijten P, Yamamoto H, Hwang K, van Breemen C: Calcium regulation in vascular smooth muscle contractility. Am J Cardiol 59:18A–23A, 1987.

9. Chiu AT, McCall DE, Thoolen M, Timmermans P: Ca^{++} utilization in the constriction of rat aorta to full and partial alpha-1 adrenoceptor agonists. J Pharmacol Exp Ther 238:224–231, 1986.
10. Nishikawa M, Hidaka H, Adelstein R: Phosphorylation of smooth muscle heavy meromyosin by calcium-activated, phospholipid-dependent protein kinase. J Biol Chem 258:14069–14072, 1983.
11. Nishikawa M, Seller JR, Adelstein RS, Hidaka H: Protein kinase C modulates *in vitro* phosphorylation of the smooth muscle heavy meromyosin by myosin light chain kinase. J Biol Chem 259:8808–8814, 1984.
12. Sperti G, Colucci WS: Phorbol ester-stimulated bidirectional transmembrane calcium flux in A7r5 vascular smooth muscle cells. Mol Pharmacol 32:37–42, 1987.
13. Litten RZ, Suba EA, Roth BL: Effects of a phorbol ester on rat aortic contraction and calcium influx in the presence and absence of BAY k 8644. Eur J Pharmacol 144:185–191, 1987.
14. Nakaki T, Roth BL, Chuang D-M, Costa E: Phasic and tonic components in 5-HT_2 receptor-mediated rat aorta contraction: Participation of Ca^{++} channels and phospholipase C. J Pharmacol Exp Ther 234:442–446, 1985.
15. Wichterman K, Baue AI, Chaundry IH: Sepsis and septic shock: A review of laboratory models and a proposal. J Surg Res 29:189–201, 1980.
16. McMillan M, Chernow B, Roth BL: Alterations in hepatic alpha$_1$-adrenergic receptors in a rat model of chronic sepsis. Circ Shock 19:185–194, 1986.
17. Meisheri KD, van Breemen C: Effects of β-adrenergic stimulation on calcium movements in rabbit aortic smooth muscle: Relationship with cyclic AMP. J Physiol (Lond) 331:429–441, 1982.
18. Sando JJ, Young MC: Identification of high-affinity phorbol ester receptor in cytosol of EL4 thymoma cells: Requirement for calcium magnesium, and phospholipids. Proc Natl Acad Sci USA 80:2642–2646, 1983.
19. Wallenstein S, Zucker CL, Fleiss JL: Some statistical methods useful in circulation research. Circ Res 47:1–9, 1980.
20. Suba EA, Roth BL: Prostaglandins activate phosphoinositide metabolism in rat aorta. Eur J Pharmacol 136:325–332, 1987.
21. Roth BL, Nakaki T, Chuang D-M, Costa E: 5 Hydroxytryptamine$_2$ receptors coupled to phospholipase C in rat aorta: Modulation of phosphoinositol metabolism by phorbol ester. J Pharmacol Exp Ther 238:480–485, 1986.
22. Roth BL, Chuang D-M: Minireview: Multiple mechanisms of serotonergic signal transduction. Life Sci 41:1051–1064, 1987.
23. Nishizuka Y: The role of protein kinase C in cell surface signal transduction and tumor promotion. Nature 308:693–698, 1984.
24. Somlyo AV, Bond M, Somlyo AP, Scarpa A: Inositol trisphosphate-induced calcium release and contraction in vascular smooth muscle. Proc Natl Acad Sci 82:5231–5235, 1985.
25. Chiu AT, Bozarth JM, Timmermans PBM: Relationship between phosphatidylinositol turnover and Ca^{++} mobilization induced by alpha$_1$-adrenoceptor stimulation in the rat aorta. J Pharmacol Exp Ther 240:123–127, 1987.
26. Soulsby ME, Bennett CL, Hess ML: Canine arterial calcium transport during endotoxin shock. Circ Shock 7:139–148, 1980.
27. van Breeman C, Leekeman S, Leijten P, Yamamoto H, Loutzenhiser R: The role of superficial SR in modulating force development induced by Ca entry into arterial smooth muscle. J Cardiovasc Pharmacol 8(Suppl 8):S111–S116, 1986.
28. Litten RZ, Carcillo JA, Roth BL: Vascular calcium metabolism and protein phosphorylation in rat intraperitoneal sepsis. Circ Shock 21:332, 1987.
29. Deaciuc IV, Spitzer JA: Rat liver free cytosolic Ca^{2+} and glycogen phosphorylase in endotoxicosis and sepsis. Am J Physiol 251:R984–R995, 1986.
30. Roth BL, Spitzer JA: Altered hepatic vasopressin and α_1-adrenergic receptors after chronic endotoxin infusion. Am J Physiol 252:E699–E702, 1987.
31. Spitzer JA, Turco ER, Deaciuc IV, Roth BL: Perturbation of transmembrane signaling mechanisms in acute and chronic endotoxemia. In Schlag G, Redl H (eds): "First Vienna Shock Forum, Part A: Pathophysiological Role of Mediators and Mediator Inhibitors in Shock." Progress in Clinical and Biological Research, Vol. 236A. New York: Alan R. Liss, Inc., 1987, pp 401–418.

The experiments described in this paper were performed in adherence to the NIH guidelines for the use of experimental animals.

Radiat. Phys. Chem. Vol. 32, No. 3, pp. 349–353, 1988
Int. J. Radiat. Appl. Instrum. Part C
Printed in Great Britain.

0146-5724/88 $3.00 + 0.00

MODELING RADICAL YIELDS IN ORIENTED DNA EXPOSED TO HIGH-LET RADIATION

J. H. MILLER,[1] W. E. WILSON,[1] C. E. SWENBERG,[2] L. S. MYERS JR[3] and D. C. CHARLTON[4]
[1]Pacific Northwest Laboratory, Richland, Wash., U.S.A.
[2]Armed Forces Radiobiology Research Institute, Bethesda, Md, U.S.A.
[3]Uniformed Services University of the Health Sciences, Bethesda, Md, U.S.A.
[4]Concordia University, Montreal, Quebec, Canada

(*Received* 16 *June* 1987)

Abstract—Monte Carlo simulation of energy absorption in oriented fibers of DNA is used to model the dependence of free radical yields on the orientation of the fibers relative to a flux of ionizing radiation. We assume a large asymmetry in the thermal conductivity of the fibers that permits rapid transport of vibrational energy along a DNA molecule, but not between different molecules. Based on this assumption, our model predicts that thymine radical anions have a significantly greater probability of undergoing a secondary protonation reaction if they are produced by a flux of high-energy protons that is incident parallel to the helical axis of DNA than if they are generated by a flux that is incident perpendicular to the DNA molecules. These results are in qualitative agreement with experimental data on the yield of 5,6-dihydrothymin-5-yl radicals when samples of oriented DNA were exposed at 77 K to neutrons.

INTRODUCTION

Understanding the mechanisms by which high-energy charged particles produce reactive chemical species in biologically significant materials is important for assessing the health effects of low-level exposure to ionizing radiation. This is particularly true for radiation with high linear-energy-transfer (LET) where correlations between track structure and target structure can have a profound effect on the nature and distribution of damage. The role of nonhomogeneous processes in radiation chemistry was recently reviewed by Magee and Chatterjee.[1] Our research in this area[2] has focused on the use of detailed Monte Carlo simulation of the spatial distribution of energy absorbed from charged particles[3] as a basis for understanding the subsequent evolution of chemically active species. In this paper we report the use of this approach to investigate production of free radicals in oriented DNA exposed to a flux of high-energy protons.

Samples of oriented DNA fibers prepared by the wet spinning technique have proven to be a valuable experimental tool for investigating the production of free radicals in DNA by both u.v. light and ionizing radiation.[4–7] The recognition that spatially correlated electron gain and loss centers may be precursors of DNA double strand breaks[8] has led to renewed interest in this experimental system for investigating radiation-induced DNA damage. Recently, Arroyo *et al.*[9] used this type of sample in conjunction with electron spin resonance (ESR) to investigate the production of radicals at 77 K by exposure to neutrons. When samples were irradiated by a flux of neutrons incident perpendicular to the helical axis of DNA, ESR spectra showed that thymine anion (T^-) and guanine cation were the principal radical species present at 77 K. However, when the neutron flux was approximately parallel to the orientation of DNA molecules, the total yield of radicals was reduced and a new ESR signal characteristic of the 5,6-dihydrothymin-5-yl ($TH^\cdot$) radical predominated.

The most obvious difference in the patterns of energy absorption in the two irradiation geometries is that charged particles that traverse the sample nearly parallel to the helical axis of DNA have a greater probability of multiple energy transfer to the same molecule than do particles incident on the sample perpendicular to the fiber orientation. This difference in the spatial distribution of energy absorption should have no effect on the production of free radicals if energy and/or charge move between DNA molecules in a fiber as freely as they are transported along a single DNA chain. Hence the unusual orientation dependence of radical yields in this system may have important implications for intramolecular energy and charge transfer in DNA.

Arroyo *et al.*[9] speculated that the reduction of radical yields in the parallel irradiation geometry was due to enhanced recombination of precursor ion pairs. This explanation seems plausible in light of recent measurements of conductivity by van Lith *et al.*[10] which suggest that the high mobility of electrons in the ice-like water layer around a biopolymer could enhance intramolecular charge transfer. Arroyo *et al.* attributed the appearance of $TH^\cdot$ radicals in the parallel irradiation geometry to intramolecular transfer of triplet excitation produced in charge recombination. The long lifetime of triplet excitons at 77 K[11] certainly favors this mechanism. However, due to the variation in triplet transfer rates,[12] triplet

excitons tend to be restricted to the neighborhood of thymine that is bounded by the nearest guanine or cytosine on each side. Hence, in DNAs with roughly equal G-C and A-T content, the range of triplet migration is not expected to be large. Ion quenching experiments[13] suggest a range of 5–30 base pairs. The short lifetime of singlet excitons[14] is probably the major factor that limits the range of their migration.

In this paper we present a model for the orientation dependence of $TH^{\cdot}$ yields that is based on an assumed asymmetry in the transport of vibrational excitation in the oriented DNA samples. Asymmetry of phonon scattering rates in oriented DNA have been observed using Raman spectroscopy;[15,16] however, these low-frequency modes should not be very effective in activating proton transfer to $T^{\cdot}$ if the activation energy is 0.2–0.7 eV as suggested by the work of Gräslund *et al.*[5] Regardless of the mechanism, our model is macroscopic in that asymmetric energy transfer is approximated by the solution of thermal diffusion equations with a coefficient of diffusion along DNA that is 1000 times greater than the coefficient for diffusion perpendicular to the helical axis. This model is developed in the next section of the paper and our numerical results for the production of $TH^{\cdot}$ radicals by proton irradiation at 0.3 and 1.0 MeV are discussed in the third section. Conclusions and the potential for improved theory and experiment are discussed in the final section.

THEORY

As suggested by Gräslund *et al.*,[5] we assume that the major source of $TH^{\cdot}$ radicals is the reaction

$$T^{\cdot} + XH^{+} \rightarrow TH^{\cdot} + X. \tag{1}$$

where the proton donor, XH^{+}, is probably water of hydration. In an excess of proton donor, this reaction will be pseudo first-order and the yield of radiation-induced $TH^{\cdot}$ radicals per DNA molecule is given by the equation

$$Y_{TH^{\cdot}} = \int \pi h^2 C_{T^{\cdot}}(x,0) P_{TH^{\cdot}}(x), \tag{2}$$

where

$$P_{TH^{\cdot}}(x) = \int_0^{t_{max}} k(x,t) \exp\left[-\int_0^t k(x,t')\,dt'\right] dt \tag{3}$$

is the probability that a thymine anion formed at position x on an oriented DNA molecule, which we approximate as a long cylinder of radius $h = 10$ Å, will be converted to $TH^{\cdot}$ by protonation. The initial concentration of $T^{\cdot}$, the rate of protonation, and the duration of the radiation-induced excess temperature are denoted by $C_{T^{\cdot}}(x,0)$, $k(x,t)$, and t_{max}, respectively.

Modeling the production of $T^{\cdot}$, which probably involves the decay of highly excited states through autoionization channels followed by capture of low-energy secondary electrons in traps with high electron affinity, is beyond the scope of this paper. Rather we simply assume that the probability to form $T^{\cdot}$ in the ith energy deposition event is proportional to the amount of energy ϵ_i absorbed locally in that event. Hence, the initial concentration of $T^{\cdot}$ is approximated by the equation

$$C_{T^{\cdot}}(x,0) = g_{T^{\cdot}} \sum_i \epsilon_i \frac{\delta(x - x_i)}{\pi h^2}, \tag{4}$$

where $g_{T^{\cdot}}$ is the average yield of $T^{\cdot}$ per unit of absorbed energy and $\delta(x)$ is the Dirac delta function. Using this approximation in equation (3) we can perform the space integration and obtain the result.

$$\frac{g_{TH^{\cdot}}}{g_{T^{\cdot}}} = \frac{\sum_i \epsilon_i P_{TH^{\cdot}}(x_i)}{\sum_i \epsilon_i}. \tag{5}$$

for the yield of $TH^{\cdot}$ relative to the yield of its precursor $T^{\cdot}$. This result is just a weighted average of the probability to convert $T^{\cdot}$ to $TH^{\cdot}$ over all the positions of energy deposition in a DNA molecule from charged particles traversing the sample at a specified angle relative to the molecular orientation. The weighting factors express the relative probability that $T^{\cdot}$ will be produced by a given energy absorption event.

The rate of proton transfer used in equation (3) to calculate $P_{TH^{\cdot}}$ depends upon the transient local temperature $T(x,t)$ through the relation

$$k(x,t) = A \exp[-Q\ T(x,t)], \tag{6}$$

where A is a constant of the order of vibration rates (10^{11} sec) and Q is the activation energy. If we completely neglect intermolecular transfer of vibrational energy and make the additional assumption that the heat capacity and thermal conductivity are independent of temperature, then $T(x,t)$ can be obtained by solution of the one-dimensional thermal diffusion equation for a cluster of point sources.[13,14] This result can be written in the form

$$T(x,t) = T_s + \sum_k T_k(x,t), \tag{7}$$

where T_s is the ambient sample temperature,

$$T_k(x,t) = T_{k0}(1 + t/\tau_{\parallel})^{-1/2} \exp\left[\frac{-(x - x_k)^2}{2\Delta^2(1 + t/\tau_{\parallel})}\right], \tag{8}$$

with

$$\tau_{\parallel} = \frac{\Delta^2}{2D_{\parallel}} \tag{9}$$

being the parallel diffusion relaxation time and

$$T_{k0} = \frac{\epsilon_k}{\sqrt{2\pi^3 h^2 \Delta \rho C}} \tag{10}$$

being the initial excess temperature at x_k due to absorption of energy ϵ_k. The sample density, specific heat and coefficient of thermal diffusion parallel to

the DNA fibers are denoted by ρ, C and $D_{\perp}$, respectively. Ultimately C and $D_{\perp}$ must be considered as adjustable parameters since we are using macroscopic material parameters to describe a microscopic process. In addition, the effective specific heat C contains a factor for the conversion of energy from electronic to vibrational excitation. As a starting point for numerical calculations, we use the specific heat and thermal diffusion coefficient of water [4×10^{7} erg (g·deg) and 10^{-3} cm^2 s, respectively]. The delocalization of vibrational excitation by subpicosecond processes is included in our model through the parameter Δ, which is the initial width of the Gaussian distribution that approximates the excess temperature induced by individual energy deposition events. We expect Δ to be of the order of the base stacking distance which is 3.4 Å in the B conformation.

The formulation of the model thus far completely neglects transport of vibrational energy perpendicular to the helical axis of the DNA molecule. This is generally adequate for small isolated clusters of excitation where the radiation-induced excess temperatures decays on a nanosecond or smaller time scale. However, when many interactions occur over an appreciable length of DNA the time dependence of the excess temperature may be affected by thermal-diffusion perpendicular to the fiber direction. Since we are assuming that $D_{\perp} \gg D_{\perp}$, it is reasonable to approximate this leakage by considering the loss of thermal energy from a long cylinder of uniform initial temperature. Including only the first term in the series expansion that is the solution of this well-known heat flow problem, we obtain an approximation for the transient local temperature that is given by

$$T(x, t) = T_{\perp} + \exp\left(-\frac{t}{\tau_{\perp}}\right) \sum_{k} T_k(x, t), \qquad (11)$$

where

$$\tau_{\perp} = \frac{b^2}{5.8 D_{\perp}} \qquad (12)$$

is the perpendicular thermal diffusion relaxation time. If the asymmetry in thermal diffusion is large (we assume $D_{\perp}/D_{\perp} = 10^{-3}$) and if the initial width parameter does not greatly exceed the radius of the molecule, then $\tau_{\perp} \gg \tau_{\perp}$ and the leakage factor in equation (11), $\exp[-t/\tau_{\perp}]$, serves only to limit the duration of the excess temperature when many excitations occur in the same molecule. Hence it mainly effects the yields calculated in the parallel irradiation geometry.

RESULTS

Application of the formalism presented in the previous section requires information about the spatial patterns of energy absorption in a DNA molecule of specified orientation relative to the flux of ionizing radiation. In our model this information consists of the positions of energy deposition events x_k and the amount of energy ϵ_k deposited locally in each event. Energy transported away from x_k by high-energy secondary electrons is not included in ϵ_k, since the detailed structure of these secondary tracks is included in our Monte Carlo simulation of the slowing down of the primary ion. To approximate the spatial distribution of energy deposited in a DNA molecule, we superimpose a long right-circular-cylinder of radius $b = 10$ Å on a computer-simulated segment of the track of a high energy proton slowing down in water. The computer simulation is carried out by a Monte Carlo code developed by Wilson and Paretzke.[14] The superposition of cylinders and track segments is random in all aspects except the angle between the axis of the cylinder and the velocity of the proton. The collection of energy transfer points in this superposition of target and track we will refer to as a "hit".

Once an energy deposition event within a hit has been randomly selected to be the site of formation of $T^{\cdot}$, the transient temperature at that position is calculated for equation (11). Typical results for hits that involve small and large amounts of energy deposited in DNA are shown in Fig. 1. If $D_{\perp}/D_{\perp} \leq 0.001$ then the leakage term in equation (11) does not significantly effect the transient temperature at times less than about 0.1 ns. However, transport of thermal energy perpendicular to the DNA fibers does influence the excess temperature associated with large hits at longer times and substantially reduces the probability that protonation will occur. Unless otherwise noted, all of the results presented in this paper are for $D_{\perp}/D_{\perp} = 0.001$.

Assuming an initial delocalization of vibrational excitation equal to 3.4 Å, Fig. 2 shows the dependence of the yield of $TH^{\cdot}$ per $T^{\cdot}$ precursor on the activation energy for the proton transfer reaction. In these calculations we have averaged over the distribution of hits that occur under a given irradiation

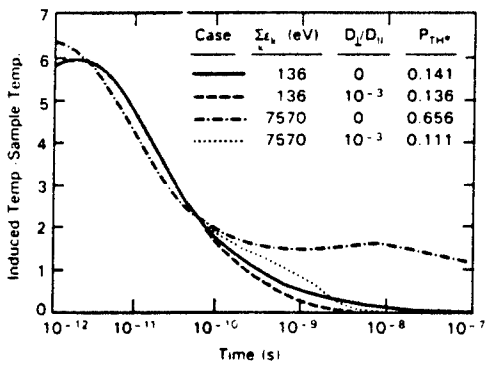

Fig. 1. Transient radiation-induced temperature changes for two typical hits with different spatial and energy characteristics. For times <0.1 ns temperature profiles are essentially the same for the two levels of asymmetry in thermal conductivity.

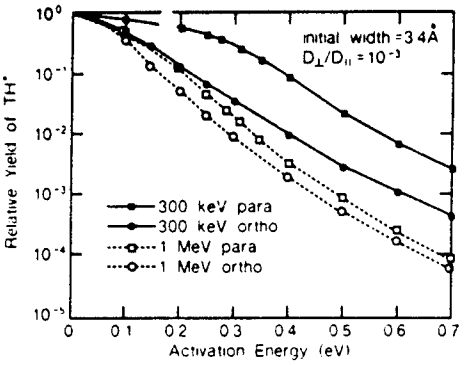

Fig. 2. Yield of TH• per T• as a function of the activation energy for proton transfer.

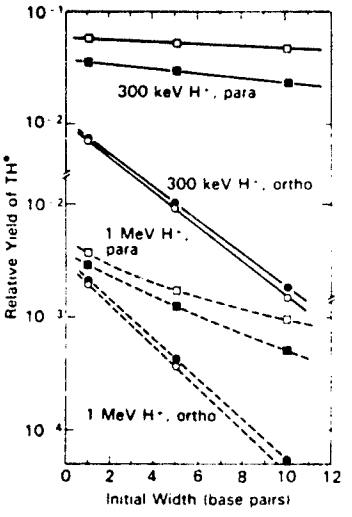

Fig. 3. Yields of TH• per T• averaged over the distribution of activation energies given in Ref. 5 as a function of the initial width parameter of the model expressed in units of the base-pair separation of DNA in the B conformation (3.4 Å). Solid symbols show the effect of a ±10 uncertainty in the orientation of DNA molecules relative to the proton flux.

condition. Typically, a sample containing on the order of 10^5 hits was examined. To obtain results for comparison with experiment we must further average the yield of TH• over a distribution of activation energies for the protonation reaction. If we use the distribution proposed by Gräslund *et al.*,[5] we obtain the results shown in Fig. 3. In this figure the ratio $g_{TH\cdot}\ g_{T\cdot}$ is plotted as a function of the initial width parameter in units of the base-pair separation, 3.4 Å.

Generally, protonation of T• decreases exponentially with increasing initial delocalization of the vibrational excitation of the medium in an individual energy deposition event. This is expected from equation (10) which shows that the initial excess temperature associated with any energy deposition event is inversely proportional to the initial width Δ. This parameter also enters the calculation through equation (8) where the effect of a larger Δ is to increase the duration of the excess temperature, which favors protonation. Apparently the former effect predominates. In Fig. 3 we see that protonation of T• in the parallel irradiation geometry is considerably less sensitive to the value of Δ than it is in the perpendicular case. In the parallel case a hit is made up of many more energy deposition events than in the perpendicular case. This makes the effectiveness of a hit for inducing protonation of T• less dependent on the excess temperature associated with individual energy deposition events.

The effects on the yield of TH• of a ±10 uncertainty in the orientation of the DNA fibers relative to the proton flux is also shown in Fig. 3. Results for the parallel orientation are more sensitive to this type of uncertainty than are those obtained for protons incident nearly perpendicular to the DNA fibers. This is a consequence of the fact that the large TH• yields in the parallel irradiation geometry result from the relatively few hits where a DNA molecule is close to the axis of a proton track for an appreciable distance. This aspect of our model is further illustrated by Table 1 which gives the average energy deposited in a DNA molecule by a hit and the root-mean-square separation of T• from other energy deposition events in a hit. The latter quantity is a measure of the distance over which thermal energy diffuses in the process of activating proton transfer to T•. Note that this energy transfer distance is essentially equal to the diameter of the target in the perpendicular case and is insensitive to a ±10 uncertainty in this orientation. However, this level of uncertainty in orientation of DNA relative to a proton flux that is parallel to the fibers causes a large reduction in the average energy transfer distance and a correspondingly large reduction in the protonation of T•.

Table 1. Characteristics of the interaction of oriented DNA with 1 MeV protons

Orientation[a]	Energy deposited (eV)	Transfer distance (Å)[b]
0	293	2240
0 ± 10	150	474
90	62	21
90 ± 10	62	22

[a] Angle in degrees between helical axis of DNA and proton velocity.
[b] Root-mean-square separation between sites of T• and other excitations.

The characteristic of our model that is most readily testable is its dependence on the LET of the radiation. This aspect of our results is better illustrated by Fig. 4 where the ratio of yields of $TH^{\cdot}$ per $T^{\cdot-}$ precursor calculated with the same model parameters in the parallel and perpendicular case, is plotted as a function of the initial width parameter in units of the base-pair separation. This ratio is an indicator of the enhancement of the protonation reaction in samples exposed to a flux of high-LET radiation parallel to the orientation of the DNA fibers. In this model, the degree to which protonation of $T^{\cdot-}$ is enhanced in the parallel irradiation geometry is strongly dependent upon the initial spatial delocalization of vibrational excitation in the DNA. As was discussed above, this results from the fact that protonation of $T^{\cdot-}$ in the parallel case is less dependent on high local excess temperature. However, the increase in the enhancement factor with increasing LET is essentially independent of this initial width parameter. Hence experimental results at one proton energy can be used to determine Δ for comparison between theory and experimental at other proton energies. This approach to experimentally testing the model assumes that Δ is independent of LET.

CONCLUSIONS

Our model calculations show that intramolecular energy transfer following radiation exposure should enhance protonation of $T^{\cdot}$ and that this is a reasonable explanation for the orientation dependence of $TH^{\cdot}$ yields that is observed when a flux of high-LET radiation is absorbed in samples of oriented DNA at 77 K.[9] The amount of enhancement predicted by the model is sensitive to the uncertainty in orientation and to the stopping power of the incident radiation. Both of these results point out the need to repeat the experiments of Arroyo *et al.*[9] with proton irradiation from an accelerator rather than a neutron source. This will reduce the uncertainty in orientation of the proton flux relative to the DNA fiber direction and allow the enhancement of $TH^{\cdot}$ radicals in the parallel irradiation geometry to be measured as a function of the LET of the incident radiation. Experiments of this type are in progress. Improvements in the model are being focused in two areas: (1) a more microscopic description of $TH^{\cdot}$ production with parameters that are more directly related to molecular properties of the system; and (2) a more complete theory that includes recombination which will allow us to predict both the enhancement of $TH^{\cdot}$ and the reduction of total radical yields in the parallel irradiation geometry. By this combined experimental and theoretical effort we expect that oriented DNA will be an even more useful tool for investigating the interplay of target structure and track structure in determining the production of reactive species in biological systems exposed to high-LET radiation.

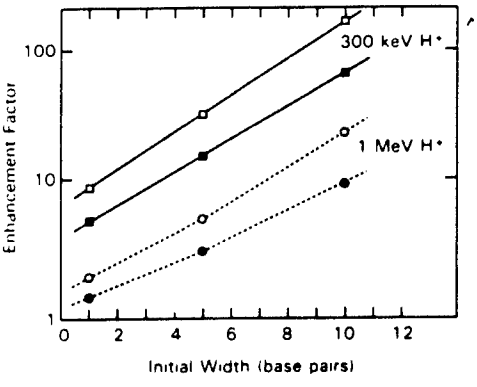

Fig. 4. Enhancement of protonation of $T^{\cdot}$ formed by irradiation with a proton flux that is parallel to the orientation of DNA relative to the yield of this secondary reaction in the perpendicular irradiation geometry. Solid symbols show the effect of a ± 10 uncertainty in orientation of DNA molecules relative to the proton flux.

Acknowledgement—This work was supported by the Office of Health and Environmental Research (OHER) U.S. Department of Energy under Contract DE-AC06-76RLO 1830.

REFERENCES

1. J. L. Magee and A. Chatterjee, in *Kinetics of Non-homogenous Processes: A Practical Introduction for Chemist, Biologist, Physicists, and Material Scientist* (Edited by G. R. Freeman) p. 171. Wiley, New York, 1986.
2. J. H. Miller, *Radiat. Res.* 1981, **88**, 280.
3. W. E. Wilson and H. G. Paretzke, *Radiat. Res.* 1981, **87**, 521.
4. A. Ehrenberg, A. Rupprecht and G. Ström, *Science* 1967, **157**, 1317.
5. A. Gräslund, A. Ehrenberg, A. Rupprecht, B. Tjalldin and G. Ström, *Radiat. Res.* 1975, **61**, 488.
6. A. Gräslund, A. Ehrenberg, A. Rupprecht and G. Ström, *Int. J. Radiat. Biol.* 1975, **28**, 313.
7. A. Gräslund, A. Ehrenberg, A. Rupprecht and G. Ström, *Photochem. Photobiol.* 1979, **29**, 245.
8. P. M. Cullis and M. C. R. Symons, *Radiat. Phys. Chem.* 1986, **27**, 93.
9. C. M. Arroyo, A. J. Carmichael, C. E. Swenberg and L. S. Myers Jr, *Int. J. Radiat. Biol.* 1986, **50**, 789.
10. D. van Lith, J. M. Warman, M. P. de Haas and A. Hummel, *J. Chem. Soc. Faraday Trans. 1*, 1986, **82**, 2933.
11. R. O. Rahn, R. G. Shulman and J. W. Longworth, *J. Chem. Phys.* 1966, **45**, 2945.
12. M. Guéron, J. Eisinger and A. A. Lamola, in *Basic Principles of Nucleic Acid Chemistry*, Vol. 1 (Edited by O. P. Ts'o) pp. 311–398. Academic Press, New York, 1974.
13. I. Isenberg, R. Rosenbluth and S. L. Baird Jr, *Biophys. J.* 1967, **7**, 365.
14. S. Georghiou, T. M. Nordlund and A. M. Saim, *Photochem. Photobiol* 1985, **41**, 209.
15. H. Urabe, Y. Tominaga and K. Kubota, *J. Chem. Phys.* 1983, **78**, 5937.
16. C. DeMarco, S. M. Lindsay, M. Pokorny, J. Powell and A. Rupprecht, *Biopolymers* 1985, **24**, 2035.
17. A. Mozumder, in *Advances in Radiation Chemistry*, Vol. 1 (Edited by M. Burton and J. L. Magee) pp. 1–99. Wiley-Interscience, New York, 1969.
18. G. H. Vineyard, *Radiat. Eff.* 1976, **29**, 245.

INT. J. RADIAT. BIOL., 1988, VOL. 53, NO. 6, 901-907

Rapid communication

Stochastic model of free radical yields in oriented DNA exposed to densely ionizing radiation at 77K

J. H. MILLER†, W. E. WILSON†, C. E. SWENBERG‡, L. S. MYERS Jr§ and D. E. CHARLTON¶

† Pacific Northwest Laboratory, PO Box 999, Richland, Washington 99352, U.S.A.
‡ Armed Forces Radiobiology Research Institute, Bethesda, Maryland 20814-5145, U.S.A.
§ Uniformed Services University of the Health Sciences, Bethesda, Maryland, U.S.A.
¶ Concordia University, Montreal, Quebec, Canada

(*Received 25 September 1987; revision received 6 January 1988; accepted 18 January 1988*)

Monte Carlo simulation techniques were used to calculate the probability that thymine radical anions ($T^{\cdot -}$), formed by the slowing-down of high-energy protons in oriented DNA, will undergo a secondary protonation reaction. By assuming a large asymmetry in the thermal conductivity of oriented DNA fibres we predict a significant enhancement of protonation of $T^{\cdot -}$ when the proton flux is incident on the sample parallel to the orientation of the DNA. These results are in qualitative agreement with experimental data on the production of $TH^{\cdot}$ radicals when oriented DNA is exposed to fast neutrons.

Oriented DNA fibres prepared by the wet spinning technique of Rupprecht (1966) have been extensively used to investigate the production of free radicals by ultraviolet (u.v.) light (Gräslund *et al.* 1971) and gamma irradiation (Gräslund *et al.* 1979, 1981, Hüttermann *et al.* 1984). Recently Arroyo and co-workers (1986) used oriented Na DNA films in conjunction with electron paramagnetic resonance (e.p.r.) to measure the orientation dependence of radicals produced by exposure at 77K to fast neutrons from the TRIGA reactor at the Armed Forces Radiobiology Research Institute. For samples irradiated by a neutron flux perpendicular to the helical axis of DNA, the e.p.r. spectra recorded at 77K were consistent with roughly equal amounts of thymine anion ($T^{\cdot -}$) and guanine cation, a result in agreement with the studies mentioned above using u.v. and gamma-irradiated samples. However, when the neutron flux was parallel to the oriented DNA fibres the total radical yield was significantly reduced, and a signal characteristic of 5,6-dihydro thymin-5-yl ($TH^{\cdot}$) radicals became the predominant feature in the e.p.r. spectrum.

Since neutrons are absorbed in hydrogenous materials mainly through the production of recoil protons, we are investigating these unusual findings through the study of free-radical production in oriented DNA by exposure to proton fluxes. This paper examines quantitatively the hypothesis that intramolecular energy transfer is responsible for the orientation dependence of radical yields reported by Arroyo *et al.*

(1986). Although the probability of multiple energy depositions in the same DNA molecule is much greater for protons with velocity nearly parallel to the fibre orientation, this difference between the patterns of energy absorption in the parallel and perpendicular case does not necessarily imply an orientation dependence of free-radical yields. For example, if each ion pair induced in DNA by the radiation exposure evolved independently, then the radiation chemistry of free radicals would be decoupled from the overall patterns of ionization in the sample. Likewise, if ion pairs in different DNA molecules interact as strongly as ion pairs in the same molecule, then the impact of this interaction on radical yields should be the same for parallel and perpendicular irradiation. This paper investigates the complex interplay between the track structure of densely ionizing radiation and the asymmetry of energy migration after deposition as a possible explanation for the unusual observations reported by Arroyo *et al.* (1986).

It is difficult to assess the degree to which secondary protons in the experiments of Arroyo *et al.* (1986) preserve the initial orientation of the neutron flux. It is also difficult to predict absolute yields of free radicals in a system as complex as DNA exposed to densely ionizing radiation. Hence we do not attempt to make quantitative comparison between the theory and experiment in this paper. The goal of this work is to calculate the probability that $T^{\pm}$ will undergo a secondary reaction to form $TH^{\cdot}$ as a function of the energy and direction of the proton track in which the thymine radical anion is produced. We predict that this secondary reaction is significantly enhanced in proton tracks with high stopping power that are nearly parallel to the DNA. This finding supports the observation by Arroyo *et al.* (1986) that $TH^{\cdot}$ is the predominant radical species formed in the parallel irradiation geometry. Similar arguments may also explain the observed reduction in total radical yields; however, to make quantitative predictions concerning the total radical yield requires more detailed information about the thermally induced decay of primary radical species than is currently available. This is particularly true with regard to the fate of radical cations (Hole *et al.* 1987).

Our model assumes the following: (a) The major source of $TH^{\cdot}$ radicals is thermally activated protonation of $T^{\pm}$, with water of hydration being the most likely proton donor. This hypothesis is consistent with the findings of Gräslund *et al.* (1975), who investigated the formation of $TH^{\cdot}$ by annealing of radicals produced by gamma irradiation of oriented DNA. (b) Intramolecular energy transfer is much more rapid than intermolecular energy transfer, even for two DNA molecules in the same oriented DNA fibre. In our macroscopic model this assumption is expressed as a large asymmetry in the coefficient of thermal diffusion. (c) Spatial pattern of energy absorption in oriented DNA molecules can be approximated by the overlap of a cylinder of uniform radius 10 Å with the track of a high-energy proton (Wilson and Paretzke 1981) that is slowing down in a homogeneous material of unit density. This approximation, which is based on inelastic scattering of protons and secondary electrons by water molecules, is assumed to be adequate for calculating the transient excess temperature that activates the protonation of $T^{\pm}$.

The production of $T^{\pm}$ probably results from autoionization of highly excited plasmon-like states followed by capture of the low-energy secondary electrons at base sites with high electron affinity. Since we cannot model these processes based on computer simulation of the slowing down of protons in water, we assume that the probability of forming $T^{\pm}$ in an energy deposition event at position x_i in a target cylinder is proportional to the amount of energy ε_i absorbed locally in that event.

This approximation leads to the expression

$$g_{TH}\ g_{T} = \sum_i \varepsilon_i P_{TH}(x_i) \Big/ \sum_i \varepsilon_i \tag{1}$$

for the yield of TH relative to the yield of its precursor $T^{\cdot}$, where $P_{TH}(x_i)$ is the probability of thermally activated proton transfer at x_i and the weighing factors ε_i reflect the bias that inelastic collisions with large energy transfer to the absorbing medium are more likely to be the type that would lead to formation of $T^{\cdot}$.

In an excess of proton donors the protonation reaction will be pseudo-first-order and the probability that protonation will occur at position x is given by

$$P_{TH}(x) = \int_0^{t_{max}} k(x,t) \exp\left[- \int_0^t k(x,t')\,dt' \right] dt \tag{2}$$

where t_{max} is the duration of the radiation-induced excess temperature. The rate of protonation, $k(x,t)$, is given by

$$k(x,t) = A \exp[-Q/T(x,t)] \tag{3}$$

where A is a constant, the order of vibrational rates, $10^{13}\,s^{-1}$, Q is the activation energy for protonation, and $T(x,t)$ is the transient temperature. We assume that both the heat capacity and thermal conductivity are temperature-independent and that thermal diffusion parallel to the DNA fibres ($D_{\parallel}$) is rapid compared to diffusion perpendicular ($D_{\perp}$) to the fibres. In the limit where only the shortest transverse relaxation time ($\tau_{\perp} = h^2/5{\cdot}8D_{\perp}$) is included

$$T(x,t) = T_0 + \exp[-t/\tau_{\perp}] \sum_k T_k(x, t/\tau_{\parallel}) \tag{4}$$

where T_0 is the ambient sample temperature, $\tau_{\parallel} = \Delta^2/2D_{\parallel}$ is the longitudinal thermal relaxation time, and T_k is the excess temperature at position x and time t due to absorption of energy ε_k at position x_k. The sum over k includes all energy depositions in the target cylinder that approximates a DNA molecule, except the one selected as the site of formation of $T^{\cdot}$.

By solving the thermal diffusion equation in one dimension, one finds

$$T_k = T_{k0}(1 + t/\tau_{\perp})\exp^{-1/2}[-(x-x_k)^2/2\Delta^2(1 + t/\tau_{\parallel})] \tag{5}$$

where

$$T_{k0} = \varepsilon_k/((2\pi^3)^{1/2} h^2 \Delta \rho C) \tag{6}$$

is the initial excess temperature at x_k due to the absorption of energy ε_k. The sample density and specific heat are denoted respectively by ρ and C. Ultimately C and $D_{\perp}$ must be treated as adjustable parameters of the model since we are using macroscopic material parameters to describe microscopic processes. As a starting point for our numerical calculations we use their water values 4×10^7 erg g-deg and $10^{-3}\,cm^2\,s^{-1}$, respectively. The initial width, Δ, of the Gaussian distribution that approximates the spatial distribution of excess temperature from an individual energy deposition event in DNA should not exceed a few base-pairs if the estimates given by Brandt and Ritchie (1974) for the delocalization of collective excitations in the water apply to DNA.

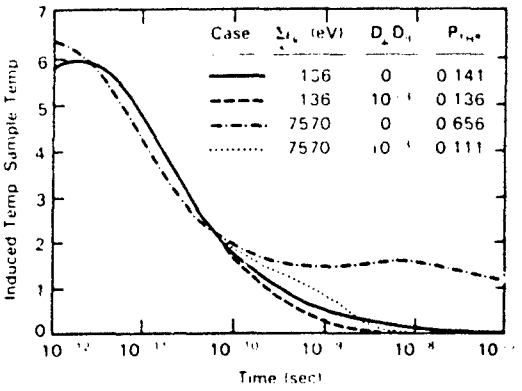

Figure 1. Typical examples of the transient radiation-induced temperature at the position of a thymine radical anion ($T^{\cdot}$) with and without transverse diffusion for small and large amounts of energy deposited in oriented DNA by a 1 MeV proton with velocity parallel to the helical axis. The effect of different temperature profiles on the probability for protonation of $T^{\cdot}$ is shown in the legend.

The collection of energy deposition events in the overlap between a proton track and a cylinder of radius b will be called a 'hit'. The number and spatial distribution of events in a hit are highly variable. Hence, to obtain results with good statistical convergence requires computer simulation of a large number of interactions between a proton track and a DNA molecule. The site of formation of $T^{\cdot}$ in a hit was selected randomly from among the energy deposition events in the target cylinder that approximates a DNA molecule. All other events are assumed to contribute to a radiation-induced excess temperature. Since we select only one $T^{\cdot}$ per hit, our model neglects any coupling between radical anions, such as competition for proton donors. As figure 1 indicates, the radiation-induced excess temperature at the site of formation of $T^{\cdot}$ and the probability for protonation, P_{TH}, are insensitive to the asymmetry in thermal diffusion when the total energy deposited in DNA by a hit is small. However, a finite transverse diffusion significantly reduces the effectiveness for producing TH in hits that involve large energy deposition in DNA because the individual excitations in these hits are dispersed over an appreciable length of the molecule. The results shown in figure 1 were obtained with an initial width of 3·4 Å and an activation energy of 0·2 eV for the protonation reaction.

The predictions of our model for the enhancement of TH yield in the parallel irradiation geometry are shown in figure 2, where an enhancement factor for protonation of $T^{\cdot}$, defined as the ratio of the yield of TH per $T^{\cdot}$ in the parallel and perpendicular irradiation geometries, is plotted as a function of the initial width parameter in units of the base-pair separation, 3·4 Å. The important role of the initial width parameter in our model can be understood from eqn (6), the relationship between energy absorbed and excess temperature. Greater delocalization of plasmon states reduces the initial excess temperature associated with individual energy deposition events. Since protonation of $T^{\cdot}$ in the perpendicular case depends upon energy transfer from a few closely spaced events, it is more dependent on high excess temperature (small initial width) than is protonation in the parallel case. Hence our predicted enhancement of TH increases with the initial width of plasmon excitations in DNA.

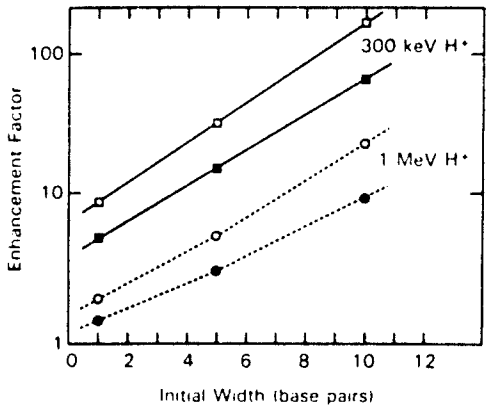

Figure 2. Predicted ratio of $TH^{\cdot}$ yields for parallel and perpendicular irradiation of oriented DNA as a function of the initial width parameter of the model expressed as base pairs separated by 3·4 A. Solid symbols show the effect of a $\pm 10^{\circ}$ uncertainty in the orientation of DNA relative to the proton flux.

Results in figure 2 denoted by closed symbols show that our predicted enhancement of the yield of $TH^{\cdot}$, although reduced, is still significant even when a $\pm 10^{\circ}$ uncertainty in the angle at which the incident particle intersects the DNA fibre axis is assumed. All of the results shown in figure 2 are based on an asymmetry of thermal diffusion equal to 10^{-3} and a distribution of activation energies for the protonation reaction suggested by Gräslund *et al.* (1975). These results predict that the enhancement of $TH^{\cdot}$ yields in the parallel irradiation geometry is dependent on the linear energy transfer (l.e.t.) of the radiation.

It is difficult to compare quantitatively the present calculations with data from the neutron experiments of Arroyo *et al.* (1986), due to the large energy and angular distribution of recoil protons from the neutron spectrum of the TRIGA reactor. However, our results do indicate that long-range intramolecular energy transfer is a possible mechanism for the observed enhancement of $TH^{\cdot}$ radicals when high-l.e.t. radiation is incident on the samples approximately parallel to the orientation of DNA molecules. Some idea of the distance over which energy must be transported if this mechanism is correct can be obtained by calculating the average distance between the site of $T^{\cdot}$ formation and other energy deposition events in the same hit. This distance is shown in table 1 for energy deposited in oriented DNA by a 1 MeV proton

Table 1. Characteristics of the interaction of oriented DNA with 1 MeV protons.

Orientation†	Energy deposited (eV)	Transfer distance (Å)‡
0	293	2240
0 ± 10	150	474
90	62	21
90 ± 10	62	22

† Angle in degrees between helical axis of DNA and proton velocity.
‡ Root-mean-square separation between sites of $T^{\cdot}$ and other excitations.

flux. As would be expected, intramolecular energy transfer distances in our model are comparable to the diameter of the DNA double helix when the proton flux is nearly perpendicular to the helical axis of DNA; however for the parallel case, the average energy-transfer distance is many times greater than the diameter of the molecule.

Our macroscopic model, based on the solution of thermal diffusion equations, does not provide much insight into molecular mechanisms of the assumed energy migration along DNA. Singlet excitons are not a likely candidate for the mobile energy state due to their short lifetime (Georghiou *et al.* 1985) and migration of triplet excitons in DNA with inhomogeneous base sequence is not expected to exceed 10–20 of base pairs (Guéron *et al.* 1974). Asymmetry in phonon-scattering rates has been detected by Raman spectroscopy of oriented DNA (Urabe *et al.* 1983, DeMarco *et al.* 1985), but these low-frequency modes are not expected to be very effective in activating proton transfer to T^-. Hence, although our model calculations show that long-range energy migration in DNA could account for the unusual orientation dependence of TH^- yields observed by Arroyo *et al.* (1986), the molecular basis of this hypothesis remains uncertain. We are currently attempting to include radical recombination in our model to investigate the orientation dependence of the total radical yield. We are also starting experiments with direct proton irradiation of oriented DNA to obtain experimental data with a more well-defined proton flux for comparison with our model predictions.

Acknowledgement

The authors gratefully acknowledge support for this work by the Office of Health and Environmental Research of the United States Department of Energy under contract DE-AC06-76RLO 1830, and by the Defense Nuclear Agency through interagency transfer of funds.

References

Arroyo, C. M., Carmichael, A. J., Swenberg, C. E., and Myers, Jr, L. S., 1986, Neutron-induced free radicals in oriented DNA. *International Journal of Radiation Biology*, **50**, 789–793.

Brandt, W., and Ritchie, R. H., 1974, Primary process in the physical stage. *Physical Mechanism in Radiation Biology*, edited by R. D. Cooper and R. W. Wood (Technical Information Center, USAEC), pp. 20–49.

DeMarco, C., Lindsay, S. M., Pokorny, M., Powell, J., and Rupprecht, A., 1985, Interhelical effects on the low-frequency modes and phase transitions of Li- and Na-DNA. *Biopolymers*, **24**, 2035–2040.

Georghiou, S., Nordlund, T. M., and Saim, A. M., 1985, Picosecond fluorescence decay time measurement of nucleic acids at room temperature in aqueous solution. *Photochemistry and Photobiology*, **41**, 209–212.

Gräslund, A., Ehrenberg, A., Rupprecht, A., and Ström, G., 1971, Ionic base radicals in γ-irradiated DNA. *Biochimica et Biophysica Acta*, **254**, 172–186.

Gräslund, A., Ehrenberg, A., Rupprecht, A., and Ström, G., 1979, U.v.-induced free radicals in oriented DNA. *Photochemistry and Photobiology*, **29**, 245–251.

Gräslund, A., Ehrenberg, A., Rupprecht, A., Tjaldin, B., and Ström, G., 1975, ESR kinetics of a free radical conversion in γ-irradiated oriented DNA. *Radiation Research*, **61**, 488–503.

Gräslund, A., Rupprecht, A., Köhnlein, W., and Hüttermann, J., 1981, Radiation-induced free radicals in oriented bromouracil-substituted DNA. *Radiation Research*, **88**, 1–10.

Guéron, M., Eisinger, J., and Lamola, A. A., 1974, Excited states of nucleic acids. *Basic Principles of Nucleic Acid Chemistry*, Vol. 1, edited by Paul O. P. Ts'o (New York: Academic Press), pp. 311–398.

Hole, E. O., Nelson, W. H., Close, D. M., and Sagstuen, E., 1987, ESR and ENDOR study of the guanine cation: secondary product in 5'-dGMP. *Journal of Chemical Physics*, **86,** 5218–5219.

Hüttermann, J., Volt, K., Oloff, H., Köhnlein, W., Gräslund, A., and Ruppricht, A., 1984, Specific formation of electron gain and loss centres in X-irradiated oriented fibers of DNA at low temperatures. *Faraday Discussions Chemical Society*, **78,** 135–149.

Ruppricht, A., 1966, Preparation of oriented DNA by wet spinning. *Acta Chemica Scandinavica*, **20,** 494–504.

Urabe, H., Tominaga, Y., and Kubota, K., 1983, Experimental evidence of collective vibrations in DNA double helix (Raman spectroscopy). *Journal of Chemical Physics*, **78,** 5937–5939.

Wilson, W. E., and Paretzke, H. G., 1981, Calculation of distributions of energy imported and ionization by fast protons in nanometer sites. *Radiation Research*, **87,** 521–537.

Reprint
Publishers: S. Karger, Basel
Printed in Switzerland

Bonavida, Gifford, Kirchner, Old (eds.), Tumor Necrosis Factor/Cachectin and Related Cytokines. Int. Conf. Tumor Necrosis Factor and Related Cytotoxins, Heidelberg 1987, pp. 246–251 (Karger, Basel 1988)

In vivo Effects and Interactions of Recombinant Interleukin 1 and Tumor Necrosis Factor in Radioprotection and in Induction of Fibrinogen

Ruth Neta

Armed Forces Radiobiology Research Institute, Bethesda, Md., USA

Although interleukin 1 (IL-1) and tumor necrosis factor (TNF) are both produced by stimulated macrophage-monocytes, they are molecularly distinct, act via separate receptors, but show striking resemblance in their biological activity. Both cytokines are pyrogenic [1], induce colony stimulating factor [2] and acute phase proteins [3], activate neutrophils [4, 5], reduce cytochrome P-450 functions [6, 7], and inhibit lipoprotein lipase [8, 9]. Furthermore, IL-1 and TNF have been reported to induce the release of one another [1, 10]. Because of this mutual induction, the relative contribution of IL-1 or TNF to the induction of a given activity becomes difficult to establish. In an attempt to determine whether these two cytokines act independently, we have compared the effect of administrating them separately or in combination on radioprotection and on the induction of an acute phase reactant – fibrinogen. We now report that IL-1 and TNF have synergistic effects on radioprotection and on the levels of circulating fibrinogen.

Materials and Methods

Mice. $B_6D_2F_1$ inbred mice were obtained from Jackson Laboratories, Bar Harbor, Me. The mice were housed in the Veterinary Department Facility at the Armed Forces Radiobiology Research Institute in cages, with Micro-Isolation unit tops, 10 mice/cage. Female mice, 8–12 weeks of age, were used for all experiments. Standard Lab chow and HCl acidified water (pH 2.4) were given ad libitum. All cage-cleaning procedures and injections were carried out in a laminar flow unit.

Cytokines. Human recombinant IL-1α was generously provided by Immunex and by Hoffmann-La Roche. The preparations were supplied in PBS pH 7.2 and 30 m*M* Tris-HCl, 400 m*M* NaCl, pH 7.8, respectively, and used on weight basis. Human recombinant TNFα, lot No. CP4026PO8, specific activity 9.6×10^6 units/mg in PBS was a generous gift from Biogen. All reagents were diluted to the desired concentration in 0.5 ml pyrogen-free saline just prior to the single intraperitoneal injection of mice, 20 h before irradiation. All cytokine preparations were assayed for LPS contamination in LAL assay and determined to contain less than 0.1 ng/inoculum.

Irradiation. Mice were placed in plexiglass containers and were given whole body irradiation at 40 rd/min by bilaterally positioned ^{60}Co elements. The number of surviving mice was recorded daily for 30 days.

Fibrinogen Assay. Mice were bled (retroorbitally) at 20 h after injection of cytokines and the plasma was collected and stored at −20 °C. Assays for fibrinogen in diluted citrated plasma were performed by measuring the rate of conversion of fibrinogen to fibrin in the presence of thrombin excess. The calibration was made using the Sigma Diagnostic Kit. Measurements of fibrin clot formation were performed on a fibrometer (Becton-Dickinson). The data are expressed as milligram fibrinogen per 100 ml plasma.

Results

Radioprotection with hrIL-1α and hrTNFα

We have compared the effect of increasing doses of hrIL-1α and of hrTNFα on protection of lethally irradiated $B_6D_2F_1$ mice ($LD_{95/30}$ = 1,050 rad). IL-1α in doses ranging from 75 to 1,000 ng protected 80–85% of mice from death. Although equivalent doses of hrTNFα had no radioprotective effect, significant radioprotection was obtained with doses ranging from 5 to 10 μg hrTNFα. The maximal degree of radioprotection achieved with the optimal dose of hrTNFα (40–50%) was significantly less than that observed with hrIL-1α. Therefore, hrTNFα is a less effective radioprotector in mice than hrIL-1α. The combination of hrIL-1α and hrTNFα resulted in a synergistic radioprotective effect, at supralethal doses of radiation, with a greater surviving number of mice than predicted from the sum of radioprotection obtained with each cytokine alone (fig. 1). A supralethal dose of 1,150 rad, rather than the usual dose of 1,050 rad, was used in this experiment in order to reduce the radioprotective effects of IL-1 and TNF by themselves, and to reveal interactions between these two cytokines.

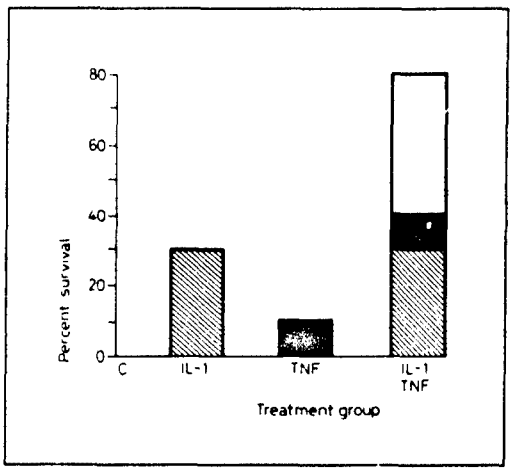

Fig. 1. $B_6D_2F_1$ mice, 8–12 weeks old, received intraperitoneally 0.5 ml saline (control), 0.1 μg IL-1, 5 μg TNF, or a combination of the two, 20 h prior to whole-body supralethal irradiation (1,150 rad). The results show the sum of three experiments consisting of 20–30 mice in each group. The percent survival in the control group was zero.

Table I. In vivo production of fibrinogen by $B_6D_2F_1$ mice in response to hrIL-1α and hrTNFα

Cytokine	Dose, μg	Fibrinogen, mg/dl	Percent increase
IL-1	0.1	256	97
	0.2	290	123
	0.5	342	163
	1.0	392	201
TNF	1.0	181	40
	2.0	225	73
	5.0	212	63
	7.5	221	70
IL-1 + TNF	0.1 + 7.5	422	225[1]
Saline		130	0

The data are representative for one of three experiments, each of which used 3 mice/dose of monokine. Data are the mean for triplicate measurements for each plasma sample. Standard deviations were less than 10% of the mean.

[1] Significantly greater than the 167% predicted increase.

Induction of Fibrinogen with hrIL-1α and/or hrTNFα

The levels of fibrinogen in the plasma of $B_6D_2F_1$ mice 20 h following administration of the two cytokines were also determined. The results in table I show that on a weight basis hrIL-1α induces higher levels of fibrinogen than hrTNFα. Furthermore, an optimal dose of hrIL-1α induces a much higher increase in fibrinogen than the optimal dose of hrTNFα. Administration of hrIL-1α and hrTNFα in combination resulted in a synergistic increase in production of fibrinogen.

Discussion

The overlapping biological effects and mutual induction of hrIL-1α and hrTNFα make it difficult to attribute a given activity to one or the other of these two cytokines. Although our results do not establish the precise contribution of each cytokine to radioprotection and fibrinogen production, the evidence suggests they have independent effects.

The requirement for much higher doses of hrTNFα than hrIL-1α cannot be attributed to lower cross-species activities of TNFα, since we also require similarly higher doses of murine TNFα to obtain radioprotection [unpubl. observations]. Furthermore, the suggestion that the effect of TNF is mediated by IL-1 is unlikely since the synergy of optimal doses of hrIL-1α and hrTNFα in protecting mice against lethal doses of radiation suggests that the effect of these two cytokines is based on different pathways. Although the mechanism of action to achieve radioprotection remains unknown, a number of the activities of IL-1α and TNFα may be related to the radioprotective effect. For example, induction of acute phase proteins, some of which (metallothionein and ceruloplasmin) with the capacity to scavenge free radicals, may contribute to radioprotection [11, 12]. Although IL-1α induction of bone marrow cell cycling [13] may present yet another critical event in radioprotection, TNFα is not known to have this capability. In fact, TNFα has been reported to be inhibitory to hematopoiesis [14, 15]. Several reports exist, however, that TNF has a role in hematopoietic differentiation [16, 17]. This differentiating effect of TNF is most pronounced when TNF is used in conjunction with other cytokines. Whether this effect of TNFα on hematopoietic cells contributes to its radioprotective effect remains to be established.

Elevated plasma levels of fibrinogen have been shown previously to be a consequence of stimulation of hepatocytes [18]. The finding that com-

bined administration of IL-1 and TNF results in more than an additive effect on fibrinogen production, again suggests that the combination of the two signals (IL-1 and TNF) induces distinct rather than overlapping responses by hepatocytes.

IL-1 and TNF are cytokines prominent in inflammation. As such they have a dual role of contributing to host defense as well as being involved in the process of healing and repair. Unfortunately, their conjoint activities, if pronounced, may also be deleterious to the host. The effects of these two cytokines may be regulated and therapeutically useful after sufficient knowledge is acquired concerning their actions and interactions.

Acknowledgements

I wish to thank Dr. J.J. Oppenheim for critical review of the manuscript and Susan D. Douches for technical assistance. This work was supported by the Armed Forces Radiobiology Research Institute, Defense Nuclear Agency, under research work unit MJB3148. The opinions or assertions contained herein are the private views of the author, no endorsement by the Defense Nuclear Agency has been given or should be inferred. The research was conducted according to principles enunciated in the 'Guide for the Care and Use of Laboratory Animals' prepared by the Institute of Laboratory Animal Resources, National Research Council.

References

1 Dinarello, C.A.; Cannon, J.G.; Wolff, S.M.; Bernheim, H.A.; Beutler, B.; Cerami, A.; Figari, I.S.; Palladino, M.A.; O'Conner, J.V.: Tumor necrosis factor (cachectin) is an endogenous pyrogen and induces production of interleukin-1. J. exp. Med. *163:* 1433–1449 (1986).

2 Vogel, S.N.; Douches, S.D.; Kaufman, E.N.; Neta, R.: Induction of colony stimulating factor in vivo by recombinant interleukin-1α and recombinant tumor necrosis factor-α. J. Immun. *138:* 2143–2148 (1987).

3 Sipe, J.D.; Vogel, S.N.; Douches, S.D.; Neta, R.: Tumor necrosis factor/cachectin is a less potent inducer of serum amyloid A synthesis than interleukin-1. Lymphokine Res. *6:* 93–101 (1987).

4 Klempner, M.S.; Dinarello, C.A.; Galin, J.I.: Human leukocytic pyrogen induces release of specific granule contents from human neutrophils. J. clin. Invest. *61:* 1330–1336 (1978).

5 Tsujimoto, M.; Yokota, S.; Vilcek, J.; Weissman, G.: Tumor necrosis factor provokes superoxide anion generation from neutrophils. Biochem. biophys. Res. Commun. *137:* 1094–1100 (1986).

6 Ghezzi, P.; Saccardo, B.; Bianchi, M.: Recombinant tumor necrosis factor depresses cytochrome P-450-dependent microsomal drug metabolism in mice. Biochem. biophys. Res. Commun. *136:* 316–321 (1986).

7 Ghezzi, P.; Saccardo, B.; Villa, P.; Rossi, V.; Bianchi, M.; Dinarello, C.A.: Role of interleukin-1 in the depression of liver drug metabolism by endotoxin. Infect. Immunity *54:* 837–840 (1986).
8 Kawakami, M.; Cerami, A.: Studies of endotoxin-induced decrease in lipoprotein lipase activity. J. exp. Med. *154:* 1631 (1981).
9 Beutler, B.A.; Cerami, A.: Recombinant interleukin-1 suppresses lipoprotein lipase activity in 3T3-L¹ cells. J. Immun. *135:* 3969–3971 (1985).
10 Philip, R.; Epstein, L.B.: Tumor necrosis factor as immunomodulator and mediator of monocyte cytotoxicity induced by itself, gamma-interferon, and interleukin-1. Nature, Lond. *323:* 86–89 (1986).
11 Goldstein, I.M.; Charo, I.F.: Ceruloplasmin: an acute phase reactant and antioxidant; in Pick, Lymphokines, vol. 8, pp. 373–411 (Academic Press, New York 1983).
12 Karin, M.: Metallothioneins: proteins in search of function. Cell *41:* 9–11 (1985).
13 Neta, R.; Sztein, M.B.; Oppenheim, J.J.; Gillis, S.; Douches, S.D.: In vivo effects of IL-1. I. Bone marrow cells are induced to cycle following administration of IL-1. Immun. *139:* 1861–1866 (1987).
14 Peetre, C.; Gullberg, U.; Nilsson, E.; Olsson, I.: Effects of recombinant tumor necrosis factor on proliferation and differentiation of leukemic and normal hemopoietic cells in vitro. J. clin. Invest. *78:* 1694–1700 (1986).
15 Murase, T.; Hotta, T.; Saito, H.; Ohno, R.: Effect of recombinant human tumor necrosis factor on the colony growth of human leukemia progenitor cells and normal hematopoietic progenitor cells. Blood *69:* 467–472 (1987).
16 Trinchieri, G.; Kobayashi, M.; Rosen, M.; Loudon, R.; Murphy, M.; Perussia, B.: Tumor necrosis factor and lymphotoxin induce differentiation of human myeloid cell lines in synergy with immune interferon. J. exp. Med. *164:* 1206–1225 (1986).
17 Munker, R.; Koeffler, P.: In vitro action of tumor necrosis factor on myeloid leukemic cells. Blood *69:* 1102–1108 (1987).
18 Pepys, M.B.; Balz, M.L.: Acute phase proteins with special reference to C-reactive protein and related proteins (pentaxins) and serum amyloid A protein. Adv. Immunol. *34:* 141–212 (1983).

Ruth Neta, PhD, Department of Experimental Hematology,
Armed Forces Radiobiology Research Institute, Bethesda, MD 20814 (USA)

CONCISE REPORT

Cytokines in Therapy of Radiation Injury

By Ruth Neta and J.J. Oppenheim

Repeated injections or infusion of hematopoietic growth factors, such as interleukin-3 (IL-3), granulocyte macrophage-colony stimulating factor (GM-CSF), or granulocyte-colony stimulating factor (G-CSF), accelerate restoration of hematopoiesis in animals compromised by sublethal doses of cytotoxic drugs or irradiation. Previous work by the investigators has shown that IL-1 induced circulating CSF in normal mice and, when used after sublethal irradiation, accelerated the recovery of endogenous splenic colonies. Therefore, IL-1, as well as IFN-γ, tumor necrosis factor (TNF), G-CSF, and GM-CSF, were evaluated as potential therapeutic agents in irradiated C3H-HeN mice. A single intraperitoneal injection, administered within three hours after a lethal dose $(LD)_{95/30}$ of irradiation that would kill 95% of mice within 30 days, protected in a dose-dependent manner up to 100% of mice from radiation-induced death due to hematopoietic syndrome. Significant therapeutic effects were also achieved with a single dose of IFN-γ or of TNF. In contrast, GM-CSF and G-CSF, administered shortly after irradiation, had no effect in the doses used on mice survival.

AS ATTESTED BY the experience with recent nuclear accidents, there is no effective treatment for patients exposed to doses of radiation that result in fatal hematopoietic failure and/or secondary infections. Clinical difficulties due to HLA mismatching, such as graft *v* host (GVH) reactions and graft rejection, minimize the successful use of bone marrow transplantation (BMT) in these situations. Therefore, agents that promote repair of bone marrow damage and improve the recovery of the surviving fraction of cells must be identified.

The investigators have reported previously that the cytokines interleukin-1 (IL-1) and tumor necrosis factor (TNF), but not IL-2, interferon (IFN)-γ, or granulocyte macrophage-colony stimulating factor (GM-CSF), when administered before lethal irradiation, protect mice from death resulting from the hematopoietic syndrome.[1,2] However, the use of IL-1 following lethal irradiation (lethal dose $[LD]_{100/30}$) did not affect survival.[3] It has been reported that the hematopoietic growth factors, IL-3, GM-CSF, G-CSF, and CSF-1, accelerate restoration of hematopoiesis in animals compromised by sublethal doses of radiation or by cytotoxic drugs.[4-9] IL-1 used after irradiation was also effective in accelerating hematopoietic recovery in sublethally (700 cGy) irradiated mice.[10] Furthermore, IL-1 and TNF both induce the appearance of high titers of CSFs in the circulation.[11] The effect of administering a single intraperitoneal dose of IL-1, TNF, GM-CSF, or G-CSF shortly after irradiation of mice has been examined. In addition, IFN-γ was studied to determine if its antiproliferative effect renders it ineffective as a restorative agent.

The investigators present data which show that a single injection of IL-1, in a dose-dependent manner, promotes survival of C3H/HeN mice from a radiation dose that results in death of 95% of control animals within 30 days $(LD_{95/30})$. IFN-γ had a similar effect, TNF also showed limited therapeutic efficacy, while G-CSF and GM-CSF were not effective in promoting survival.

MATERIALS AND METHODS

Mice. A total of 450 C3H/HeN mice were purchased from Animal Genetics and Production Branch, NCI (Frederick, MD), for use in these experiments. Mice were quarantined on arrival and screened for evidence of disease before being released from quarantine. They were maintained in an AAALAC accredited facility in plastic Micro-isolator cages (Lab Products, Maywood, NY) on hardwood chip contact bedding and provided with commercial rodent chow and acidified tap water (HCl to a pH of 2.5) ad libitum. Animal holding rooms were maintained at 70 ± 2°F with 50% ± 10% relative humidity using at least ten air changes per hour of 100% conditioned fresh air. The mice were on a 12-hour light-dark full spectrum lighting cycle with no twilight. Mice were 8 to 10 weeks of age when used. All cage cleaning, handling, and injections were carried out in a laminar flow clean air unit.

Cytokines. Human recombinant IL-1α was generously provided by Immunex (Seattle) and by Hoffman-La Roche (Nutley, NJ). The preparations were supplied in phosphate buffered saline (PBS) at pH 7.2 or in 30 mmol/L tris-HCl, 400 mmol/L NaCl, pH 7.8, respectively, and used on a weight basis. Human recombinant TNF α, lot number CP4026PO8, specific activity 9.6×10^6 U/mg in PBS was a generous gift from Biogen (Cambridge, MA). Murine recombinant GM-CSF was provided by Immunex as a lyophilized powder with sucrose as a stabilizing agent. Human recombinant G-CSF, specific activity 8×10^7 U/mg was a gift from Amgen (Thousand Oaks, CA). Murine recombinant IFN-γ, lot 4296, specific activity 6.8×10^6 U/mg was a gift from Genentech (San Francisco). All reagents were diluted to the desired concentration in pyrogen-free saline just before the single intraperitoneal injection of 0.5 mL to mice, one to three hours after irradiation. All cytokine preparations were assayed for lipopolysaccharide (LPS) contamination in a

From the Department of Experimental Hematology, Armed Forces Radiobiology Research Institute, Bethesda; and Laboratory of Molecular Immunoregulation, National Cancer Institute, Frederick, MD.

Submitted April 5, 1988; accepted May 25, 1988.

Supported by the Armed Forces Radiobiology Research Institute, Defense Nuclear Agency, under research work unit MJB3148. The opinions or assertions contained herein are the private views of the author, no endorsement by the Defense Nuclear Agency has been given or should be inferred. The research was conducted according to principles enunciated in the Guide for the Care and Use of Laboratory Animals *prepared by the Institute of Laboratory Animal Resources, National Research Council.*

Address reprint requests to Ruth Neta, PhD, Defense Nuclear Agency Armed Forces Radiobiology Research Institute, Bethesda, MD 20814.

The publication costs of this article were defrayed in part by page charge payment. This article must therefore be hereby marked "advertisement" in accordance with 18 U.S.C. section. 1734 solely to indicate this fact.

0006-4971/88/7203-0048$3.00/0

limulus ameboycte assay and determined to contain less than 0.1 ng per inoculum.

Irradiation. Mice were placed in plexiglass containers and were given whole body irradiation at 40 cGy/min by bilaterally positioned ^{60}Co elements. The number of surviving mice was recorded daily for 30 days. Preliminary studies established 800 cGy to be the lethal dose for 95% of mice.

Statistical analysis. Statistical evaluation of the results was done using chi-square analysis.

RESULTS

Effect of IL-1. Doses of IL-1 ranging from 0.1 to 0.5 μg, previously shown to be radioprotective, were administered 20 hours before irradiation.[1,2] In this report a broader range of 0.1 to 5.0 μg doses of IL-1 for therapeutic effects was tested. In six consecutive experiments, a dose-dependent beneficial effect of treatment with IL-1 on survival of 800 cGy irradiated mice was observed (Fig 1A). The most effective doses ranged from 1.0 to 5.0 μg. Up to 100% of mice survived if given a single injection of IL-1 within one to three hours after irradiation with an $LD_{95/30}$ dose.

Treatment with TNF. Administration of a high dose of 5.0 μg TNF significantly improved survival ($P < .001$) (Fig 1B). However, on a weight basis, TNF did not equal the therapeutic potency of IL-1.

Effect of GM-CSF and G-CSF. A single injection of a range of doses of either GM-CSF or G-CSF was administered one to three hours after irradiation. None of these treatments had any effect on mice survival (Fig 1C). This differs from reports indicating that multiple injections of these two growth factors accelerate recovery of the hematopoietic system.[4-9]

Treatment with IFN-γ. Administration of 1.25 μg of IFN-γ following irradiation of mice with an $LD_{95/30}$ dose promoted survival ($P < .001$) (Fig 1D). This result is in contrast to the previous observation that IFN-γ was not radioprotective when used before lethal irradiation.[12]

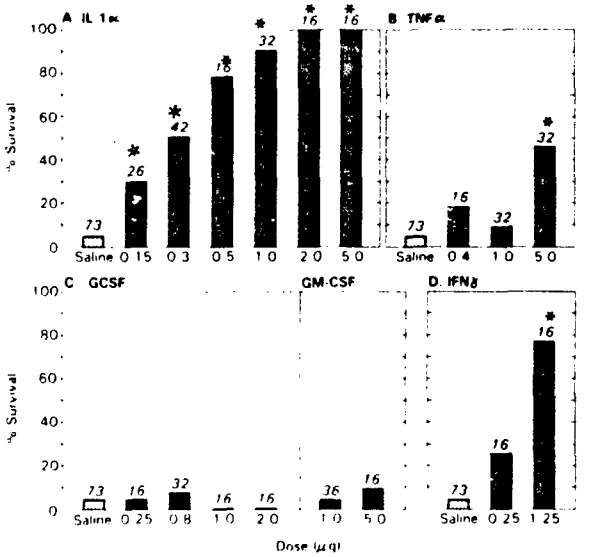

Fig 1. Effect of treatment with cytokines IL-1α (A), TNF-α (B), G-CSF and GM-CSF (C) and IFN-γ (D) after irradiation with 800 rads on survival of C3H-HeN mice. C3H-HeN mice, 8 to 10 weeks old were exposed to ^{60}Coγ irradiation and one to three hours later given intraperitoneal injections of cytokines in doses as specified, or saline. The numbers at the top of the bars represent the total number of mice given each treatment. The data presented summarize the results of six experiments. *$P < .001$, compared with saline controls.

DISCUSSION

The results demonstrated that IL-1, TNF, and IFN-γ can promote survival of $LD_{95/30}$ irradiated mice from radiation-induced death. A single intraperitoneal dose of either cytokine administered one to three hours after irradiation was sufficient to increase mice survival 45% to 100%. Therefore, these data suggest the possibility that IL-1, TNF, and IFN-γ act directly or indirectly to aid in the recovery from radiation damage.

Early studies of damage induced by whole-body exposure to ionizing radiation established the existence of a hematopoietic degenerative phase.[13] This phase lasts for several days depending on the species and is characterized by an initial neutrophilia that lasts for several hours and by the appearance of numerous abnormal myelocytic cells first observed in the marrow and several days later in the blood. The elevated numbers of neutrophils in the blood and the elevation in levels of fibrinogen (Neta, unpublished data, 1988), are indicative of an inflammatory reaction to the radiation induced damage. Furthermore, several laboratories previously reported that ionizing radiation causes an increase in phagocytic and bacteriocidal activity of mature neutrophils and macrophages.[14-16] The inflammatory response in turn presumably assists in recovery from irradiation by removal of damaged tissues and by promoting the restoration of normal function.

Another characteristic of degenerative phase that develops in parallel with neutrophilia is a temporary mitotic inhibition of the dividing cells, the duration of which is radiation-dose-dependent and lasts for several hours in the $LD_{50/30}$ dose ranges.[13] As dividing cells are the most sensitive to radiation damage, it is the repair of these rapidly dividing cells that may be critical for survival. It is therefore possible that IL-1, TNF, and IFN-γ may change the kinetics of proliferation and recovery and/or promote the repair of damaged cells.

The fact that IL-1 is not effective when used after irradiation in treatment of mice given higher radiation doses than $LD_{95/30}$ may indicate that a small number of surviving stem cells or progenitor cells may be the necessary targets of IL-1. An additional explanation may depend on the repair of the damaged progenitor cells that may be achieved with IL-1. The reported production of IL-1 following irradiation[17-20] suggests that endogenously produced IL-1 may also aid in damage repair.

These studies, as well as studies from other laboratories of effect of cytokines on recovery of damage from radiation or cytotoxic drugs are still preliminary. Given the observed success in improving recovery from radiation damage, the effect of cytokines as adjuncts or substitutes for BMT should be carefully evaluated.

ACKNOWLEDGMENT

We wish to thank Drs M.L. Patchen and T.J. MacVittie for critical review of this manuscript, W.E. Jackson for statistical analysis of the results, and S.D. Douches and M. White for technical assistance.

REFERENCES

1. Neta R, Douches SD, Oppenheim JJ: Interleukin-1 is a radioprotector. J Immunol 136:2483, 1986

2. Neta R, Oppenheim JJ, Douches SD: Interdependence of the radioprotective effects of human recombinant Interleukin-1α, tumor necrosis factor α, granulocyte colony stimulating factor and murine recombinant granulocyte-macrophage colony stimulating factor. J Immunol 140:108, 1988

3. Neta R, Douches SD, Oppenheim JJ: Radioprotection by interleukin-1, in Goldstein G, Bach JF, Wigzal H (eds): Immunoregulation by Characterized Polypeptides. UCLA Symposia on Molecular and Cellular Biology. New York, Liss, 1986, pp 429

4. Sieff CA: Hematopoietic growth factors. J Clin Invest 79:1549, 1987

5. Groopman JE: Hematopoietic growth factors: From methyl cellulose to man. Cell 50:5, 1987

6. Cohen AM, Zsebo KM, Inoue H, Hines D, Boone TC, Chazin VR, Tsai L, Ritch T, Souza LM: In vivo stimulation of granulopoiesis by recombinant human granulocyte colony stimulating factor. Proc Natl Acad Sci USA 84:2484, 1987

7. Shimanura M, Kobayashi Y, Yno A, Urabe A, Okabe T, Komatsu Y, Itoh S, Takaku F: Effect of human recombinant granulocyte colony stimulating factor on hematopoietic injury in mice induced by 5-fluorouracil. Blood 69:353, 1987

8. Nienhuis AW, Donahue RE, Karlsson S, Clark SC, Agricola B, Antinoff N, Pierce JE, Turner P, Anderson WF, Nathan DG: Recombinant human GM-CSF shortens the period of neutropenia after autologous bone marrow transplantation in a primate model. J Clin Invest 80:573, 1987

9. Monroy RL, Skelly RR, MacVittie TJ, Davis TA, Sauber JJ, Clark SC, Donahue RE: The effect of recombinant GM-CSF on the recovery of the monkeys transplanted with autologous bone marrow. Blood 70:1996, 1987

10. Neta R, Oppenheim JJ, Douches SD, Giclas PC, Imbra RI, Karin M: Radioprotection with Interleukin-1: Comparison with other cytokines, in Cinader B, Miller RG (eds): Progress in Immunology. San Diego, Academic Press, vol 6, 1986, p 900

11. Vogel SN, Douches SD, Kaufman EN, Neta R: Induction of colony stimulating factor in vivo by recombinant Interleukin-1 and tumor necrosis factor. J Immunol 138:2143, 1987

12. Neta R, Vogel SN, Oppenheim JJ, Douches SD: Cytokines in radioprotection. Comparison of the radioprotective effects of IL-1 to IL-2, GM-CSF, and IFN-gamma. Lymphokine Res 5:105-110, 1986 (suppl)

13. Bond VP, Fliedner TM, Archambeau JO: Mammalian Radiation Lethality. A Disturbance in Cellular Kinetics. San Diego, Academic Press, 1965

14. Mukherjee AK, Starra AJ: The role of the phagocyte in host-parasite interactions. XIV. Effects of concurrent X-irradiation on phagocytosis. J Reticuloendothelial Soc 5:134, 1968

15. Geiger B, Gallily R: Effect of X-irradiation on various functions of murine macrophages. Clin Exp Immunol 16:643, 1974

16. Meyer OT, Dannenberg AM Jr: Radiation, infection, and macrophage function. II. Effect of whole body radiation on the number of pulmonary alveolar macrophages and their levels of hydrolytic enzymes. J Reticuloendothelial Soc 7:79, 1970

17. Geiger B, Fality R, Gery I: The effect of irradiation on the release of lymphocyte activating factor (LAF). Cell Immunol 7:177, 1973

18. Granstein RD, Sander DN: Whole body exposure to ultraviolet radiation results in increased serum Interleukin-1 activity in humans. Lymphokine Res 6:187, 1987

19. Ansel JC, Luger TA, Green I: The effect of in vitro and in vivo UV irradiation on the production of ETAF by human and murine Keratenocytes. J Invest Dermatol 81:519, 1983

20. Ansel JC, Luger TA, Green I: Fever and increased serum IL-1 activity as a systemic manifestation of acute phototoxicity in New Zealand white rabbits. J Invest Dermatol 89:32, 1987

Brain Research, 456 (1988) 49–56
Elsevier

BRI 13782

Effects of dithiothreitol, a sulfhydryl reducing agent, on CA_1 pyramidal cells of the guinea pig hippocampus in vitro

J.M. Tolliver* and T.C. Pellmar

Physiology Department, Armed Forces Radiobiology Research Institute, Bethesda, MD 20814-5145 (U.S.A.)

(Accepted 9 February 1988)

Key words: Dithiothreitol; Hippocampus; Radioprotectant; Intracellular recording

The radioprotectant, dithiothreitol (DTT) has been shown to increase excitability in the hippocampal slice preparation. In the present study, intracellular recording techniques were used to further examine the actions of DTT. Electrophysiological recordings from CA_1 pyramidal cells were obtained prior to, during and after DTT exposure. DTT caused a small depolarization without altering membrane resistance. DTT induced spontaneous firing and occasional burst firing in normally silent neurons. These effects were accompanied by a reduction in spike frequency adaptation but no change in the afterhyperpolarization following a train of action potentials. Following DTT exposure, orthodromic stimulation produced multiple firing. Subthreshold excitatory postsynaptic potentials (EPSPs) were significantly prolonged. Isolating the CA_1 subfield, attenuated the prolongation of the EPSP by DTT. Recurrent inhibitory postsynaptic potentials were unaffected by DTT. The actions of DTT are likely to result from DTT-induced reduction of disulfide bonds since the reduced form of DTT does not cause a similar hyperexcitability.

INTRODUCTION

The hippocampus is vulnerable to radiation damage. Following exposure to X-radiation, spiking activity appears in electroencephalographic recordings from this area of the brain[12,15,33]. Single unit recordings in vivo show that neuronal firing patterns in the hippocampus are disrupted by radiation[2]. In vitro studies indicate that γ-radiation can impair both synaptic and extrasynaptic mechanisms in the hippocampus[41].

Dithiothreitol (DTT), a disulfide reducing agent[4], has been used as a radioprotectant in cellular and enzyme systems[17,18,31,32]. It is thought to act both by scavenging free radicals[18,31,32] and by donating hydrogen to damaged macromolecules[18]. Many studies have demonstrated that DTT affects neurotransmitter systems including acetylcholine[3,16,21,25,30] dopamine[37], opiates[27], norepinephrine[24,28] and histamine[10,11]. All these transmitters are effective agents in the hippocampal slice (for review see ref. 6). A previous study showed that DTT increases hippocampal excitability, causing spontaneous and evoked burst firing[40]. Both synaptic and extrasynaptic mechanisms were implicated. The present study uses intracellular recording techniques to examine the mechanism(s) whereby DTT increases neuronal excitability. Preliminary results have been presented elsewhere[39].

MATERIALS AND METHODS

Hippocampal slices (400–450 μm thick) were prepared from euthanized male Hartley guinea pigs as previously described[20,40]. Slices were incubated at room temperature in oxygenated solution (see below) for at least 2 h to allow recovery from the dissection. One slice was then placed in a submerged slice chamber (Zbicz design)[44]. The tissue was continuously superfused (0.8–1.0 ml/min) with a solution

* Present address: Drug Enforcement Administration, Office of Diversion Control, Washington, D.C. 20537, U.S.A.
Correspondence: T. Pellmar, Physiology Department, Armed Forces Radiobiology Research Institute, Bethesda, MD 20814-5145, U.S.A.

containing (in mM): NaCl 124, KCl 3.0, $CaCl_2$ 2.4, $MgSO_4$ 1.3, KH_2PO_4 1.24, $NaHCO_3$ 26.0 and glucose 10.0, oxygenated with 95% O_2–5% CO_2 and maintained at 30° ± 1 °C.

DTT, obtained from Calbiochem (Lot numbers 233153 and 410163), was dissolved in the bathing solution immediately prior to use to give a final concentration of 0.5 mM. After obtaining control data, the slices were superfused with the DTT solution for 25 min. This dose and exposure time were chosen because they consistently increased excitability in the field potential recordings. Subsequent to DTT exposure, slices were superfused with normal solution for the remainder of the experiment. Data were collected for a minimum of 60 min after the initial exposure to DTT.

Concentric, bipolar stainless steel electrodes were used to provide constant-current stimuli (up to 0.5 mA, 200 μs duration, 0.2 Hz) to hippocampal pathways. Cells in the CA_1 region of hippocampus were orthodromically activated by stimulation of afferent fibers in the stratum radiatum. Antidromic potentials were elicited by stimulation of the alveus.

Intracellular recordings from CA_1 pyramidal cells were obtained through electrodes filled with either 2 M KCl (20–40 MΩ) or 4 M potassium acetate (70–100 MΩ). A conventional bridge circuit (Dagan 8100) allowed potential recording and intracellular current injection via the same electrode. The bridge was balanced frequently by passing pulses of current and monitoring the potential on the oscilloscope. Data were recorded on a Gould chart recorder and a Tektronix oscilloscope, and were digitized and stored on an LSI 11-03 minicomputer. In all experiments, somatic field potentials were monitored concurrently using electrodes (1–10 MΩ) filled with 2 M NaCl. Field potentials were amplified using a high-gain differential preamplifier. They were either photographed directly off the oscilloscope or digitized, and stored on an LSI 11-03 minicomputer.

The effects of DTT on the following electrophysiological parameters were examined: membrane potential, input resistance, spike frequency adaptation, afterhyperpolarization (AHP), excitatory postsynaptic potentials (EPSPs) and inhibitory postsynaptic potentials (IPSPs). Membrane resistance was calculated from the membrane potential change produced by injections of 0.25 or 0.50 nA hyperpolarizing current. To study spike frequency adaptation, suprathreshold depolarizing current pulses of 700 ms duration were applied via the recording electrode at 0.05–0.1 Hz. An AHP was elicited every 10–20 s by injecting a train of 4 suprathreshold depolarizing current pulses (8 ms duration, 80 Hz). EPSPs were evoked by stimulation (10–75 μA) of the stratum radiatum and recurrent IPSPs by stimulation (25–100 μA) of the alveus. In several experiments the CA_1 region was isolated; CA_2 and CA_3 were removed by cutting the slice with a scalpel blade. No attempt was made to verify histologically that all of the CA_2 and CA_3 region was removed in these experiments. The slice was allowed to recover from the isolation procedure for at least 45 min before attempting to impale CA_1 neurons.

RESULTS

As previously reported[40], field potential recordings in field CA_1 of hippocampus revealed an increase in excitability following exposure to 0.5 mM DTT for 25 min. Twenty to 40 min after initial exposure to DTT, the baseline 'noise' level increased in the extracellular recordings from stratum radiatum. This was followed by an increase in the amplitude of the orthodromic population spike and the emergence of multiple (3–7) peaks in the orthodromic field potential (Fig. 1A). This effect was sustained for the duration (1–2 h) of the experiment.

The increased excitability produced by DTT was further examined in CA_1 pyramidal cells with intracellular recording techniques. Prior to drug exposure, CA_1 pyramidal cells were generally silent; spontaneous action potentials were rare. Twenty to 40 min following initial exposure to 0.5 mM DTT, spontaneous activity was always evident (Fig. 1B). This effect coincided with the appearance of 'noise' in the extracellular recording. In approximately 60% of the cells, spontaneous doublets and burst firing occurred in an irregular pattern. Similar spontaneous bursting activity was observed in field potential recordings[40].

The intracellular changes were accompanied by a small, but statistically significant depolarization of the membrane potential. The mean (± S.E.M.) resting potential of all 25 cells before exposure to DTT was −64.6 ± 0.8 mV. Sixty minutes after initial expo-

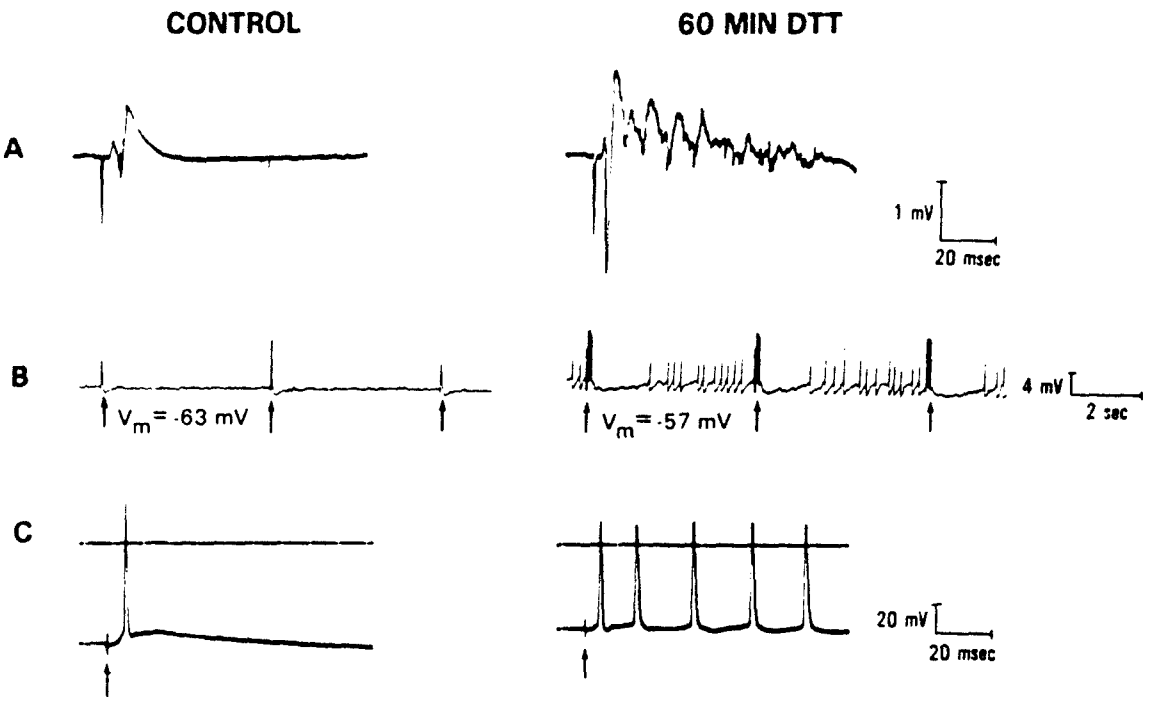

Fig. 1. DTT altered the orthodromic activity in CA_1 of the hippocampal slice. A: orthodromic field potentials in response to stimulation of the stratum radiatum prior to and 60 min after beginning exposure to DTT (0.5 mM). DTT increased the amplitude of the initial population spike and caused multiple spiking. B: DTT induced spontaneous action potential firing, increased synaptic input and caused some membrane depolarization. At the arrows, stratum radiatum was stimulated. Action potentials were truncated by the chart recorder. C: orthodromic action potentials recorded from CA_1 pyramidal cell. Straight line indicates zero potential. The onset of multiple spiking in the orthodromic field potential coincided with the appearance of multiple firing recorded intracellularly.

sure to DTT the membrane potential was depolarized to -61.6 ± 0.7 mV (Student's t-test for paired samples, $n = 25$, $P < 0.05$). DTT did not significantly alter the input resistance of CA_1 pyramidal cells. The input resistance in control was 41.7 ± 4.7 MΩ and following exposure to DTT was 44.0 ± 5.0 MΩ ($n = 12$, $P > 0.05$).

Increased excitability of CA_1 pyramidal cells was evident when they were stimulated orthodromically. In control, the stimulus applied to the stratum radiatum was adjusted to elicit an EPSP with a single action potential (Fig. 1C, Control). After exposure to DTT, the same orthodromic stimulus evoked multiple (3–7) action potentials (Fig. 1C). The onset of multiple firing of pyramidal cells in response to orthodromic stimulation coincided with the appearance of multiple spiking in the orthodromic field potential (Fig. 1A, C). Even when membrane potential was maintained at pre-DTT levels, multiple spikes were elicited by orthodromic stimulation. Subthreshold EPSPs were examined in 5 cells. Comparisons of EPSPs before and after DTT exposure were always made at the same membrane potential. The rate of rise and the amplitude of the early component of the EPSP were not significantly affected by DTT (Fig. 2A). The mean amplitude in control was 6.2 ± 0.5 mV while after exposure to DTT was 5.9 ± 0.6 mV ($n = 5$, $P > 0.05$). The rate of rise of the EPSP was 1.4 ± 0.2 mV/ms in control and 1.5 ± 0.2 mV/ms after DTT exposure ($n = 5$, $P > 0.05$). Similarly, the extracellularly recorded population synaptic response showed no change in the initial slope[40]. DTT did, however, consistently, prolong the EPSP (Fig. 2A). DTT increased the mean duration from 40.5 ± 4.4 to 91.4 ± 13.3 ms ($n = 4$, $P < 0.05$) measured from the initial depolarization to the time it returned to the resting membrane potential. The shape of the EPSP depended on stimulus strength. Stimulation with very low currents could evoke only a delayed depolarizing potential with no initial EPSP. As the stim-

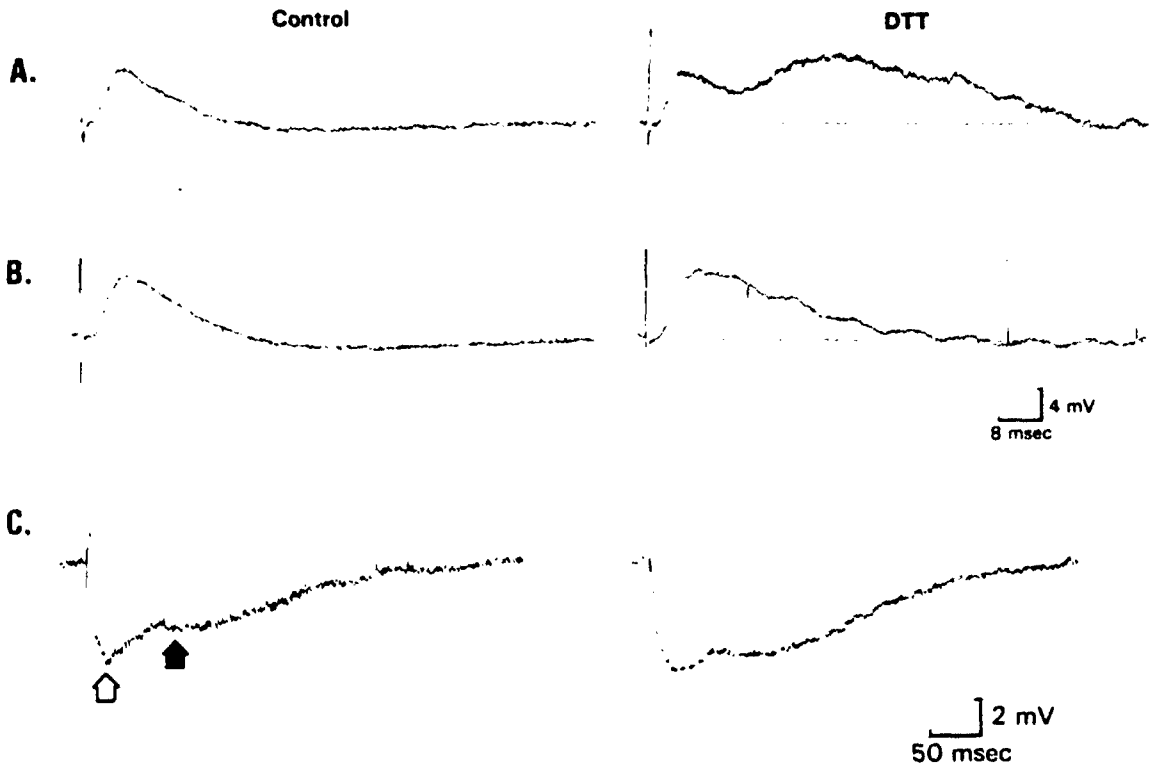

Fig. 2. DTT prolonged the EPSP but did not block recurrent inhibition. A: EPSPs recorded from a CA_1 pyramidal cell prior to and 45 min after starting superfusion with 0.5 mM DTT. DTT had little effect on the rate of rise or the amplitude of the EPSP. The EPSP was, however, prolonged. Both traces were recorded at a membrane potential of −68 mV. B: EPSPs recorded from a pyramidal cell located in the isolated CA_1 region. EPSP prior to DTT exposure (control) and 45 min after initial exposure to DTT. DTT was less effective in prolonging the EPSP in the isolated CA_1 region than in the intact slice. Traces in B were recorded at a membrane potential of −63 mV. C: recurrent IPSPs were elicited in CA_1 pyramidal cell by subthreshold stimulation of the alveus. DTT (0.5 mM) did not block the early (open arrow) or late (filled arrow) phase of the IPSP. IPSP was measured with membrane potential at −60 mV.

ulus strength was increased, both the initial EPSP and the delayed depolarizing potential became larger. With further increases in stimulus strength, the EPSP and the later depolarizing potential merged together to form the prolonged EPSP. At sufficient stimulus strength, the longer latency depolarizing potential reached threshold, resulting in action potential firing.

Stimulation of stratum radiatum might antidromically activate CA_2-CA_3, which could cause late synaptic activation of CA_1 pyramidal cells, and thus prolong the EPSP. To examine this possibility, the effects of DTT on the EPSP were examined in slices in which CA_1 was isolated by removal of CA_2-CA_3. Slices were allowed to recover for at least 45 min before intracellular recording. Cells in the isolated sections did not show any signs of injury. Resting membrane potential (−62.4 ± 1.2 mV, $n = 3$) and membrane resistance (44.7 ± 5.4 MΩ, $n = 3$) were not significantly different from control values in intact slices. In the isolated CA_1 regions, DTT increased the EPSP duration from 49.3 ± 6.6 to 69.6 ± 11.8 ms ($n = 3$, $P < 0.05$) (Fig. 2B). Two of the 3 cells tested showed a minimal increase in duration (40–54.3 ms and 40–51.4 ms). The EPSP of the third cell, however, was greatly prolonged (68–103 ms). These results contrasted with those of the intact slice where the EPSP of all 5 cells showed a substantial increase in duration. The variability observed in the isolated sections may be due to the degree of isolation of CA_1 actually achieved.

DTT might also increase excitability by decreasing recurrent inhibition. IPSPs were elicited by subthreshold stimulation of the alveus. Despite the ap-

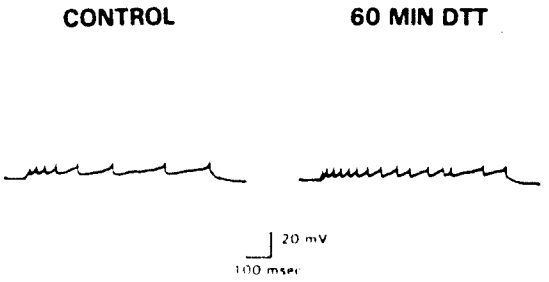

Fig. 3. DTT decreased spike frequency adaptation recorded from CA_1 pyramidal cell. Spike frequency adaptation was examined by stimulating a cell with depolarizing current pulses of 700 ms duration. Recordings were made prior to (Control) and 60 min after starting DTT exposure. Membrane potential remained at -65 mV.

pearance of increased excitability, DTT did not reduce the amplitude of the early or the late phase of the recurrent IPSP (early IPSP, control 5.4 ± 0.6 mV, DTT 5.2 ± 0.5 mV; late IPSP, control 2.3 ± 0.6 mV, DTT 2.1 ± 1.3 mV, $n = 3$, $P > 0.05$) (Fig. 2C). The duration of the IPSP also did not change following exposure to DTT (control, 319.2 = 38.6 ms; DTT, 301.8 ± 60.0 ms, $n = 3$, $P > 0.05$).

A depolarizing current pulse of 700 ms duration produced a train of action potentials that decreased in frequency during the step (Fig. 3). This phenomenon, spike frequency adaptation, has been well described in hippocampal neurons[26]. Spike frequency adaptation was examined prior to and after DTT exposure in 4 cells (Fig. 3). DTT decreased spike frequency adaptation in all cells examined. DTT more than doubled (2.29 ± 0.25 times, $n = 3$) the number of action potentials elicited by 700 ms depolarizing step. The increased number of action potentials did not result from a change in the resting membrane potential or input resistance. There was no obvious change in the shape of the evoked action potentials.

Spike frequency adaptation is, in part, due to the temporal summation of the calcium-dependent slow AHP. The effects of DTT on the AHP produced by a train of 4 action potentials were examined in 4 cells. As shown in Fig. 4, DTT did not alter the early or late phase of the AHP. In control, the late AHP was 6.75 ± 1.60 mV while after exposure to DTT, the AHP was 6.38 ± 1.55 mV ($n = 4$, $P > 0.05$).

DISCUSSION

This study demonstrates that DTT increases the excitability of CA_1 pyramidal cells in the hippocampal slice. This increased excitability is manifested by the appearance of the following phenomena recorded from CA_1 pyramidal cells: (1) spontaneous spiking and occasional spontaneous bursting activity; (2) abnormal repetitive firing in response to orthodromic stimulation; and (3) a reduction in spike frequency adaptation. The appearance of these intracellular events coincides with the onset of changes in the orthodromic field potential recordings reported previously[40].

A prolongation of the EPSP appears to be responsible for the repetitive firing elicited by orthodromic stimulation following treatment with DTT. One mechanism that could account for the increased EPSP duration is the blockade of inhibitory inputs to the pyramidal cells. The convulsants bicuculline and penicillin prolong the EPSP through this action[6-9,34]. In contrast to these agents DTT does not alter the recurrent IPSP. Feedforward inhibition was not tested, however, and may be affected by DTT.

An alternative mechanism for EPSP prolongation is inhibition of the reuptake of the excitatory neurotransmitter. The transmitter released by Schaffer collaterals at the CA_1 pyramidal cells is thought to be the excitatory amino acid, glutamate[5,36]. Considering that DTT (0.5 mM) decreases γ-aminobutyric acid reuptake[20], it is feasible that through a similar mech-

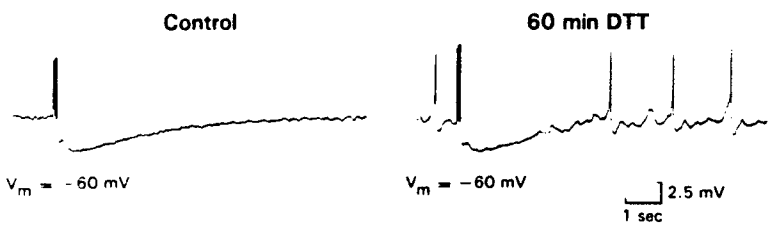

Fig. 4. DTT did not alter the early or the late phase of the AHP following 4 action potentials evoked by a train of 4 suprathreshold current pulses (8 ms, 80 Hz). Traces were recorded prior to and 60 min following the start of DTT superfusion.

anism. DTT could impair the reuptake of excitatory amino acids. The multiphasic shape of the prolonged EPSP following DTT exposure is inconsistent with this possibility.

A third mechanism for prolongation of the EPSP is that DTT alters the interaction of the CA_1 and the CA_2 CA_3 subfields. Stimulation of the stratum radiatum to elicit an orthodromic response in CA_1 also antidromically activates the CA_2 CA_3 region. If the excitability of this region was elevated by DTT, then stimulation of the stratum radiatum could result in a reverberating circuit between CA_1 and the CA_2 CA_3 subfields. Thus a reactivation of CA_1 resulting from the delayed firing of the CA_2 CA_3 region would prolong the EPSP[14,43]. Support for this hypothesis comes from the observation that DTT seems to be less effective in prolonging the EPSP in isolated CA_1 regions than in intact slices. In addition, it was possible to stimulate the stratum radiatum at a sufficiently low stimulus strength to evoke a long latency potential in the absence of an early EPSP. This longer latency potential most likely represents activation of CA_1 resulting from the delayed firing of the CA_2-CA_3 region in response to the stimulation of the stratum radiatum.

DTT probably does not increase excitability of CA_1 pyramidal cells by increasing transmitter release or by enhancing sensitivity of the receptor mediating normal synaptic excitation. If these mechanisms were responsible for the increased excitability, DTT would be expected to increase the amplitude and rate of rise of the EPSP. Instead, DTT had minimal effects on these parameters. Although the neurotransmitter mediating the EPSP produced by Schaffer collateral stimulation is uncertain, it is likely to be glutamate[5,36]. To date, no effects of DTT on the excitatory amino acid receptors have been reported. DTT does not alter the response of *Onchidium* esophageal ganglia to applied L-glutamate[22]. Other sulfhydryl modifying reagents such as mercuric chloride, *n*-chloromercuribenzoate and *n*-ethylmaleimide depress rather than enhance glutamate and kainate responses recorded from pyramidal neurons of the rat hippocampus[23].

Extracellular recordings suggested that DTT increased excitability through both synaptic and extrasynaptic mechanisms[40]. Most neurons were somewhat depolarized following exposure to DTT. Similarly Terrar[38] observed that a 30-min exposure to DTT caused a small depolarization in muscle. Such a mechanism is not likely to explain all the actions of DTT, however. The oxidized form of DTT (*trans*-4,5 dihydroxy-1,2 dithiane, OxDTT) was found in extracellular experiments to be ineffective in inducing multiple spiking in the orthodromic field potential[40]. Preliminary intracellular experiments indicate that, although OxDTT causes a similar depolarization (3–8 mV), it does not induce burst firing.

DTT decreased spike frequency adaptation. This effect would promote repetitive firing since normal mechanisms to attenuate trains of actions potentials are impaired. The calcium-dependent potassium current contributes significantly to regulation of firing frequency in hippocampal pyramidal cells[26]. A decrease in this current, however, is unlikely to be the mechanism since the AHP (resulting from the calcium-dependent potassium current[1,13,19,35,42]) is unaffected by DTT.

In conclusion, DTT increases the excitability of the hippocampus in vitro. This effect probably results from DTT-induced reduction of disulfide bonds since the reduced form, OxDTT, does not cause similar hyperexcitability. DTT is known to interact with a number of neurotransmitter systems which are present in the hippocampus. Although stimulation of stratum radiatum predominantly activates the Schaffer collaterals and therefore an excitatory amino acid pathway, other inputs and other transmitter systems are likely to be activated. It is not unlikely that alteration of these systems would contribute to the dysfunction of the hippocampus following DTT exposure. The abnormal activity produced by DTT in neural tissue would limit its usefulness as a radioprotectant.

ACKNOWLEDGEMENTS

Supported by the Armed Forces Radiobiology Research Institute, Defense Nuclear Agency, under work unit 00105. Views presented in this paper are those of the authors; no endorsement by the Defense Nuclear Agency has been given or should be inferred. Research was conducted according to the principles enunciated in the 'Guide for the Care and Use of Laboratory Animals' prepared by the Institute of Laboratory Animal Resources, National Research Council.

REFERENCES

1 Alger, B.E. and Nicoll, R.A., Epileptiform burst afterhyperpolarization: a calcium dependent potassium potential in hippocampal CA1 pyramidal cells, *Science*, 210 (1980) 1122–1124.

2 Bassant, M. and Court, L., Effect of whole-body irradiation on the activity of rabbit hippocampal neurons, *Radiat. Res.*, 75 (1978) 593–606.

3 Brown, D.A. and Kwiatkawski, D., A note on the effect of dithiothreitol (DTT) on the depolarization of isolated sympathetic ganglia by carbachol and bromoacetylcholine, *Br. J. Pharmacol.*, 56 (1976) 128–130.

4 Cleland, W.W., Dithiothreitol, A new protective reagent for SH groups, *Biochemistry*, 3 (1964) 480–482.

5 Cotman, C.W. and Nadler, J.V., Glutamate and aspartate as hippocampal transmitters: biochemical and pharmacological evidence. In P.J. Roberts, J. Storm-Mathisen and G.A.R. Johnson (Eds.), *Glutamate: Transmitter in the Central Nervous System*, Wiley and Sons, New York, 1981, pp. 117–154.

6 Dingledine, R., Hippocampus: synaptic pharmacology. In R. Dingledine (Ed.), *Brain Slices*, Plenum, New York, 1984, pp. 87–112.

7 Dingledine, R. and Gjerstad, L., Penicillin blocks hippocampal i.p.s.p.s unmasking prolonged e.p.s.p.s, *Brain Research*, 168 (1979) 205–209.

8 Dingledine, R. and Gjerstad, L., Reduced inhibition during epileptiform activity in the in vitro hippocampal slice, *J. Physiol. (Lond.)*, 305 (1980) 297–313.

9 Dingledine, R., Hynes, M.A. and King, G.L., Involvement of *N*-methyl-D-aspartate receptors in epileptiform bursting in the rat hippocampal slice, *J. Physiol. (Lond.)*, 380 (1986) 175–189.

10 Donaldson, J. and Hill, S.J., Enhancement of histamine N_1-receptor agonist activity by 1,4-dithiothreitol in guinea-pig cerebellum and cerebral cortex, *J. Neurochem.*, 47 (1986) 1476–1482.

11 Donaldson, J. and Hill, S.J., 1,4-Dithiothreitol-induced alteration in histamine H_1-agonist binding in guinea-pig cerebellum and cerebral cortex, *Eur. J. Pharmacol.*, 129 (1986) 25–31.

12 Gangloff, H., Acute effects of X-irradiation on brain electrical activity in cats and rabbits. In *Effects of Ionizing Radiation on the Nervous System*, International Atomic Energy Agency, Vienna, 1962, pp. 123–135.

13 Gustafsson, B. and Wigstrom, H., Evidence for two types of afterhyperpolarization in CA1 pyramidal cells in the hippocampus, *Brain Research*, 206 (1981) 462–468.

14 Hablitz, J.J., Picrotoxin-induced epileptiform activity in hippocampus: role of endogenous versus synaptic factors, *J. Neurophysiol.*, 51 (1984) 1011–1027.

15 Haley, T.J., Changes induced in brain activity by low doses of X-irradiation. In *Effects of Ionizing Radiation on the Nervous System*, International, Atomic Energy Agency, Vienna, 1962, pp. 123–135.

16 Hedlund, B. and Bartfai, T., The importance of thiol and disulfide groups in agonist and antagonist binding to the muscarinic receptor, *Mol. Pharmacol.*, 15 (1979) 531–544.

17 Held, K.D., Interactions of radioprotectors and oxygen in cultured mammalian cells. I. Dithiothreitol effects on radiation-induced cell killing, *Radiation Res.*, 101 (1985) 424–433.

18 Held, K.D., Harrop, H.A. and Michael, B.D., Effects of oxygen and sulfhydryl-containing compounds on irradiated transforming DNA. II. Glutathione, cysteine, and cysteamine, *Int. J. Radiat. Biol.*, 45 (1984) 615–626.

19 Hotson, J.R. and Prince, D.A., A calcium-activated hyperpolarization follows repetitive firing in hippocampal neurons, *J. Neurophysiol.*, 43 (1980) 409–419.

20 Iversen, L.L. and Johnston, G.A.R., GABA uptake in rat central nervous system: comparison of uptake in slices and homogenates and the effects of some inhibitors, *J. Neurochem.*, 18 (1971) 1939–1952.

21 Karlin, A. and Bartels, E., Effects of blocking sulphydryl groups and of reducing disulphide bonds on the acetylcholine-activated permeability system of the electroplax, *Biochim. Biophys. Acta*, 126 (1966) 525–535.

22 Kato, M., Oomura, Y. and Maruhashi, J., Effects of chemical modification on the L-glutamate receptors on the *Onchidium* neurons, *Jap. J. Physiol.*, 33 (1983) 535–546.

23 Kiskin, N.I., Krishtal, O.A., Tsyndrenko, A.Ya. and Akaike, N., Are sulfhydryl groups essential for function of the glutamate-operated receptor–ionophore complex, *Neurosci. Lett.*, 66 (1986) 305–310.

24 Lucas, M., Hanoune, J. and Bockaert, J., Chemical modification of the beta adrenergic receptor coupled with adenylate cyclase by disulfide bridge-reducing agents, *Mol. Pharmacol.*, 14 (1978) 227–236.

25 Lukas, R.J. and Bennett, E.L., Chemical modification and reactivity of sulfhydryls and disulfides of rat brain nicotinic-like acetylcholine receptors, *J. Biol. Chem.*, 255 (1980) 5573–5577.

26 Madison, D.V. and Nicoll, R.A., Control of the repetitive discharge of rat CA1 pyramidal neurones in vitro, *J. Physiol. (Lond.)*, 354 (1984) 319–331.

27 Marzullo, G. and Hine, B., Opiate receptor function may be modulated through an oxidation-reduction mechanism, *Science*, 208 (1980) 1171–1173.

28 Pederson, S.E. and Ross, E.M., Functional activation of beta-adrenergic receptors by thiols in the presence or absence of agonists, *J. Biol. Chem.*, 260 (1985) 14150–14157.

29 Pellmar, T.C., Electrophysiological correlates of peroxide damage in guinea pig hippocampus in vitro, *Brain Research*, 364 (1986) 377–381.

30 Rang, H.P. and Ritter, J.M., The effects of disulphide bond reduction on the properties of cholinergic receptors in chick muscle, *Mol. Pharmacol.*, 7 (1971) 620–631.

31 Redpath, J.L., Pulse radiolysis of dithiothreitol, *Radiation Res.*, 54 (1973) 364–374.

32 Redpath, J.L., Radioprotection of enzyme and bacterial systems by dithiothreitol, *Radiation Res.*, 55 (1973) 109–117.

33 Schoenbrun, R.L., Campeau, E. and Adey, W.R., Electroencephalographic and behavioral effects from x-irradiation of the hippocampal system. In T.J. Haley and R.S. Snider (Eds.), *Response of the Nervous System to Ionizing Radiation, Second International Symposium*, Little and Brown, Boston, 1964, pp. 411–428.

34 Schwartzkroin, P.A. and Prince, D.A., Changes in excitatory and inhibitory potentials leading to epileptogenic activity, *Brain Research*, 183 (1980) 61–76.

35 Schwartzkroin, P.A. and Stafstrom, C.E., Effects of EGTA on the calcium-activated afterhyperpolarization in hippocampal CA3 pyramidal cells, *Science*, 210 (1980) 1125–1126.

36 Storm-Mathisen, J., Localization of transmitter candidates in the brain: the hippocampal formation as a model, *Prog.*

Neurobiol., 8 (1977) 119–181.

37 Suen, E.T., Stefanini, E. and Clement-Cormier, Y.C., Evidence for essential thiol groups and disulfide bonds in agonist and antagonist binding to the dopamine receptor, *Biochem. Biophys. Res. Commun.*, 96 (1980) 953–960.

38 Terrar, D.A., Effects of dithiothreitol on end-plate currents, *J. Physiol. (Lond.)*, 276 (1978) 403–417.

39 Tolliver, J.M. and Pellmar, T.C., Intracellular analysis of dithiothreitol effects on guinea pig CA1 pyramidal cells, *Soc. Neurosci. Abstr.*, 12 (1986) 676.

40 Tolliver, J.M. and Pellmar, T.C., Dithiothreitol elicits epileptiform activity in CA1 of the guinea pig hippocampal slice, *Brain Research*, 404 (1987) 133–141.

41 Tolliver, J.M. and Pellmar, T.C., Ionizing radiation alters neuronal excitability in hippocampal slices of the guinea pig, *Radiation Res.*, 112 (1987) 555–563.

42 Wong, R.K.S. and Prince, D.A., Afterpotential generation in hippocampal pyramidal cells, *J. Neurophysiol.*, 45 (1981) 86–97.

43 Wong, R.K.S. and Traub, R.D., Synchronized burst discharge in disinhibited hippocampal slice. I. Initiation in CA2-CA3 region, *J. Neurophysiol.*, 49 (1983) 442–458.

44 Zbicz, K.L. and Weight, F.F., Transient voltage and calcium dependent outward currents in hippocampal CA3 pyramidal neurons, *J. Neurophysiol.*, 40 (1985) 1038–1058.

INFECTION AND IMMUNITY, Oct. 1988, p. 2650–2657
0019-9567/88/102650-08$02.00/0

Vol. 56, No. 10

Recombinant Interleukin-1α and Recombinant Tumor Necrosis Factor α Synergize In Vivo To Induce Early Endotoxin Tolerance and Associated Hematopoietic Changes

STEFANIE N. VOGEL,[1]* ERIC N. KAUFMAN,[1] MICHELE D. TATE,[1] AND RUTH NETA[2]

Department of Microbiology, Uniformed Services University of the Health Sciences, 4301 Jones Bridge Road,[1] and Department of Experimental Hematology, Armed Forces Radiobiology Research Institute,[2] Bethesda, Maryland 20814

Received 25 April 1988/Accepted 11 July 1988

Endotoxin, the lipopolysaccharide (LPS) derived from gram-negative bacteria, invokes a wide range of responses in susceptible hosts. It is known that virtually all responses to LPS are mediated by the action of macrophage-derived cytokines (such as interleukin-1 [IL-1], tumor necrosis factor [TNF], and others) which are produced principally by macrophages and maximally within several hours of LPS administration. One manifestation of LPS administration which is not well understood is the phenomenon of "early endotoxin tolerance." In response to a single sublethal injection of LPS, experimental animals become refractory to challenge with a homologous or heterologous LPS preparation 3 to 4 days later. Animals rendered tolerant exhibit mitigated toxicity and a reduced capacity to produce circulating cytokines (i.e., colony-stimulating factor or interferon) in response to the challenge LPS injection. Previous studies have also shown that this state of transient, acquired hyporesponsiveness to LPS is accompanied by a marked increase in the size of cells in the bone marrow which are enriched in numbers of macrophage progenitors. In this study, we examined the capacity of recombinant IL-1 or recombinant TNF or both to induce early endotoxin tolerance and its associated hematopoietic changes. Neither cytokine alone was able to mimic LPS for induction of tolerance. Combined administration of recombinant IL-1 and recombinant TNF doses which were not toxic when administered individually led to synergistic toxicity (as assessed by death or weight loss). However, within a nontoxic range, the two cytokines synergized to induce a significant reduction in the capacity to produce colony-stimulating factor in response to LPS, as well as the characteristic increase in bone marrow cell size and macrophage progenitors shown previously to be associated with LPS-induced tolerance.

Endotoxin, the lipopolysaccharide (LPS) component of gram-negative bacterial outer membranes, induces in vivo many of the pathophysiologic changes associated with systemic gram-negative bacterial infection (reviewed by S. N. Vogel and M. M. Hogan, *in* J. J. Oppenheim and E. Sherach, ed., *Immunophysiology: Role of Cells and Cytokines in Immunity and Inflammation*, in press). Among these are fever, hypoglycemia, hypotension, shock, and even death. Several lines of evidence support the hypothesis that the macrophage is the principal cellular mediator of endotoxicity and, more specifically, that LPS-induced, macrophage-derived soluble factors are the direct mediators of endotoxic phenomena. First, LPS-stimulated macrophages produce in vitro many of the same soluble factors which circulate in the serum following in vivo administration of LPS. These include interleukin-1 (IL-1), tumor necrosis factor (TNF; also referred to as cachectin), interferon, colony-stimulating factor (CSF), and prostaglandins of the E series. When purified and injected into experimental animals in the absence of LPS, many of these soluble factors have been shown to induce one or more of the effects of in vivo LPS treatment. Agents which increase macrophage activation greatly increase endotoxin sensitivity in vivo, even in the genetically LPS-hyporesponsive C3H/HeJ mouse strain (23, 27). Increased sensitivity to LPS correlates well with quantifiable increases in levels of circulating LPS-induced factors (5, 13, 24, 27, 32). In studies in which antisera against specific cytokines have been administered prior to or simultaneously with LPS, many of its biologic effects have been mitigated. For instance, anti-IL-1 serum has been shown to block LPS-induced fever (8). Similarly, injection of anti-TNF antibodies afforded significant protection against lethal challenge with LPS (4). Lastly, in mouse strains that bear the defective allele for LPS responsiveness, *Lps*^{d}, protein-free preparations of LPS fail to elicit the production of macrophage-derived factors, either in vivo or in vitro (reviewed by Vogel and Hogan [in press]).

A single injection of LPS results in the appearance of a temporal hierarchy of factors within the serum (reviewed by Vogel and Hogan [in press]). The first group of cytokines (i.e., IL-1, TNF, and interferon) appears maximally within 2 h of injection, and they have been referred to as "early acute-phase reactants." By 4 to 8 h postinjection, circulating levels of these factors are greatly decreased. Production of granulocyte-macrophage CSF activity is somewhat delayed, with peak activity occurring at 4 to 6 h following LPS and declining to basal levels by 24 h. A third group of soluble factors which appears maximally in the serum 18 to 24 h postinjection has been collectively referred to as "late acute-phase reactants" and includes C-reactive protein, serum amyloid A, fibrinogen, and others. This last group of factors is produced primarily by hepatocytes and is induced by the action of early acute-phase reactants on these cells.

For many years, it has been recognized that initial sublethal exposure to LPS renders experimental animals refractory to a subsequent challenge with homologous or heterologous LPS several days later. This effect was referred to as "early-phase endotoxin tolerance" (reviewed in reference 9). Until recently, very little was known about the mechanisms which underlie this phenomenon. Early studies dem-

* Corresponding author.

onstrated that macrophages derived from mice which had received a tolerance-inducing injection of LPS failed to respond to subsequent LPS challenge in vitro to produce endogenous pyrogen or prostaglandins (7, 21). In this sense, macrophages from mice rendered tolerant are phenotypically similar to macrophages rendered refractory to LPS by pharmacological means (e.g., by treatment with glucocorticoids; 3, 28). Williams et al. (31) demonstrated that a splenic adherent cell population was necessary for abrogation of early-phase endotoxin tolerance in transfer experiments, supporting the cellular nature of this phenomenon. In studies performed in this laboratory, it was demonstrated that early-phase endotoxin tolerance is associated with alterations in bone marrow-derived macrophage precursor pools (10, 11). Specifically, cell-sizing profiles of bone marrow cells from mice rendered tolerant showed enrichment for a population of cells significantly larger than control bone marrow populations, and by density gradient sedimentation it was shown that the denser population of cells contained increased numbers of macrophage progenitors. The induction, maintenance, and loss of these hematopoietic changes coincided temporally with the acquisition, maintenance, and loss of the tolerant state. These changes were observed in a variety of outbred and inbred mouse strains, including those with defects or deficiencies within certain lymphoid cell subsets. For example, early-phase endotoxin tolerance, as well as the associated hematopoietic changes, were observed in athymic (nude), B-cell-deficient (*xid*), and splenectomized mice (12). As an additional control, LPS-hyporesponsive C3H/HeJ mice did not exhibit any of the hematopoietic alterations observed in fully LPS-responsive mice rendered tolerant by injection of LPS (11).

In this study, we tested the possibility that cytokines which are normally produced in response to a tolerance-inducing dose of LPS may mediate the induction of early endotoxin tolerance or the accompanying hematopoietic alterations or both. Our findings indicate that combined treatment of mice with recombinant IL-1α (rIL-1) and recombinant TNFα (rTNF) induces a significant, synergistic level of toxicity, but at sublethal-dose ranges they induce a significant degree of endotoxin tolerance, as well as changes in bone marrow cell-sizing profiles and enrichment for macrophage progenitors previously associated with the tolerant state.

MATERIALS AND METHODS

Mice. Female C57BL/6J mice 5 to 6 weeks old were purchased from Jackson Laboratory (Bar Harbor, Maine) and used within 2 weeks of their receipt. Mice were allowed access to food and acid water ad libitum.

Reagents. Protein-free LPS was prepared from *Escherichia coli* K235 by the phenol-water extraction method of McIntire et al. (14). Human rIL-1α (lot SM59) was the generous gift of Hoffmann-LaRoche Inc. (Nutley, N.J.) and possessed a specific activity of 5×10^6 U/mg. The activity of this material was verified frequently in a standard thymocyte comitogenic assay (25) throughout the course of this study. The concentration of contaminating LPS in this rIL-1 preparation was 1.5 ng/1.3×10^6 U. Human rTNFα (lots NP102 and NP200B) was the generous gift of Cetus Corporation (Emeryville, Calif.) and possessed a specific activity of approximately 2×10^7 U/mg. The activity of the rTNF was also verified in a standard actinomycin D-treated L929 fibroblast cytotoxicity assay (29). The concentration of LPS in the rTNF preparations was <0.03 ng/0.3 mg. All reagents were maintained at −20°C, either in lyophilized form or as intermediate stocks at high protein concentrations, before dilution in pyrogen-free saline just before injection.

Measurement of CSF activity in serum. Serum was tested for CSF activity in a bone marrow colony assay in semisolid agar as described previously (11). Briefly, serum was obtained from pooled blood collected from mice injected (as indicated) with saline, rIL-1, rTNF, or LPS. Serial dilutions of serum were made in six-well tissue culture plates (Costar, Cambridge, Mass.). Bone marrow cells were obtained from the femurs and tibias of C3H/HeJ mice and processed by density gradient centrifugation in lymphocyte separation medium (Litton Bionetics, Kensington, Md.). The cells were then collected from the gradient interface and diluted to a final concentration of 10^5 cells per ml in a mixture of tissue culture medium and molten agar. One milliliter of the cell suspension was added to each of the wells, which contained 0.2 ml of the serum dilution. The wells were mixed by swirling and allowed to solidify. Cultures were incubated at 37°C (6% CO_2) for 7 days, at which time bone marrow colonies (≥25 cells) were enumerated with an inverted microscope.

Determination of the number of macrophage progenitor cells in bone marrow. The number of macrophage progenitor cells was determined as described elsewhere (11). Briefly, mice from each experimental group were sacrificed, and the bone marrow cells were obtained from the femurs and tibias by flushing with serum-free medium. The bone marrow cells were centrifuged and suspended in tissue culture medium. Cell counts and cell-sizing profiles were obtained with a model ZM Coulter Counter and a C1000 Channelyzer (Coulter Electronics, Inc., Hialeah, Fla.) calibrated as directed by the manufacturer.

To determine the number of macrophage progenitors, a double-layer, semisolid agar colony assay was used as described previously (11). An excess of partially purified murine macrophage CSF (CSF-1) was incorporated into the bottom layer of the assay system. Bone marrow cells (5×10^4 or 1×10^5) were then suspended in a molten agar medium mixture and overlaid onto the CSF-1-containing layer. Colonies (≥50 cells) were enumerated after 10 days in culture, and the number of progenitors per 10^5 input bone marrow cells was calculated.

Injection schedule for induction of early endotoxin tolerance. The protocol for induction of early endotoxin tolerance was identical to that used in previous studies (10–12, 31). Briefly, mice were injected intraperitoneally with 25 μg of *E. coli* K235 LPS in a volume of 0.5 ml on day 0. Three days later, mice were challenged with 25 μg of LPS and bled 6 h later for measurement of CSF in serum. Controls included mice injected on days 0 and 3 with pyrogen-free saline and mice injected on day 0 with saline and on day 3 with LPS. Mice which received rIL-1 or rTNF or both were also injected on day 0 with the indicated concentrations of cytokines but challenged on day 3 with saline or LPS.

RESULTS

Toxicity of rIL-1 and rTNF when administered individually or in combination. In our previous studies, an early-phase endotoxin tolerance system was established in which injection of 25 to 50 μg of LPS (approximately 0.05 to 0.1 50% lethal dose) was shown to render mice significantly less responsive to an LPS challenge 3 to 4 days later. Since LPS has been shown to induce both IL-1 and TNF concurrently, and since both cytokines have been shown to mimic LPS

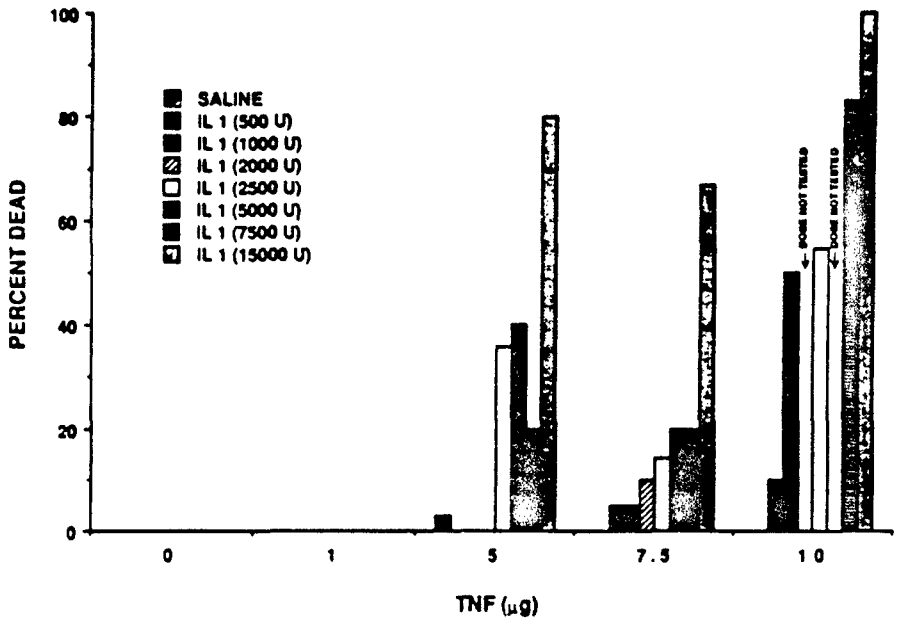

FIG. 1. Toxicity in response to injection with rIL-1 or rTNF or both. Mice were injected intraperitoneally with 0.5 ml of the indicated doses of rTNF (*x* axis) or rIL-1 (bar graph legends) or both, and the percentage of deaths (*y* axis) was scored over a 3-day period. Each point represents the total percentage of deaths observed for a given combination. Each combination was tested in 1 to 10 independent experiments in which six mice (average) per treatment per experiment were injected.

when administered in vivo (reviewed in reference 6 and by Vogel and Hogan [in press]), we sought to test the hypothesis that rIL-1 or rTNF or both could mediate induction of early endotoxin tolerance. Previous studies demonstrated that injection of high doses of either rIL-1 or rTNF resulted in production of levels of CSF comparable to those induced by 25 μg of LPS, i.e., the dose used for induction of early endotoxin tolerance (11). Therefore, the doses of rIL-1 and rTNF chosen for preliminary studies bracketed those used previously. Figure 1 illustrates the toxicity of these two cytokines over a very broad dose range when administered individually or in combination. The dose of rTNF injected is shown along the *x* axis, and the dose of rIL-1 injected is indicated by the bar graph legends. The percentage of deaths is plotted on the *y* axis. Injection of high doses of rTNF (up to 2×10^5 U per mouse; 10 μg) alone occasionally resulted in deaths (maximal toxicity never exceeded 3%). Injection of rIL-1 alone (up to 15,000 U per mouse; ~3 μg) was never lethal for mice. However, when ≥7.5 μg of rTNF was injected in combination with increasing doses of rIL-1, deaths (up to 100%) were observed in a dose-dependent fashion. In 10 separate experiments, 25 μg of LPS led to deaths in only 3.1% of the mice, consistent with our previous estimates of the 50% lethal dose for this particular endotoxin preparation (11, 26). On the basis of a recent report by Rothstein and Schreiber (22) which showed that rTNF synergized with LPS to induce deaths, we calculated the concentrations of contaminating LPS injected along with each cytokine. For the maximum dose of rTNF injected (i.e., 10 μg), <0.001 ng of LPS was injected. For the maximum dose of rIL-1 injected (i.e., 15,000 U), 0.017 ng of LPS was injected. Thus, even with the largest dose combination (i.e., 10 μg of rTNF and 15,000 U of rIL-1), only 0.018 ng of LPS was injected. This amount of LPS is >1,000-fold less than that required by Rothstein and Schreiber to induce a minimal level of synergy (resulting in death) with 10 μg of rTNF. Thus, our data suggest the possibility that the two cytokines, rIL-1 and rTNF, might synergize to mediate toxicity similar to that observed following administration of high doses of LPS. These data also defined the experimental limits for subsequent experiments with respect to the range of usable cytokine dosage combinations; i.e., a range of 500 to 2,000 U of rIL-1 per mouse could be used in combination with 5 or 7.5 μg of rTNF to achieve lethality consistently below 10%.

Another toxic manifestation associated with injection of LPS is induction of weight loss, which is maximal at 48 to 72 h postinjection (27). In addition to the lethality observed in response to combinations of rIL-1 and rTNF (Fig. 1), weight loss was measured 3 days after injection of sublethal doses of rIL-1 and rTNF administered alone or in combination. At 3 days after injection, 1,000 or 2,000 U of rIL-1 resulted in ≤4.1% weight loss, and injection of rTNF (5 or 7.5 μg) resulted in ≤6.9% weight loss when compared with saline-injected controls (Fig. 2). However, in combination, rIL-1 plus rTNF synergized to induce weight losses in mice which ranged from 17.2 to 27.3%, similar to or exceeding that induced by a tolerance-inducing dose (25 μg) of LPS (18.6 ± 2.1%).

Effect of administration of rIL-1 or rTNF or both on day 0 on ability to respond to LPS on day 3. In early endotoxin tolerance models established previously in several laboratories (11, 31), 25 μg of LPS was found to induce a state of tolerance to subsequent injection with LPS 3 days later, as assessed by the decreased capacity to produce CSF 6 h after endotoxin challenge. Since a single nonlethal injection of LPS has been shown to induce both IL-1 and TNF shortly after administration, the capacity of these two cytokines to induce a state of early endotoxin tolerance was tested. Figure 3 illustrates the capacity of mice injected on day 0 to respond to LPS on day 3 by producing CSF. As reported previously, the ability of mice treated on day 0 with LPS

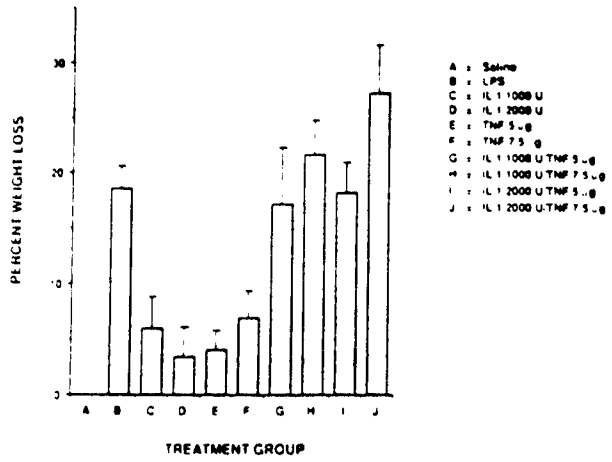

FIG. 2. Weight loss in response to injection with nonlethal doses of rIL-1 or rTNF or both. Mice were injected with saline, LPS (25 μg), or the indicated doses of rIL-1 or rTNF or both. Mice were weighed 3 days after injection, and the percent weight loss was calculated on the basis of the mean weight of saline-injected mice (17.2 ± 3 g). The data represent the arithmetic means ± the standard errors of the means of four separate experiments in which four to nine mice were injected per treatment group per experiment.

(treatment group B) to respond to LPS again on day 3 was <20% of the response of control mice (i.e., those which received saline on day 0; treatment group A). When mice were injected on day 0 with either rIL-1 or rTNF (treatment groups C to G), the ability to respond to LPS 3 days later was comparable to that of saline-pretreated mice. However, when mice were injected on day 0 with rIL-1 and rTNF in combination (treatment groups H to M), dose-dependent inhibition of LPS responsiveness on day 3 was observed. In addition, experiments in which doses as high as either 15,000 U of rIL-1 or 10 μg of rTNF were administered on day 0 led to no significant alteration in the ability to respond to LPS on day 3 (data not shown). These data indicate that in combined treatment of mice with rIL-1 and rTNF the two compounds synergize to mimic the tolerance-inducing effects of a sublethal dose of LPS.

Effect of administration of rIL-1 or rTNF or both on day 0 on bone marrow cell-sizing profiles and the number of macrophage progenitors on day 3. In previous studies, Madonna and co-workers (10–12) demonstrated that administration of a tolerance-inducing dose of LPS on day 0 led to a characteristic alteration in the cell-sizing profiles of bone marrow cells on day 3; i.e., there was enrichment for a population of larger mononuclear cells. Density gradient sedimentation studies showed that this larger population of cells contained increased numbers of progenitors which could respond to CSF-1 to form colonies in soft agar (11). Figure 4 shows a histogram analysis of the day 3 cell-sizing profiles of bone marrow cells derived from mice injected on day 0 with saline, LPS, rIL-1, rTNF, or rIL-1 plus rTNF. Figure 4A confirms the results of previous studies. When compared with saline injection of controls, injection of a tolerance-inducing dose of LPS on day 0 resulted in a marked shift in the cell-sizing profiles to a population of larger cells. Injection of either rIL-1 or rTNF resulted in a slight increase in the size of bone marrow cells (Fig. 4B; note the slight decrease in the proportion of cells in the 6.3- to 8.6-μm-diameter range and the compensatory increases within in the 8.7- to 11.4- and 11.5 to 14-μm-diameter ranges in mice treated with either rIL-1 or rTNF). These findings confirm and extend the results of a previous study in which rIL-1 was shown to increase bone marrow cell-sizing profiles (19). However, this IL-1-induced increase in population cell size fails to approach the magnitude of that observed in mice which received LPS on day 0 (Fig. 4A). Figures 4C and D show the effects of combined rIL-1 and rTNF treatment (on day 0) on the day 3 cell-sizing profiles. As observed after treatment with the tolerance-inducing dose of LPS (Fig. 4A), combined treatment with the two cytokines led to a marked shift in the cell-sizing profiles to a population enriched for significantly larger cells. In mice treated with both cytokines, there was enrichment for progenitor cells which respond to CSF-1 to form colonies in soft agar (Table 1). Thus, treatment of mice with both rIL-1 and rTNF resulted in the hematopoietic alterations previously reported to accompany a state of early endotoxin tolerance induced by LPS (11).

DISCUSSION

For many years, it has been recognized that the physiological changes that occur in experimental animals in response to gram-negative LPS are mediated principally by soluble factors produced by macrophages (reviewed by Vogel and Hogan [in press]). Perhaps the most convincing evidence for the participation of a particular cytokine in an LPS-induced response is demonstration of inhibition of a particular response by administration of anti-cytokine antibodies. To this end, the participation of IL-1 and TNF in

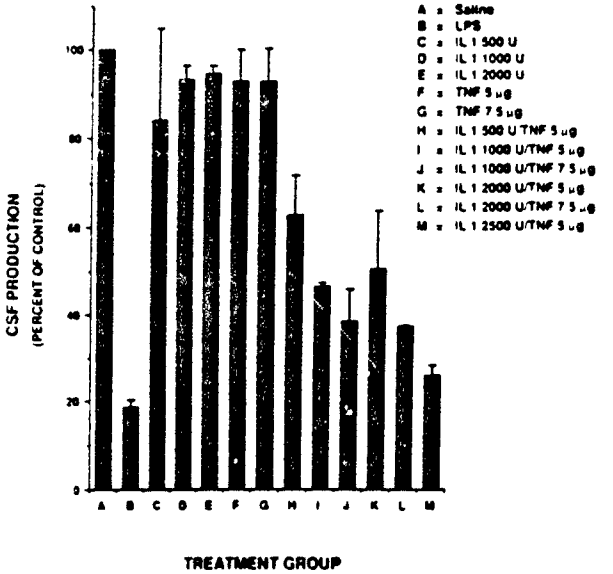

FIG. 3. Effect of injection of rIL-1 or rTNF or both on subsequent LPS responsiveness. Mice (four to seven mice per treatment group per experiment) were injected on day 0 with saline, LPS (25 μg), or the indicated doses of rIL-1 or rTNF or both. On day 3, mice were challenged with 25 μg of LPS and bled 6 h later. The pooled sera were subsequently tested for CSF activity (as described above). The data are expressed as percentages of the control (saline on day 0, LPS on day 3). The mean CSF activity of serum pools from mice which received saline on day 0 and LPS on day 3 was 6,237 ± 1,301 CFU/ml (five separate experiments). The results represent the arithmetic means ± the standard errors of the means for three to five separate experiments per treatment group.

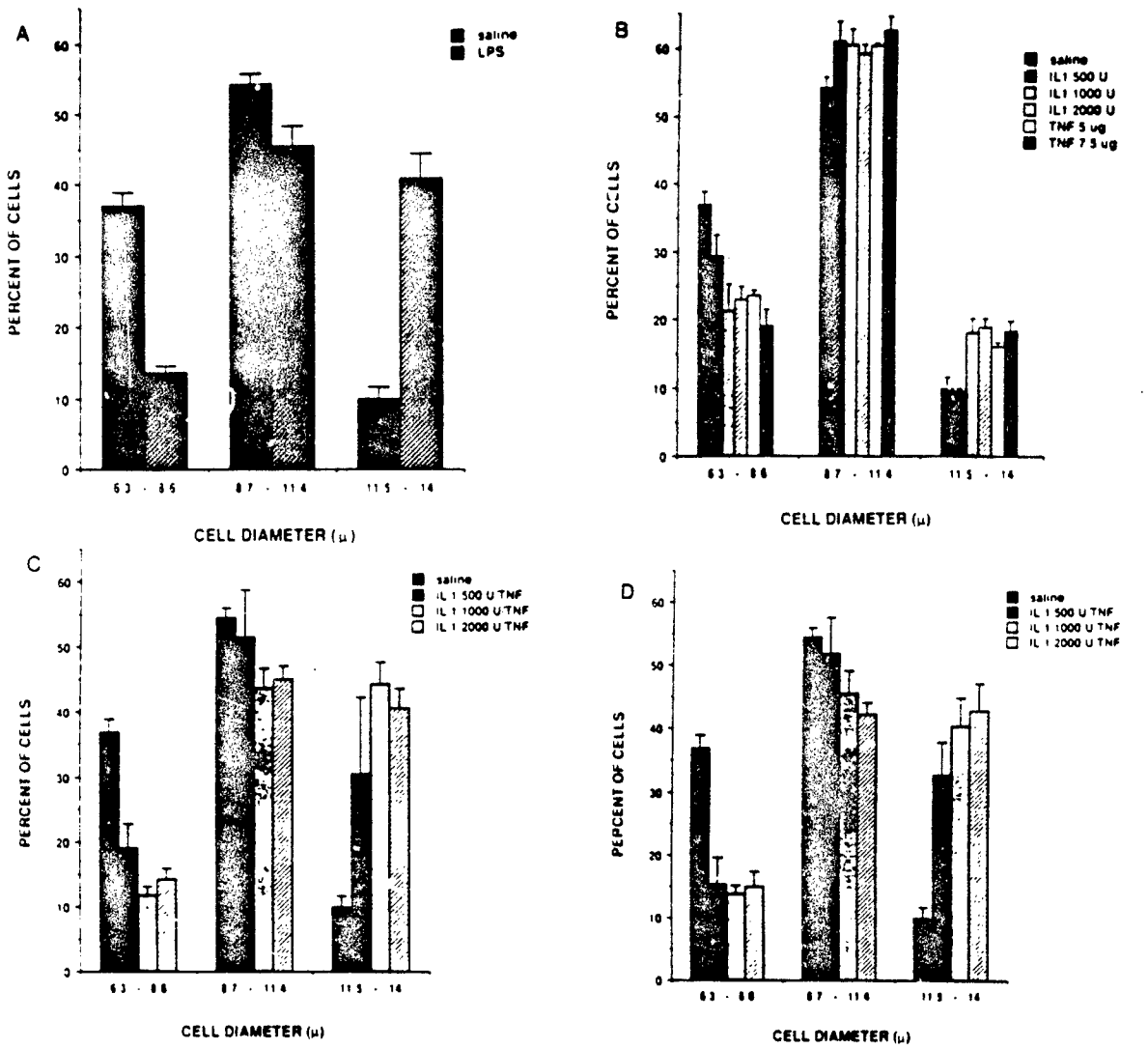

FIG. 4. Effect of rIL-1 or rTNF or both on cell-sizing profiles of bone marrow cells. Mice (two to three mice per treatment group per experiment) were injected on day 0 with saline, LPS (25 μg), or the indicated doses of rIL-1 or rTNF or both. On day 3, the bone marrow cells were obtained from the femurs and subjected to cell-sizing analysis with a Coulter Channelyzer as described in the text. Approximately 10,000 cells per treatment were analyzed for cell size in each experiment. The results represent the arithmetic means ± the standard errors of the means from three to seven separate experiments per treatment group. Panels: A, cell-sizing profiles from mice injected with saline versus LPS; B, saline versus various doses of either rIL-1 or rTNF; C, saline versus various doses of rIL-1 in combination with 5 μg of rTNF; D, saline versus various doses of rIL-1 in combination with 7.5 μg of rTNF.

LPS-mediated responses (e.g., fever and lethality) has been firmly established (4, 8). However, the availability of reagents such as anti-murine IL-1 and anti-murine TNF antibodies has been markedly limited, particularly for use in in vivo studies. It is also important to recognize that this experimental approach, although definitive for the participation of a particular factor, cannot preclude the possibility that the factor under study acts in combination with other coordinately induced mediators.

Another major approach which has been taken to assess the contribution of specific soluble factors in the mediation of LPS-induced effects is to test specific cytokines for their capacity to mimic LPS-induced responses. The recent availability of purified recombinant cytokines, such as rIL-1 and rTNF, has allowed for such an assessment without the earlier concerns which plagued studies in which natural cytokines were tested (i.e., the quantity of cytokine required for in vivo studies, as well as the persistent possibility that contaminating cytokines in the purified natural preparations actually induced the observed effect or in some way modified the response to the cytokine under question). Most recent studies using cloned reagents have focused on the administration of a single cytokine to induce a particular effect in vivo. In this regard, a plethora of information has come forth which indicates that, in vivo, both rIL-1 and rTNF induce many of the same LPS-like manifestations (reviewed in reference 6 and by Vogel and Hogan [in press]), even though these two factors bear no structural homology and bind to distinct receptors (2). For instance, both IL-1 and TNF have been shown to induce fever independently, via production of

TABLE 1. Effect of rIL-1 or rTNF or both on the numbers of CSF-1-responsive progenitors in bone marrow[a]

Treatment (amt)	Mean (± SEM) no. of CSF-1 progenitors/10^5 bone marrow cells (P value)[b]
Saline	47 ± 1.5
rIL-1 (1,000 U)	37 ± 10.8 (0.334)
rTNF (5 μg)	52 ± 7.8 (0.754)
rTNF (7.5 μg)	67 ± 3.5 (0.010)
rIL-1 (1,000 U)+rTNF (5 μg)	89 ± 5 (0.002)
rIL-1 (1,000 U)+rTNF (7.5 μg)	121 ± 1.9 (0)

[a] Bone marrow cells were derived on day 3 from mice (two to three mice per treatment group per experiment) which had received saline or the indicated dose of rIL-1 or rTNF or both on day 0. The results are expressed as the number of CSF-1-responsive progenitors per 10^5 bone marrow cells. The results represent three separate experiments.

[b] An unpaired, two-tailed Student t test was used.

prostaglandins (8). In this regard, they are both classical "endogenous pyrogens." In addition, at high doses, rTNF was shown to induce IL-1 in vivo (8). This particular example provides a good illustration of both cytokine redundancy (in the sense that two distinct cytokines can induce the same biological effect) and the potential for an inductive cascade which, in turn, could prolong a given manifestation in vivo. Injection of either rIL-1 or rTNF has been demonstrated in vivo to induce many of the same physiologic alterations seen in response to LPS in addition to fever, such as hypoglycemia, shock and death, increased resistance to infection, radioprotection, resistance to neoplasia, induction of CSF and late acute-phase reactants, and others (reviewed by Vogel and Hogan [in press]).

In this study, we sought to determine whether induction of early endotoxin tolerance by LPS is mediated by soluble factors produced in response to the tolerance-inducing injection (i.e., the sublethal injection of LPS given on day 0 to induce a state of resistance to a subsequent challenge 3 to 4 days later). In these studies, it was shown that neither rIL-1 nor rTNF injected individually (at doses which induced levels of circulating CSF in vivo comparable to that induced by a tolerance-inducing injection of LPS) induced a state of early endotoxin tolerance. This was assessed by production of normal levels of CSF in response to LPS administered 3 days later. Since IL-1 and TNF are coordinately produced in response to LPS, we hypothesized that induction of tolerance depends upon the simultaneous presence of both soluble factors. When administered individually, rIL-1 and rTNF rarely induced overt signs of toxicity; however, simultaneous administration of high doses of the two cytokines resulted in frank toxicity and often death. It is highly unlikely that this is due to synergy between rTNF and contaminating LPS, since the maximum amount of contaminating LPS injected was >1,000-fold less than that shown previously to induce minimal synergy with rTNF, resulting in death (22). Synergy between rTNF and rIL-1 was evident, even within a combined-dose range which rarely led to deaths, as measured by induction of weight loss greater than or equivalent to that induced by 25 μg of LPS. Within this same sublethal-dose range, the two cytokines induced refractoriness to LPS challenge in a dose-dependent fashion (Fig. 3). The amount of contaminating LPS injected with a more typical tolerance-inducing dose combination (e.g., 7.5 μg of rTNF and 2,000 U rIL-1) was <0.003 ng. Thus, it is more likely that the synergistic toxicity observed by Rothstein and Schreiber (22) is due to LPS induction of IL-1, which in turn synergizes with rTNF. These tolerance-inducing combinations of rIL-1 and rTNF also led to the hematopoietic alterations shown previously to be associated with LPS-induced early endotoxin tolerance (11), i.e., an increase in the size of bone marrow cells (Fig. 4) with concurrent enrichment for macrophage precursors (Table 1). With respect to the latter, it is interesting that injection of 7.5 μg of rTNF alone, but not 5 μg of rTNF, led to a statistically significant increase in the number of macrophage progenitors in the bone marrow. This may reflect the fact that high doses of TNF administered in vivo have been shown to induce IL-1 production (8). Thus, rTNF-induced IL-1 may act synergistically with administered rTNF to increase the number of CSF-1-responsive progenitors.

Taken collectively, these findings suggest that, in vivo, LPS-induced early endotoxin tolerance is mediated by the synergistic action of LPS-induced IL-1 and TNF. For most of the studies performed, combined administration of IL-1 and TNF has been shown to result in an additive effect; however, a precedent for synergy between these two factors exists. For example, Beck et al. (1) showed that intradermal injection of natural IL-1, like LPS, led to attraction of ^{51}Cr-labeled neutrophils to the site of injection. Movat et al. (17) confirmed these findings by using rIL-1 and extended them by demonstrating that the combined action of rIL-1 and rTNF was synergistic in producing infiltration. Similar findings were recently reported by Wankowicz et al. (30). Movat et al. (16) also demonstrated that intradermal injection of rIL-1 and rTNF led to synergistic induction of a local Schwartzman reaction in rabbits challenged intravenously with endotoxin 18 h later. Neta et al. (18) have shown that at doses of radiation which closely approach 100% lethality, the radioprotective effects of rIL-1 and rTNF are additive; however, at higher levels of irradiation, the radioprotection afforded by combined rIL-1 and rTNF injection was much greater than would be predicted by summing the protection afforded by injection of the cytokines individually. For induction of certain acute-phase reactants, such as serum amyloid P, simultaneous administration of rIL-1 and rTNF resulted in an additive response; however, combined administration of these two cytokines led to synergistic induction of fibrinogen (15). Recently, it was pointed out that IL-1 and TNF are strongly synergistic for generation of hypotension and the capillary leak syndrome (6, 20). In studies performed with C3H/HeJ mice, synergistic protection from infection by *E. coli* was afforded by treatment of mice with a combined rIL-1 and rTNF regimen (G. Saydoff, personal communication).

The mechanisms by which LPS induces a transient reversal of sensitivity to homologous or heterologous challenge with LPS, i.e., early endotoxin tolerance, are not very well understood. Early studies in which peritoneal macrophages or Kupffer cells of animals rendered tolerant to endotoxin were found to be refractory to stimulation with LPS in vitro (7, 21) strongly suggested that tolerance was a function of a failure to produce those soluble macrophage factors, such as endogenous pyrogen or prostaglandins, shown previously to be associated with endotoxin-mediated toxicity. Subsequent studies by Williams et al. (31) strengthened the role of macrophages in the induction of tolerance by showing that injection of either a splenic adherent cell population or peritoneal exudate macrophages along with splenic nonadherent cells was essential for overriding the inability to produce CSF in recipients rendered tolerant to endotoxin. Lastly, in work by Madonna and co-workers (10–12), the tolerance-inducing dose of LPS was followed by normal induction of macrophage-derived products, such as CSF and

interferon, but resulted in a depressed capacity to produce these same factors upon LPS challenge 3 to 4 days later. The kinetics of tolerance induction was correlated with acquisition of a characteristic change in the cell-sizing pattern of the bone marrow towards larger cells, and within this increased population of larger cells a marked increase in the number of CSF-1-responsive macrophage progenitors was observed. It was therefore proposed that (i) early endotoxin tolerance results from a developmental blockade which results in accumulation of immature macrophages in the bone marrow which, in turn, limits the number of fully mature, LPS-responsive macrophages in the periphery or (ii) initial exposure of mature macrophages to LPS renders them refractory to subsequent stimulation because of a blockade or down regulation of the LPS receptor.

The data presented in this report, that rIL-1 and rTNF synergize to induce refractoriness to LPS, as well as the hematopoietic changes reported previously, suggest that tolerance is induced in the absence of LPS and is mediated indirectly, rather than by a mechanism which involves a blockade of the LPS receptor. Another possibility which might be invoked to explain the failure to respond to a challenge injection of LPS is that the initial injection of the two cytokines results in induction of a state of tachyphylaxis to IL-1 or TNF produced in response to the LPS challenge. If this were so, then one would expect to observe diminished toxicity in the face of normal levels of circulating IL-1 or TNF produced in response to the LPS challenge. Preliminary experiments have indicated that, similar to the reduced levels of CSF and interferon in circulation following LPS challenge, animals rendered endotoxin tolerant produced significantly less circulating TNF upon challenge than did control animals (data not shown), consistent with earlier findings (7, 21) that macrophages derived from animals rendered tolerant produce depressed levels of soluble factors in vitro (e.g., endogenous pyrogen and prostaglandins) when exposed to LPS. Thus, failure to produce adequate levels of cytokines is more likely to underlie the observed decrease in toxicity, rather than cytokine-induced tachyphylaxis to TNF. Confirmation of these conclusions will depend upon the availability of high-titered anti-murine IL-1 and anti-murine TNF antibodies and the demonstration that injection of either reagent abrogates induction of LPS-induced tolerance in vivo. As indicated above, the hematopoietic changes observed in response to a tolerance-inducing dose of LPS are only a correlate of early LPS-induced tolerance. The demonstration that anti-IL-1 or anti-TNF or both antibodies also abrogate the hematopoietic responses to a tolerance-inducing dose of LPS would strengthen this relationship.

ACKNOWLEDGMENTS

This work was supported by Uniformed Services University of the Health Sciences protocol RO7338 and the Armed Forces Radiobiology Research Institute, Defense Nuclear Agency, under research work unit MJ B3148 (Uniformed Services University of the Health Sciences protocol G27384).

LITERATURE CITED

1. **Beck, G., G. S. Habicht, J. L. Benach, and F. Miller.** 1986. Interleukin 1: a common endogenous mediator of inflammation and the local Schwartzman. J. Immunol. 136:3025–3031.
2. **Beutler, B., and A. Cerami.** 1985. Recombinant interleukin 1 suppresses lipoprotein lipase activity in 3T3-L1 cells. J. Immunol. 135:3969–3977.
3. **Beutler, B., N. Krochin, I. Milsark, C. Luedke, and A. Cerami.** 1986. Control of cachectin (tumor necrosis factor) synthesis: mechanisms of endotoxin resistance. Science 232:977–980.
4. **Beutler, B., I. W. Milsark, and A. C. Cerami.** 1985. Passive immunization against cachectin-tumor necrosis factor protects mice from lethal effect of endotoxin. Science 229:869–871.
5. **Carswell, W. A., L. J. Old, R. L. Kassel, S. Green, N. Fiore, and B. Williamson.** 1975. An endotoxin induced serum factor that causes necrosis of tumors. Proc. Natl. Acad. Sci. USA 72:3666–3670.
6. **Dinarello, C. A.** 1988. Biology of interleukin-1. (Fed. Am. Soc. Exp. Biol. J. 2:108–115.
7. **Dinarello, C. A., P. T. Bodel, and E. Atkins.** 1968. The role of the liver in the production of fever and in pyrogenic tolerance. Trans. Assoc. Am. Physicians 81:334.
8. **Dinarello, C. A., J. G. Cannon, S. W. Wolff, H. A. Bernheim, B. Beutler, A. Cerami, I. S. Figari, M. A. Palladino, and J. V. O'Connor.** 1986. Tumor necrosis factor (cachectin) is an endogenous pyrogen and induces production of interleukin 1. J. Exp. Med. 163:1433–1450.
9. **Greisman, S. E.** 1983. Induction of endotoxin tolerance, p. 149–178. *In* A. Nowotny (ed.), Beneficial effects of endotoxins. Plenum Publishing Corp., New York.
10. **Madonna, G. S., J. E. Peterson, E. E. Ribi, and S. N. Vogel.** 1986. Early-phase endotoxin tolerance: induction by a detoxified lipid A derivative, monophosphoryl lipid A. Infect. Immun. 52:6–11.
11. **Madonna, G. S., and S. N. Vogel.** 1985. Early endotoxin tolerance is associated with alterations in bone marrow-derived macrophage precursor pools. J. Immunol. 135:3763–3771.
12. **Madonna, G. S., and S. N. Vogel.** 1986. Induction of early-phase endotoxin tolerance in athymic (nude) mice, B-cell-deficient (*xid*) mice, and splenectomized mice. Infect. Immun. 53:707–710.
13. **Mannel, D. N., R. N. Moore, and S. E. Mergenhagen.** 1980. Endotoxin-induced tumor cytotoxic factor, p. 141–143. *In* D. Schlessinger (ed.), Microbiology—1980. American Society for Microbiology, Washington, D.C.
14. **McIntire, F. C., H. W. Sievert, G. H. Barlow, R. ... Finley, and A. Y. Lee.** 1967. Chemical, physical, and biological properties of a lipopolysaccharide from *Escherichia coli* K235. Biochemistry 6:2363–2372.
15. **Mortenson, R. F., J. Shapiro, B.-F. Lin, S. Douches, and R. Neta.** 1988. Interaction of recombinant IL-1 and recombinant tumor necrosis factor in the induction of mouse acute phase proteins. J. Immunol. 140:2260–2266.
16. **Movat, H. Z., C. E. Burrowes, M. I. Cybulsky, and C. A. Dinarello.** 1987. Role of complement, interleukin-1, and tumor necrosis factor in a local Shwartzman-like reaction, p. 69–78. *In* H. Movat (ed.), Leukocyte emigration and its sequelae. S. Karger, Basel.
17. **Movat, H. Z., M. I. Cybulsky, I. G. Colditz, M. K. W. Chan, and C. A. Dinarello.** 1987. Acute inflammation in gram-negative infection: central role of endotoxin, interleukin-1, tumor necrosis factor, and the neutrophil leukocyte. Fed. Proc. 46:97–104.
18. **Neta, R., J. J. Oppenheim, and S. D. Douches.** 1988. Interdependence of the radioprotective effects of human recombinant interleukin 1α, tumor necrosis factor α, granulocyte colony-stimulating factor, and murine recombinant granulocyte-macrophage colony-stimulating factor. J. Immunol. 140:108–111.
19. **Neta, R., M. B. Sztein, J. J. Oppenheim, S. Gillis, and S. D. Douches.** 1987. The *in vivo* effects of interleukin 1. I. Bone marrow cells are induced to cycle after administration of interleukin 1. J. Immunol. 139:1861–1866.
20. **Okusawa, S., J. A. Gelfand, T. Ikejima, R. J. Connolly, and C. A. Dinarello.** 1988. Interleukin 1 induces a shock-like state in rabbits. Synergism with tumor necrosis factor and the effect of cyclooxygenase inhibition. J. Clin. Invest. 81:1162–1172.
21. **Rietschel, E. T., U. Schade, O. Lüderitz, H. Fischer, and B. A. Peskar.** 1980. Prostaglandins in endotoxicosis, p. 66–72. *In* D. Schlessinger (ed.), Microbiology—1980. American Society for Microbiology, Washington, D.C.
22. **Rothstein, J. L., and H. Schreiber.** 1977. Synergy between tumor necrosis factor and bacterial products causes hemorrhagic necrosis and lethal shock in normal mice. Proc. Natl. Acad. Sci. USA 85:607–611.

23. **Sultzer, B. M., and G. W. Goodman.** 1977. Characteristics of endotoxin-resistant low-responder mice, p. 304–309. *In* D. Schlessinger (ed.), Microbiology—1977. American Society for Microbiology, Washington, D.C.
24. **Urbaschek, R. M., R. K. Shadduck, C. Bona, and S. E. Mergenhagen.** 1980. Colony-stimulating factor in nonspecific resistance and in increased susceptibility to endotoxin, p. 115–119. *In* D. Schlessinger (ed.), Microbiology—1980. American Society for Microbiology, Washington, D.C.
25. **Vogel, S. N., S. D. Douches, E. N. Kaufman, and R. Neta.** 1987. Induction of colony stimulating factor *in vivo* by recombinant interleukin 1α and tumor necrosis factor α. J. Immunol. 138: 2143–2148.
26. **Vogel, S. N., K. E. English, and A. D. O'Brien.** 1982. Silica enhancement of murine endotoxin sensitivity. Infect. Immun. 38:681–685.
27. **Vogel, S. N., R. N. Moore, J. D. Sipe, and D. L. Rosenstreich.** 1980. BCG-induced enhancement of endotoxin sensitivity in C3H/HeJ mice. I. *In vivo* studies. J. Immunol. 124:2004–2009.
28. **Wahl, S.** 1982. Mononuclear cell-mediated alterations in connective tissue, p. 225–234. *In* R. J. Genco and S. E. Mergenhagen (ed.), Host-parasite interactions in periodontal diseases. American Society for Microbiology, Washington, D.C.
29. **Wang, A. M., A. A. Creasey, M. B. Ladner, L. S. Lin, J. Strickler, J. N. VanArsdell, R. Yamamoto, and D. F. Mark.** 1985. Molecular cloning of the complementary DNA for human tumor necrosis factor. Science 228:149–154.
30. **Wankowicz, Z., P. Megyeri, and A. Isackstz.** 1988. Synergy between tumour necrosis factor α and interleukin-1 in the induction of polymorphonuclear leukocyte migration during inflammation. J. Leukocyte Biol. 43:349–356.
31. **Williams, Z., C. F. Hertogs, and D. H. Pluznik.** 1983. Use of mice tolerant to lipopolysaccharide to demonstrate requirement of cooperation between macrophages and lymphocytes to generate lipopolysaccharide-induced colony-stimulating factor in vivo. Infect. Immun. 41:1–5.
32. **Youngner, J. S., and W. R. Stinebring.** 1965. Interferon appearance stimulated by endotoxin, bacteria, or viruses in mice pre-treated with *Escherichia coli* endotoxin or infected with *Mycobacterium tuberculosis*. Nature (London) 208:456–458.